COMPUTER AIDED DESIGN

of

HARRISON TWIN PIVOT

and

TWIN BALANCE GRASSHOPPER ESCAPEMENT GEOMETRIES

Computer Aided Design of Harrison Twin Pivot and Twin Balance Grasshopper Escapement Geometries

PART ONE and most of the APPENDIX of this publication supersede 'Perfecting the Harrison Grasshopper Escapement' and 'Perfecting the Harrison Twin Pivot Grasshopper Escapement', both published in 2009. As a consequence of recent discoveries within Harrison's illustrated work, twin pivot 'end/start ratio' replaces 'mean torque arm ratio' and corrections for varying forces are not applied. Mathematical modelling is displaced by a more versatile and capable graphical technique, most accurately (although not essentially) executed using widely available Computer Aided Design (CAD) software.

PART TWO and part of the APPENDIX present further analysis of Harrison's illustrated work and a graphical design technique specific to his twin balance (longitude timekeeper, or 'sea clock') grasshopper escapement geometry, again most accurately executed using CAD software.

1st Edition, 16th November 2011

TABLE OF CONTENTS

PART ONE
THE TWIN PIVOT GRASSHOPPER ESCAPEMENT

PART TWO
THE TWIN BALANCE GRASSHOPPER ESCAPEMENT

APPENDIX

PREFACE

John 'Longitude' Harrison (1693-1776) created his first grasshopper escapement with the simple objectives of eliminating sliding friction, the detrimental effects of wear and the unpredictable inconsistencies of lubrication. He later discovered that versatile impulse characteristics and a capacity for high escaping arcs could also be manipulated to his advantage, as he strove to extract unprecedented performance from entirely mechanical timekeepers exposed to the Earth's atmosphere. Perhaps unintentionally, Harrison also created one of the most beautiful and mesmerising mechanical escapements ever devised.

After almost two and a half centuries of neglect, the single and twin pivot grasshopper escapements have recently enjoyed something of a revival, the motive in almost all cases being an understandable desire to reproduce the fascinating 'kicking grasshopper' motions, from which the escapement derives its popular name. Sadly, the remarkable performance advantages and the means by which they should be achieved have been almost universally overlooked, ignored or misunderstood. As a consequence, recent history is littered with hideous grasshopper mutations, more likely to turn Harrison in his grave than permit the escape wheel to rotate as he intended. There can, however, be little argument that Harrison's own failure to record a clear explanation of his invention has been responsible for a great deal of the neglect and ignorance.

In an attempt to resolve this sorry and unnecessary situation, ‘Computer Aided Design of Harrison Twin Pivot and Twin Balance Grasshopper Escapement Geometries’ will gather, analyse, interpret and explain every one of Harrison's recorded intentions for the performance of his astonishing invention and offer straightforward techniques for their simultaneous incorporation within the geometries of twin pivot and twin balance grasshopper escapements.

David Heskin, Lancashire, England, November 2011

PART ONE

*

THE TWIN PIVOT GRASSHOPPER ESCAPEMENT

INTRODUCING THE TWIN PIVOT GRASSHOPPER ESCAPEMENT

The first grasshopper escapement ever created was almost certainly of the twin pivot configuration. A young carpenter and self-taught clockmaker by the name of John Harrison (1693-1776) had designed and constructed a tower clock for the stables at Brocklesby Park, Lincolnshire, the original escapement of which proved to be unreliable, apparently due to excessive friction and/or the deficiencies of eighteenth century lubricants. In a typically direct and thorough fashion, Harrison invented an entirely new, effectively frictionless escapement, adequately represented in **Figure 1**, to no particular scale. Harrison's *'Contrivance of Pallats'*, more recently referred to as the 'grasshopper' escapement due to its 'kicking' motions, functions entirely without lubrication. Two wooden arms, illustrated largely in brown, pivot upon two separate pivots, from which the name 'twin pivot' has been derived.

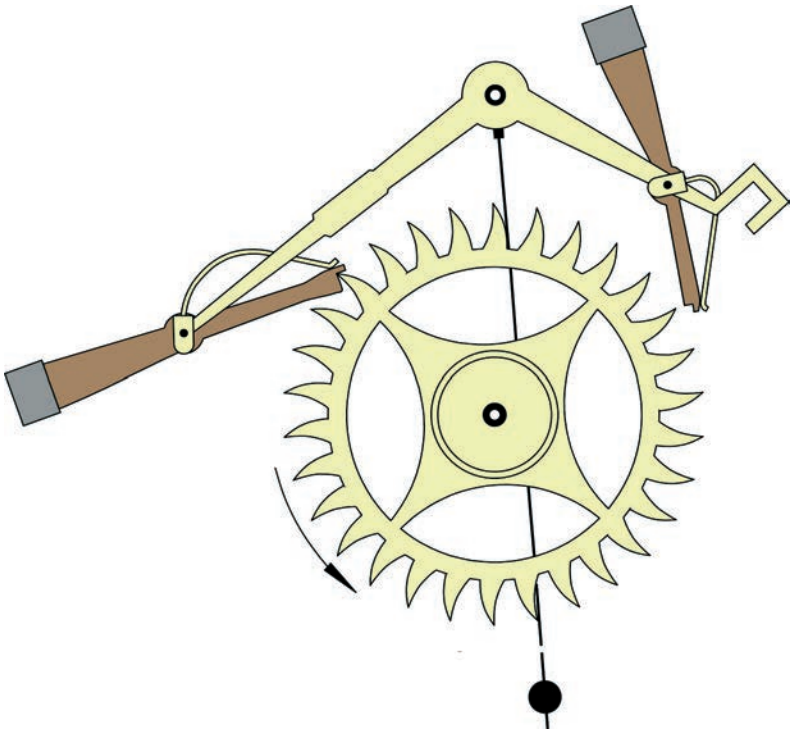

Figure 1 - Representation of Harrison's 'Brocklesby Park' twin pivot grasshopper escapement.

The Brocklesby Park escapement may have been the only twin pivot grasshopper ever made by Harrison, although it is not entirely impossible that he installed but subsequently replaced the configuration within some of his early wooden movement longcase regulators, constructed to his own design not long after the Brocklesby commission. It is clear (to this observer, at least) that he favoured a different configuration, currently installed in almost all of his longcase regulators, referred to herein as the 'single pivot' grasshopper escapement.

Logical reasons for Harrison's apparent abandonment of the twin pivot grasshopper escapement have yet to be identified. His manuscripts and illustrations would appear to offer no clues, merely declaring, without elaboration or proof, that the inherently asymmetrical impulse of the single pivot configuration is of no consequence. In defence of the twin pivot grasshopper, the Brocklesby Park escapement has delivered satisfactory service for almost three centuries, apart from damage due to mishandling and/or problems elsewhere in the clock. There can therefore be little doubt, albeit with the benefit of hindsight, that the twin pivot grasshopper is an exceptionally reliable and durable escapement. The observations, analyses and proposals offered herein will also demonstrate that the twin pivot configuration has no obvious vices and, unlike the single pivot, will incorporate symmetrical impulse features with ease.

Although mechanical design and construction are topics beyond the intended scope and size of this publication, it should also be mentioned that the twin pivot arrangement is more straightforward in those respects than the single pivot.

MECHANICAL ARRANGEMENT

In comparison with common escapements, such as the anchor and dead beat, the mechanical arrangement of the twin pivot grasshopper escapement is slightly more involved, rather unusual and far more interesting. **Figure 2**, to no particular scale, illustrates the assembled components of a complete twin pivot grasshopper escapement, directly attached to a greatly shortened, symbolic representation of a simple pendulum. The upper figure is a view from above looking vertically downwards and the lower figure is a view from the front looking horizontally rearwards. In reality (although not illustrated, in the interests of simplicity), the pendulum would be independently suspended and rigidly linked to the escapement frame by a conventional crutch.

The illustrated escapement and its escape wheel of sixty teeth will be especially well suited to a detailed explanation of the principles of operation, offered shortly. It should however be mentioned that, for his single pivot configuration, Harrison clearly stipulated an escape wheel rotating one every four minutes in association with a pendulum beating seconds. As will be demonstrated in due course, those stipulations require that an escape wheel of one hundred and twenty teeth be fitted. That, together with additional design and performance stipulations, will be incorporated later, when a fully compliant Harrison twin pivot geometry is created from first principles.

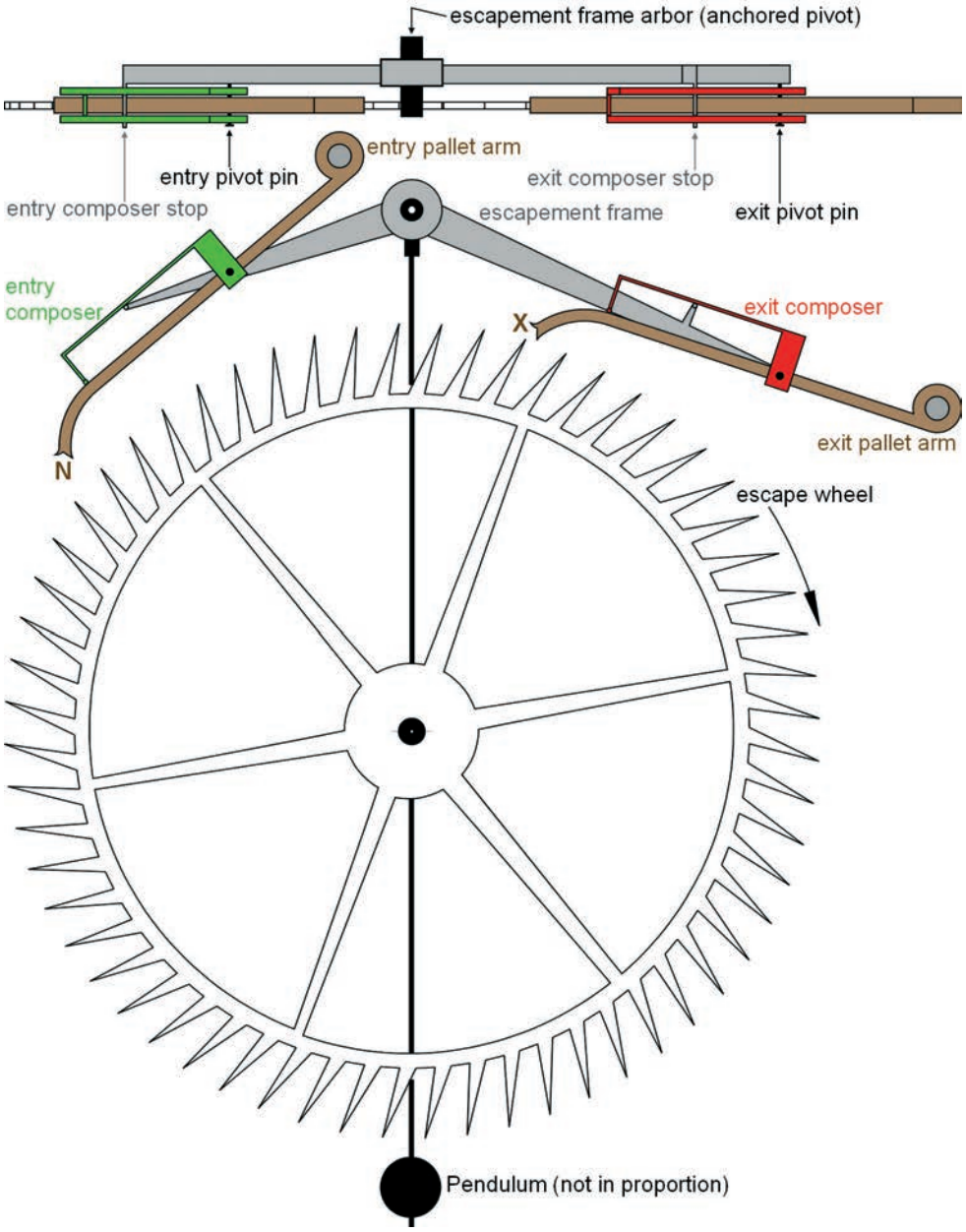

Figure 2 - Simplified representation of a twin pivot grasshopper escapement.

The twin pivot grasshopper escapement of Figure 2 incorporates the following components:

■ **ESCAPEMENT FRAME -** The grey **'escapement frame'** incorporates two rigidly attached pivot pins, illustrated in black and labelled **'entry pivot pin'** and **'exit pivot pin'** and two rigidly incorporated projections, illustrated in grey and labelled **'entry composer stop'** and **'exit composer stop'**. The escapement frame may only rotate in unison with the rigidly attached **'escapement frame arbor'** about the anchored escapement frame arbor axis.

■ **ENTRY AND EXIT PALLET ARMS AND NIBS -** The brown **'entry pallet arm'**, typically of hardwood, is mounted, with freedom to rotate, upon the entry pivot pin. The brown **'exit pallet arm'**, also typically of hardwood, is mounted, with freedom to rotate, upon the exit pivot pin. The **'entry pallet nib'**, labelled N, is the forked end of the entry pallet arm met by the tips of escape wheel teeth as they 'enter' the escapement assembly. The **'exit pallet nib'**, labelled X, is the forked end of the exit pallet arm left behind by escape wheel teeth tips as they 'exit' the escapement assembly. For reasons to be explained shortly, the pallet arms are weighted at their **'tail'** ends, in this case with metal inserts (illustrated as solid grey circles), such that, when subjected only to the Earth's gravity acting vertically downwards, either arm is tail-heavy about its pivot.

■ **ENTRY AND EXIT COMPOSERS -** Also mounted upon upon each pivot pin, with freedom to rotate, are components commonly referred to as **'composers'**, typically of brass. The **'entry composer'** is illustrated in green and the **'exit composer'** is illustrated in red. Both composer are nose-heavy, the 'nose' being the free end, furthest from the pivot. For reasons to be explained in due course, the torque (turning effort) generated by either nose-heavy composer about its pivot pin is arranged to be greater than the opposite torque generated by the paired, tail-heavy pallet arm about the same, shared pivot pin, when the escapement is subjected only to the Earth's gravity acting vertically downwards.

It will be obvious from the above that each escapement component is only capable of rotation about specific arbor axes and/or pivot pins, all of which are parallel to the escape wheel axis. No other motions are possible.

COMPONENT BEHAVIOUR

This section begins with descriptions of the behaviour of individual escapement components and ends with simple explanations of their basic interactions.

KEY TO ILLUSTRATIONS

All views are from the front of an imaginary timekeeper movement, looking horizontally rearwards. A seconds-beating pendulum will be assumed throughout. Normal escape wheel advancement is clockwise.

■ **'Anchored pivot'** (shown here greatly enlarged). In effect, a pivot anchored rigidly to the Earth.
Movement (translation) of the pivot is not possible.
Free rotation of components mounted upon the pivot is possible.
No other motions of components mounted upon the pivot are possible.

■ **'Travelling pivot'** (shown here greatly enlarged). Rigidly incorporated within a moveable object.
Can only move in unison with the incorporating object.
Free rotation of components mounted upon the pivot is possible.
No other motions of components mounted upon the pivot are possible.

■ **'Rigid attachment'** (shown here greatly enlarged).
Rigidly joins objects together.
In this example, objects A, B and C are rigidly joined at D.

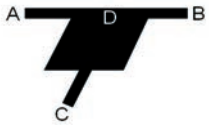

■ **Symbolic pushing hand** (shown here greatly enlarged).
Indicates that a component is being pushed (with undefined force, unless stated) in the indicated direction (in this case horizontally to the right) by an imaginary, extremely small assistant. Considerably smaller than an average adult male human hand.

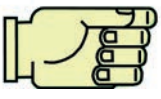

Figure 3 (below) - Illustrates the view from a position directly in front of the twin pivot grasshopper escapement of Figure 2 after both pallet arms and both composers have been removed. As described earlier, the rigid assembly of the escapement frame, escapement frame arbor, both pivot pins and both composer stops is only capable of rotation about the escapement frame arbor axis, which is, in effect, anchored to the Earth. No other motions are possible. For simplicity, the upper part of a seconds-beating pendulum is illustrated as a bold, broken, black line, vertical in this instance, directly attached to the escapement frame assembly. The opposing hands of our extremely small assistant indicate that the entire, rigid assembly of the pendulum, frame, pins and stops is currently being held stationary in the illustrated position.

For future reference, the minimum theoretical pendulum angular displacement for successful escapement operation, commonly referred to as the **'escaping arc',** will be defined by two short, broken radials from the escapement frame arbor axis, referred to as **'displacement markers'**, symmetrically disposed to the left and right of a short, broken, vertical line through the same axis (visible in Figure 4, below). In reality, the driving weight (or the spiral spring) of any timekeeper must be adjusted to supply a small excess of energy to the escapement, to guarantee reliable, continuous operation, despite unavoidable and unpredictable influences, such as the Earth's ever-changing atmosphere. It must be ensured that the small excess of energy is sufficient to generate left and right pendulum motions slightly beyond the left and right minimum displacement markers in all circumstances.

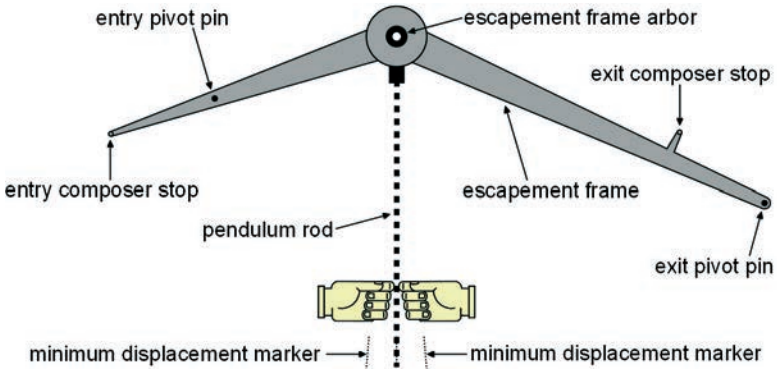

Figure 3 - Rigid assembly of the escapement frame, escapement frame arbor, both pivot pins, both composer stops and a symbolic upper portion of the pendulum being held in the illustrated position.

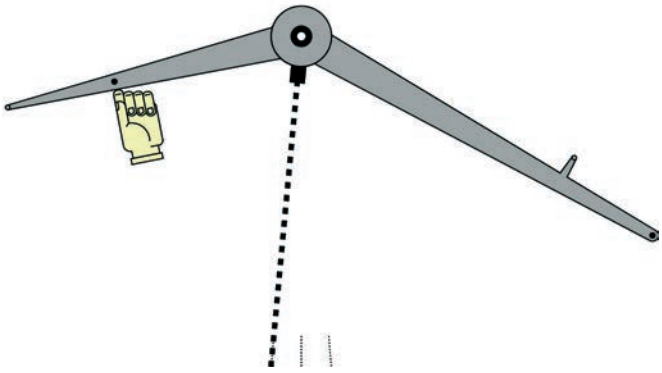

Figure 4 - Clockwise torque applied to the escapement frame about its arbor axis.

Figure 4 (above) - Illustrates the effect of releasing the pendulum and applying and maintaining clockwise torque to the escapement frame about its arbor axis, as represented by the pushing hand.

The rigid assembly of the pendulum, escapement frame, escapement frame arbor, both pivot pins and both composer stops has rotated clockwise, in its otherwise unaltered entirety, about the escapement frame arbor axis, in opposition to the Earth's gravity, which acts vertically downwards through the centre of mass of the assembly. When the applied torque and the opposing torque due to gravity are in balance about the escapement frame arbor axis, the assembly will adopt a stationary position, with the pendulum somewhere to the left of vertical, as illustrated. An increase in the applied torque would increase the illustrated deflection of the pendulum and a reduction in the applied torque would reduce the illustrated deflection of the pendulum.

During normal escapement operation, the forces and torques required to maintain the correct motions and brief pauses of the pendulum need only be sufficient in magnitude to make up for small energy losses to due air resistance etc. and various unavoidable and unpredictable influences and disturbances. It should therefore be bourne in mind that normal operating forces and torques are likely to be lower than the stationary situations depicted in Figures 4 to 19 inclusive might suggest.

Figure 5 (below) - Illustrates the effect of withdrawing all previous inputs and applying and maintaining anticlockwise torque to the escapement frame about its arbor axis, generated by the symbolic pushing hand. The rigid assembly of the pendulum, escapement frame, escapement frame arbor, both pivot pins and both composer stops has rotated anticlockwise, in its otherwise unaltered entirety, about the escapement frame arbor axis. The pendulum has swung somewhere to the right of vertical, until a balance of applied torque and resistance due to gravity has been established, at which point all motion has ceased.

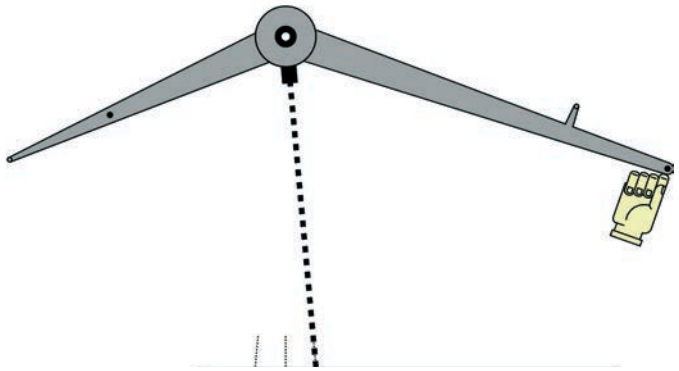

Figure 5 - Anticlockwise torque applied to the escapement frame about its arbor axis.

Figure 6 (below) - All previous inputs have been removed and the pendulum and escapement frame are being held stationary in the illustrated position. The entry and exit composers, currently illustrated in light grey, have been fitted to the entry and exit pivot pins, respectively, in their correct orientations. Recall that both composers are nose-heavy and that each composer in isolation is free to rotate about its own pivot pin. The entry composer is therefore constantly inclined to rotate anticlockwise about the entry pivot pin and, entirely independently, the exit composer is constantly inclined to rotate anticlockwise about the exit pivot pin. Two broken circles highlight the inevitable points of contact between each composer limb and the relevant composer stop, which prevent further anticlockwise rotation of the composers about their pivot pins. Both composers are thereafter obliged to **'rest'** upon their stops in the illustrated positions.

NB - In this and all subsequent illustrations, any 'resting' composers will be coloured light grey.

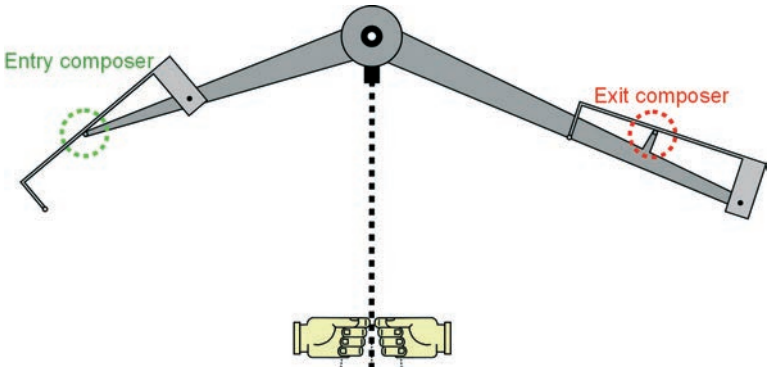

Figure 6 - Both nose-heavy composers independently 'resting' upon their composer stops.

Figure 7 (below) - The noses of both composers have been **'lifted'** by entirely separate external forces, applied by the hands of a second assistant. For clarity of illustration, the 'lifts' of both composers are greater than they would be during normal escapement operation. The limb of the nose-heavy entry composer, shown in green, has been lifted away from the entry stop and the entry composer is generating continuous resistance to the applied force. The limb of the exit composer, shown in red, has been lifted away from the exit composer stop and is generating its own continuous, resistance to the applied force. Observe that the lift of the entry composer is entirely independent of the lift of the exit composer and vice versa. Thus, for example, if the hand input to either composer was to be removed, that composer would rotate freely and independently anticlockwise until brought to rest by its composer stop. The other composer, still subjected to an applied force, would independently remain in its lifted position.

NB - In this and all subsequent illustrations, the entry composer will be coloured green when it is not resting upon its composer stop and the exit composer will be coloured red when it is not resting upon its composer stop.

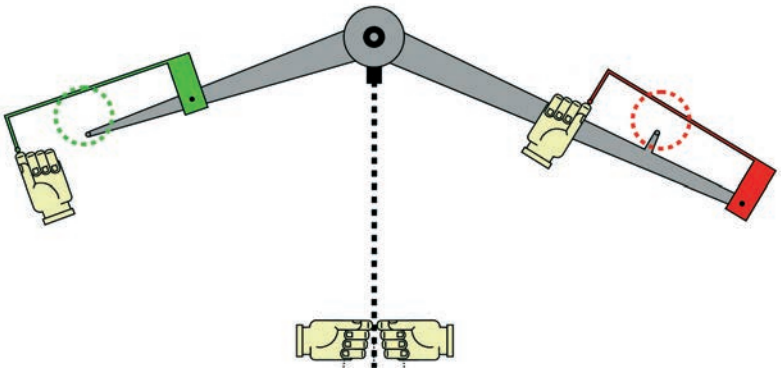

Figure 7 - Composer noses independently 'lifted'.

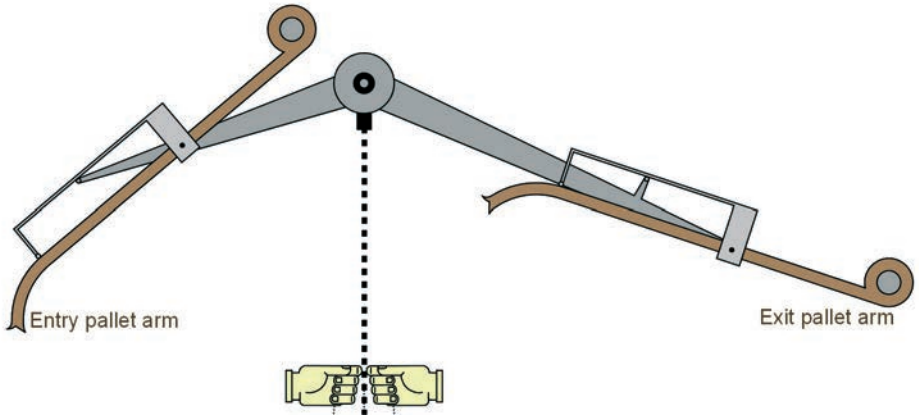

**Figure 8 - Each tail-heavy pallet arm rests against its paired composer nose.
Each more dominantly nose-heavy composer rests upon its composer stop.**

Figure 8 (above) - All previous inputs have been removed, apart from restraint of the pendulum and escapement frame. The entry and exit pallet arms, illustrated in brown, have been fitted to the entry and exit pivot pins, respectively, in their correct orientations. Recall that both pallet arms are tail heavy about their pivots and that each arm in isolation is free to rotate about its own pivot pin. The entry pallet arm is therefore constantly inclined to rotate clockwise about the entry pivot pin and, entirely independently, the exit pallet arm is constantly inclined to rotate clockwise about the exit pivot pin. **Of greatest importance to correct functioning of the escapement, the continuous clockwise torque generated by either tail-heavy pallet arm about its pivot pin is arranged to be less than the continuous anticlockwise torque independently generated by its paired, nose-heavy composer about the same pivot pin.**

On the entry side of the escapement, the clockwise torque of the tail-heavy entry pallet arm is holding the pallet arm in continuous contact with the nose of the entry composer, whilst the more dominant anticlockwise torque generated by the nose-heavy entry composer is holding the entry composer in continuous contact with the entry composer stop.

On the exit side of the escapement, the clockwise torque of the tail-heavy exit pallet arm is holding the exit pallet arm in continuous contact with the nose of the exit composer, whilst the more dominant anticlockwise torque generated by the nose-heavy exit composer is holding the exit composer in continuous contact with the exit composer stop. Observe that the behaviour of the entry pallet arm and entry composer pairing is entirely independent of the behaviour of the exit pallet arm and exit composer pairing.

Note that the anticlockwise torque generated by the mass of the illustrated escapement frame, entry pallet arm, entry composer, entry pivot pin and entry composer stop to the left of the escapement frame arbor axis will clearly fail to balance the clockwise torque generated by the illustrated mass of the escapement frame, exit pallet arm, exit composer, exit pivot pin and exit composer stop to the right of the escapement frame arbor axis. Although balance about the escapement frame arbor axis could be achieved by adding mass to the left and/or removing mass from the right, perfect balance will henceforth be assumed, but will not be illustrated. The assumption will avoid unnecessary complication.

Figure 9 (below) - The pendulum has been pushed and held stationary to the left of vertical, obliging the escapement frame, escapement frame arbor, both pivot pins, both composer stops and both resting pallet arm and composer pairings to rotate en masse clockwise about the escapement frame arbor axis, through the same angle as the pendulum. No component has moved relative to any other component. Thus, each nose-heavy composer remains at rest upon its composer stop and each tail-heavy pallet arm remains at rest against its paired composer nose.

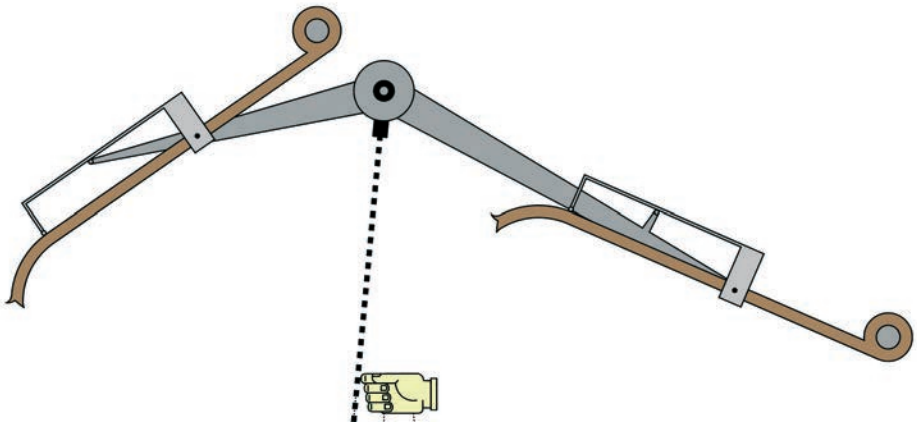

Figure 9 - Pendulum pushed and held to the left. No relative motions occur.

Figure 10 (below) - The pendulum has been pushed and held stationary to the right of vertical, obliging the escapement frame, escapement frame arbor, both pivot pins, both composer stops and both resting pallet arm and composer pairings to rotate en masse anticlockwise about the escapement frame arbor axis, through the same angle as the pendulum. No component has moved relative to any other component. Thus, each composer remains at rest upon its composer stop and each pallet arm remains at rest against its paired composer nose.

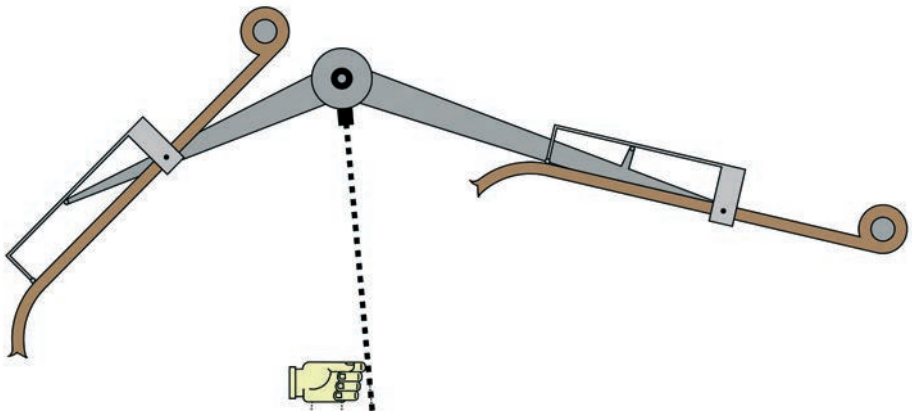

Figure 10 - Pendulum pushed and held to the right. No relative motions occur.

Figure 11 (below) - The pendulum and escapement frame are being held stationary in the illustrated position, whilst sufficient, separate forces have been applied to the nib ends of the pallet arms, in the illustrated directions. The entry pallet arm and composer pairing has rotated clockwise about the entry pivot pin and the entry composer colour has changed from light grey (when it was resting) to green (when no longer resting). Entirely independent of entry component behaviour, the exit pallet arm and composer pairing has rotated clockwise about the exit pivot pin and the exit composer colour has changed from light grey (resting) to red (not resting). Entry and exit composer lifts are highlighted by broken green and red circles, respectively. Both pallet arm and composer pairings are now independently generating continuous resistance to the applied forces.

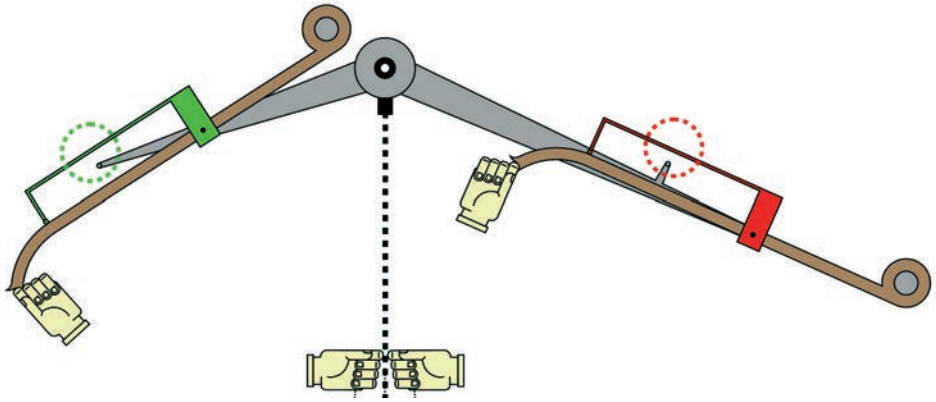

Figure 11 - Entirely independent consequences of separately lifting the nib end of each pallet arm.

Figure 12 (below) - The pendulum and escapement frame assembly is being held stationary in the illustrated position, whilst sufficient, separate forces have been applied to each pallet arm, as illustrated. The sole intention is to demonstrate the effects of reversing the forces applied in Figure 11, although the most convenient points of application and the required magnitudes of those forces will not necessarily be the same.

Clockwise torque generated about the entry pivot pin by the tail-heavy entry pallet arm has been overcome by sufficient force applied close to the entry nib, as illustrated, obliging the entry pallet arm to rotate anticlockwise about the entry pivot pin. Since the nose-heavy entry composer can rotate no further anticlockwise than its resting position, it has been left behind, resting upon the entry composer stop. Separation of the entry pallet arm from the entry composer is emphasised by a broken green circle.

Entirely independent of entry component behaviour, clockwise torque generated about the exit pivot pin by the tail-heavy exit pallet arm has been overcome by sufficient force applied to the tail end, as illustrated, obliging the exit pallet arm to rotate anticlockwise about the exit pivot pin. Since the nose-heavy exit composer can rotate no further anticlockwise than its resting position, it has been left behind, resting upon the exit composer stop. Separation of the exit pallet arm from the exit composer is emphasised by a broken red circle.

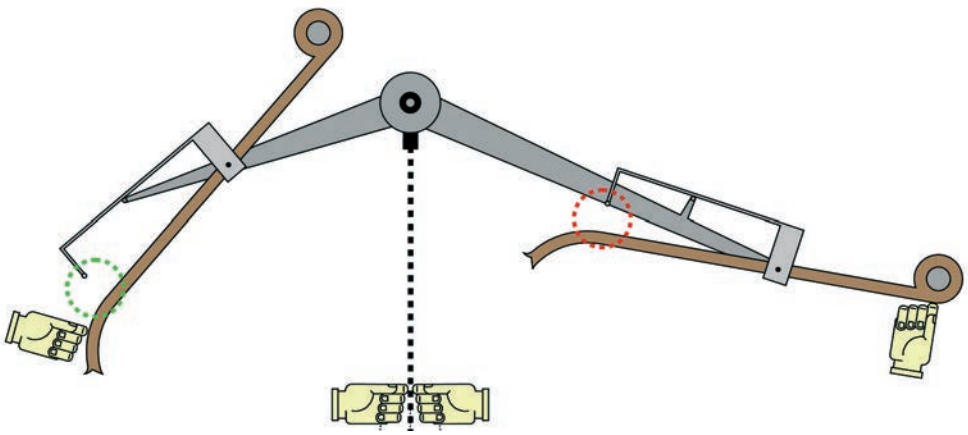

Figure 12 - Entirely independent consequences of separately lowering the nib end of each pallet arm.

STARTING THE GRASSHOPPER

Figures 13 to **19** inclusive and the accompanying text describe a proven sequence of operations for safely starting a twin pivot grasshopper escapement, beginning with an unwound movement and a stationary pendulum.

Understanding and care are essential to the avoidance of simultaneous detachment of both pallet nibs from any of the escape wheel teeth tips (referred to herein as escapement '**trip**'), permitting free-running of a driven escape wheel (referred to as escape wheel **'runaway'**). Since one of the primary purposes of any movement train is to greatly increase the number of turns of the escape wheel relative to the number of turns of the weight (or spring) barrel, a free, driven escape wheel will accelerate with likely rapidity to a no doubt considerable rotational speed. Any subsequent contact between the speeding escape wheel teeth, either pallet nib or the operator could all too easily result in damage or injury, potentially severe. Further damage or injury might also arise from the continuous fall of the driving weight, resulting in impact with the clock case and/or the operator.

Despite such potentially dire consequences of ignorance or carelessness, unfair conclusions must be avoided, for Harrison's grasshopper escapement is one of the most dependable, consistent, maintenance-free and durable mechanical escapements ever devised. **It does not, however, suffer fools at all gladly.**

Figure 13 (below) illustrates the complete escapement and a relevant portion of the escape wheel. A crossed white arrow indicates that the escape wheel is stationary, whilst a brief note confirms that no torque is being applied to the escape wheel arbor by a completely unwound movement. Until instructed otherwise, the pendulum must be stationary during start-up, as the opposing hands of our extremely small assistant currently serve to emphasise.

In the illustrated situation, with the pendulum vertical, the entry pallet nib is well clear of the escape wheel and may be ignored for now. The exit nib is, however, extremely close to, but not quite within, the circular path of the teeth tips, as highlighted by the broken red circle. In such a situation, if clockwise torque was to be foolishly applied to the escape wheel arbor by winding the timepiece, unrestrained escape wheel rotation would not be prevented by any part of the escapement and the escape wheel would 'runaway' at potentially high speed, with risk of damage and/or injury, as warned earlier.

Sufficient extension of the lower prong of the forked exit pallet nib would obstruct the path of the escape wheel teeth tips and might prevent runaway. Unfortunately, continuous, reliable cycling of the escapement relies upon adequate working clearances, which impose a limit upon the maximum length of the lower prong.

Escape wheel runaway might also be prevented during start-up by manually holding the pendulum sufficiently to the left of vertical before winding the timepiece. The entire escapement frame assembly, including the exit pallet nib, would thereby rotate clockwise about the escapement frame arbor axis, lowering the exit nib into the path of the escape wheel teeth tips. For maximum security and compliance with the correct geometry, the internal corner of the forked exit nib must be aligned with the path of the escape wheel teeth tips.

An alternative and no less secure approach to preventing escape wheel runaway during start-up would be to avoid any displacement of the illustrated, stationary pendulum and manually raise the tail of the exit pallet arm until the internal corner of the forked exit pallet nib aligned with the path of the escape wheel teeth tips. A detailed description of the entire procedure based upon such an approach accompanies Figures 14 to 19 inclusive.

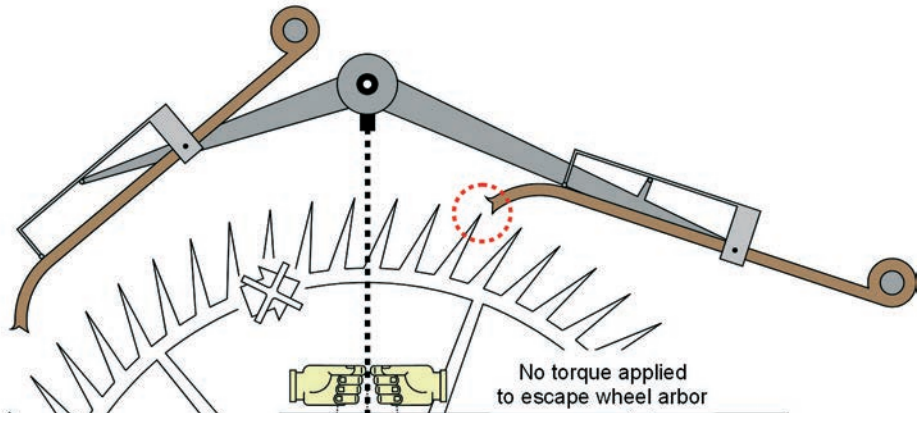

Figure 13 - Pendulum vertical. Escapement and escape wheel at rest. Unwound movement. Runaway of the illustrated escape wheel is not prevented. Do not wind the timepiece.

Figure 14 (below) - The pendulum must be stationary, until instructed otherwise, as the opposing hands of our assistant continue to emphasise. The exit pallet arm has been gently raised at the tail end and the escape wheel manually rotated (e.g. directly, or via an accessible part of the movement train) until the internal corner formed at the end of the exit nib (henceforth referred to as the exit nib **'locking corner'**) engages with an escape wheel tooth tip, as highlighted by the broken red circle. The black infill to the first engaged escape wheel tooth will serve as a useful point of reference during subsequent explanations. As the tail of the exit pallet arm is raised, the arm will separate from the resting exit composer, as highlighted by the broken orange circle. Subject to the extent of pallet arm tail weighting, escape wheel material (typically brass) and pallet nib material (see below), sufficient torque to the escape wheel will generate enough static friction between the black escape wheel tooth tip and the exit nib locking corner to hold the tail-heavy exit pallet arm in the illustrated position, even if the manual input to the tail was to be removed. This condition will henceforth be referred to as nib locking corner **'capture'**.

Pallet nibs of selected, sound, seasoned, dry hardwood are usually suitable for the intended purpose. Lower friction materials, such as metal, some plastics or naturally 'greasy' woods, such as lignum vitae, would all generate lower static friction in combination with brass escape wheel teeth tips, demanding higher escape wheel torque to achieve reliable nib locking corner capture. A potentially undesirable consequence might be a pronounced excess of energy to the pendulum during the continuous cycle of operation. For the same reasons, the pallet nibs must never be lubricated and pallet arm tail weighting should ideally be no greater than reliable operation requires.

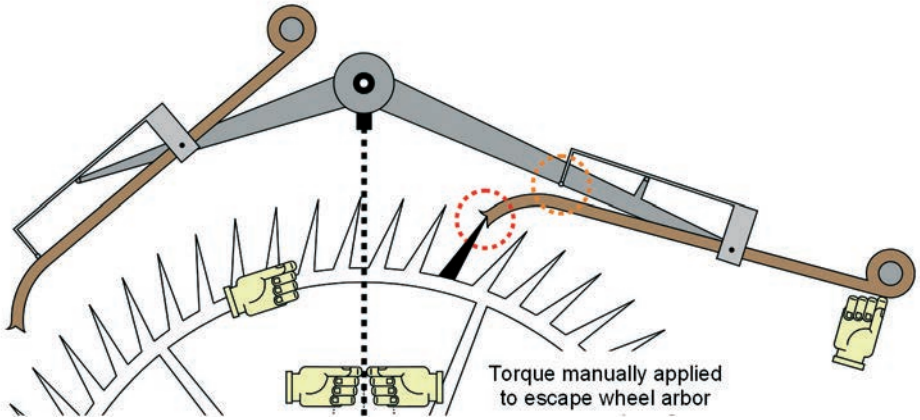

Figure 14 - Exit pallet nib locking corner manually aligned with an escape wheel tooth tip. Sufficient, continuous escape wheel torque manually applied. Exit pallet nib locking corner captured by static friction.

Figure 15 (below) - Illustrates the outcome of maintaining sufficient manual input to the escape wheel to sustain pallet nib locking corner capture, removing the manual input to the exit pallet arm, winding the timepiece and *only then* removing the manually applied torque to the escape wheel, strictly in that order. The pendulum will adopt a stationary position very slightly to the right of its free position, as illustrated, as continuous clockwise escape wheel torque is transmitted, in sequence, to the exit nib, exit pallet arm, exit pivot pin, escapement frame and pendulum, becoming anticlockwise in the process. It is absolutely vital that adequate torque to the escape wheel is continuously maintained, otherwise sufficient static friction between the captured nib locking corner and the black escape wheel tooth tip will be lost and the nib of the tail-heavy exit pallet arm will swing away from the escape wheel (escapement 'trip'), permitting potentially damaging high speed rotation of the driven escape wheel (escape wheel 'runaway').

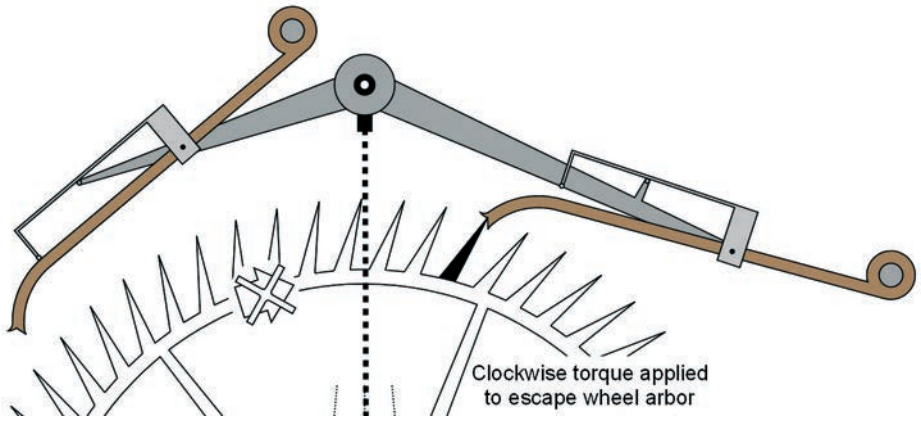

Figure 15 - Manual input to the exit pallet arm removed. Timepiece wound before manual torque removed from the escape wheel. Pendulum adopts a stationary position slightly right of its free position.

Figure 16 (below) - Illustrates a situation in which several slight, but instructive departures from Figure 15 are beginning to occur. Our assistant has pushed the pendulum very slightly to the right of the previously illustrated position and the rigidly attached escapement frame assembly has rotated very slightly anticlockwise about the escapement frame arbor axis, as indicated by the grey arrow. Slight anticlockwise rotation of the exit pivot pin about the escapement frame arbor axis induces anticlockwise rotation of the exit pallet arm about the exit pivot pin, as the captured exit nib locking corner pivots about the black escape wheel tooth tip, at the location highlighted by the small red circle. The driven escape wheel rotates slightly clockwise, as it transmits energy to the exit nib locking corner, exit pallet arm, exit pivot pin, escapement frame and pendulum, in that order. The resting entry composer and entry pallet arm pairing rotates very slightly anticlockwise about the escapement frame arbor axis, which begins to lower the entry nib towards the escape wheel.

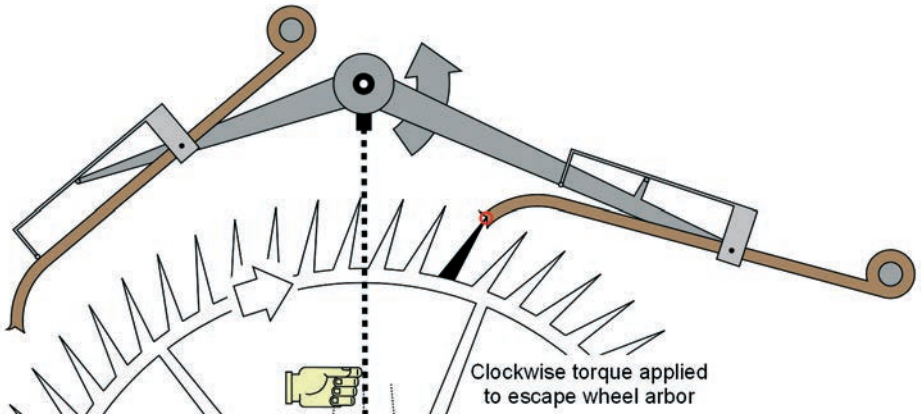

Figure 16 - Slight pendulum displacement to the right.

Figure 17 and Figure 18 (below and next page) - These separate figures represent numerous events occurring virtually simultaneously, but most clearly explained in two separate stages.

Figure 17 (below) - The pendulum has been pushed markedly further to the right, rotating the escapement frame and exit pivot pin further anticlockwise about the escapement frame arbor axis. The exit pallet arm, still captured at its nib locking corner by the black escape wheel tooth tip, must therefore rotate further anticlockwise about the exit pivot pin. The resting entry pallet nib, which has been rotating anticlockwise about the escapement frame arbor axis, has just contacted the escape wheel, as emphasised in green. The geometry must be designed such that contact between the entry pallet nib and the appropriate escape wheel tooth tip occurs precisely at the entry nib locking corner, at the exact instant the pendulum coincides with its right-hand minimum displacement marker. Contact between the entry nib locking corner and the appropriate tooth tip immediately prevents further clockwise advancement of the escape wheel. Imprecise contact between the entry nib and the engaging tooth tip (due, for example, to incorrect design, manufacture and/or set-up) would result in forbidden sliding friction between those components and might even permit escapement trip, leading to potentially damaging escape wheel runaway.

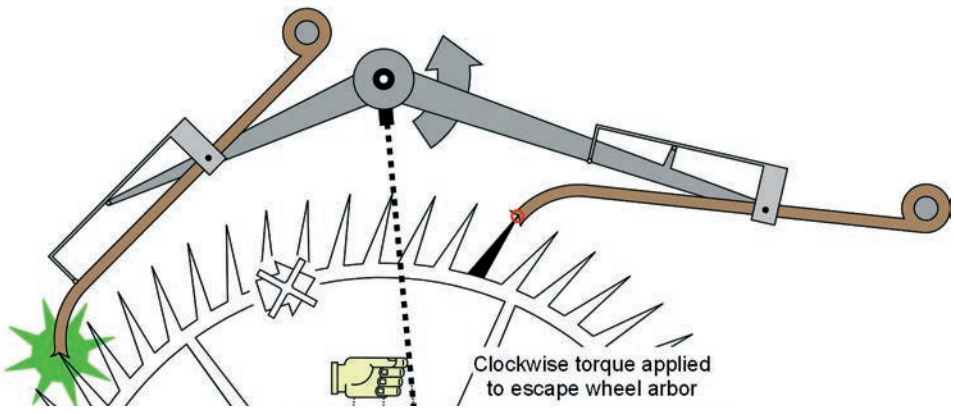

**Figure 17 - Pendulum coincides with right hand minimum displacement marker.
Entry pallet nib locking corner contacts an escape wheel tooth tip. Escape wheel halted.**

Figure 18 (below) - Virtually coincident with the events depicted in Figure 17, the pendulum has been pushed further to the right by an imperceptibly small amount. The entry pivot pin continues to rotate anticlockwise about the escapement frame arbor axis, obliging the entry pallet arm to rotate clockwise about the entry pivot pin. Such motions can only be accommodated by forcing the escape wheel into **'recoil'** (rotation in reverse) as indicated by the red arrow. As a further consequence of clockwise entry pallet arm rotation, the entry composer is imperceptibly lifted away from the entry composer stop and the illustrated entry composer colour changes from light grey to green.

At the instant recoil begins, escape wheel impulse captures the entry nib locking corner, but is removed from the exit nib locking corner. Static friction between the exit nib locking corner and the black escape wheel tooth tip is thereby lost. This is an event referred to herein as **'release'**, when a pallet nib locking corner is released from captivity by a recoiling escape wheel tooth tip. The released, tail-heavy exit pallet arm rotates freely and independently clockwise about the exit pivot pin, until it encounters the nose of the resting (light grey) exit composer. Subject to the tail weighting, inertia, travel and momentum of the exit pallet arm, the free motion and encounter could be anything from slow, gentle and virtually silent, to rapid and hard, generating an audible 'click'. In extreme cases there may be bouncing of the pallet arm upon contact, generating one or more further 'clicks' of diminishing volume, whilst a weak and/or light composer might even bounce upon its composer stop. Note carefully that, unlike common escapements such as the anchor and dead beat, the described sounds are not immediately created by contact between an escape wheel tooth tip and a pallet nib locking corner and would therefore be of limited or no value when setting the timekeeper in beat.

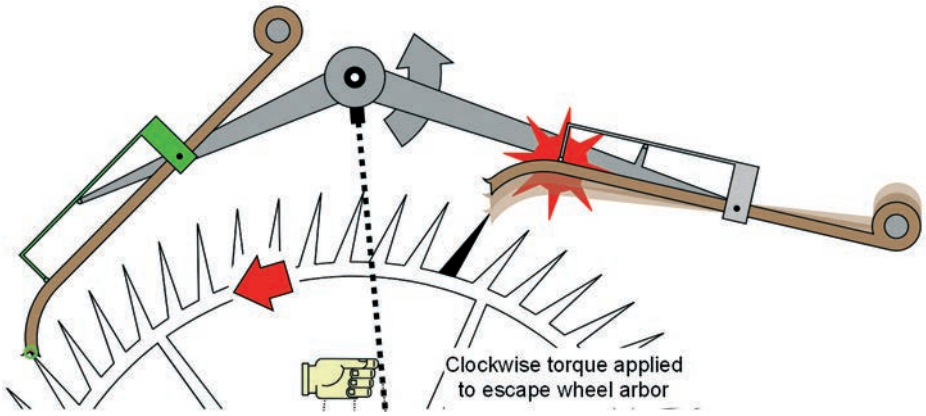

Figure 18 - Virtually coincident with Figure 17. Entry pallet nib locking corner captured. Entry composer imperceptibly lifted away from entry composer stop. Escape wheel recoil begins. Exit pallet arm released and arrested by exit composer.

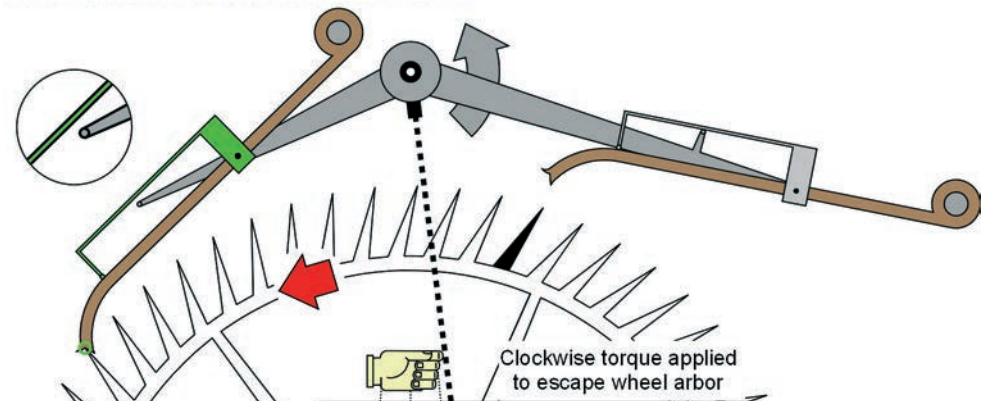

Figure 19 - Overswing to the right. Escape wheel recoil continues. Entry pallet nib still captured. Maximum recoil and entry composer 'lift' (see inset) will occur at the limit of overswing.

Figure 19 (above) - The pendulum has been pushed beyond the right-hand minimum displacement marker. This additional motion will be referred to as **'overswing'** of the pendulum and rigidly connected escapement (despite 'supplementary arc' being the accepted term). Harrison used the expression 'overplus'. It is worthy of mention that, subject to the clearances incorporated during mechanical design, excessive overswing might cause deranging and/or damaging conflicts between components during this or subsequent events.

During the illustrated pendulum overswing to the right, the entry pallet arm has been forced to rotate further clockwise about the entry pivot pin, which has lifted the entry composer further away from the entry composer stop, as clearly illustrated in the magnifying inset. As a consequence, the escape wheel has been obliged to recoil further anticlockwise.

Subject to the application of adequate overswing to the right, withdrawal of the manual input to the pendulum would represent the end of the escapement start-up procedure and the simultaneous start of continuous escapement cycling, sustained entirely by the raised driving weight (or the tensioned spiral spring) of the timekeeper.

COMPLETE CYCLE OF OPERATION

Figure 20 (below) - All manual inputs have been removed from the situation depicted in Figure 19. Clockwise torque to the pendulum is being generated by the clockwise-driven escape wheel, which is transmitting its energy to the pendulum via the captured entry nib locking corner, entry pallet arm, entry pivot pin and escapement frame, in that order. Under the combined influences of clockwise escapement torque and the Earth's gravity, the overswung pendulum, rigidly attached escapement frame, frame arbor, both pivot pins, both composer stops and the resting exit pallet arm and composer pairing are accelerating en masse clockwise about the escapement frame arbor axis. The captured entry pallet arm is therefore obliged to rotate anticlockwise about the entry pivot pin. The lifted (green), entry composer, which is moving in unison with the entry pallet arm, is also, therefore, obliged to rotate anticlockwise about the entry pivot pin, lowering the entry composer limb closer to the entry composer stop, as clearly shown in the magnifying inset. Note the position of the black escape wheel tooth, which will serve to record advancement of the escape wheel during one complete cycle of operation.

It should be mentioned that pallet arm and composer weightings will influence the delivery of impulse to the pendulum, although the effects during each escapement cycle are slight and may be ignored for the purposes of this publication.

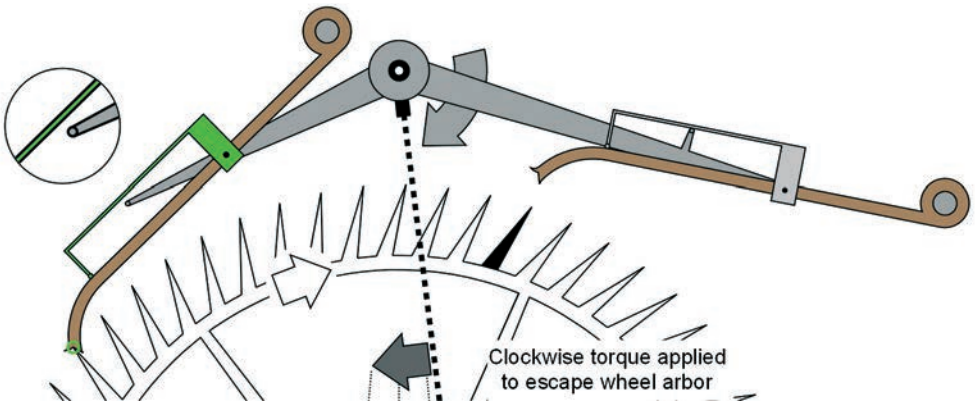

Figure 20 - No manual inputs. Returning from the limit of overswing to the right. Normal (clockwise) escape wheel rotation. Entry pallet nib locking corner impulse assists gravity, accelerating the pendulum from right to left. Decreasing entry composer lift.

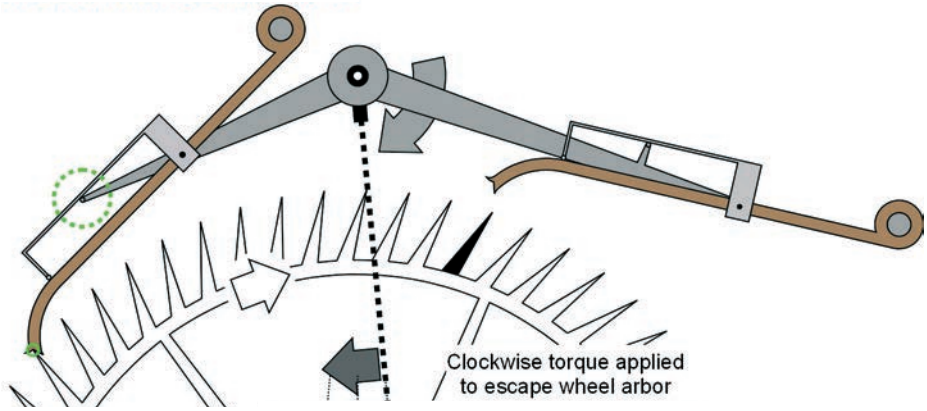

Figure 21 - Cessation of overswing to the right. Entry pallet nib locking corner impulse and gravity sustain pendulum acceleration to the left. Entry composer contacts entry composer stop.

Figure 21 (previous page) - Under the continuing influences of clockwise escapement torque and gravity, the pendulum, rigidly attached escapement frame, both pivot pins, both composer stops and the resting exit pallet arm and composer pairing are still accelerating clockwise about the escapement frame arbor axis. The pendulum is now passing through its right-hand minimum displacement marker, at the cessation of overswing to the right. At that same instant, the anticlockwise rotations of the entry pallet arm and entry composer pairing about the entry pivot pin have reached the point at which the entry composer has contacted the entry composer stop, highlighted by the broken green circle and by the illustrated entry composer colour changing from green to light grey. Entry composer arrest is normally gentle and barely, if at all, audible.

Figure 22 (below) - The pendulum is now passing through mid-swing, from right to left. The entry pallet arm continues to rotate anticlockwise about the entry pivot pin, but the entry composer has been left behind, resting upon the entry composer stop. By mid swing, the entry pallet arm has separated from the entry composer to an obvious extent, highlighted by the broken green circle. Observe that the nib of the resting exit pallet arm is swinging towards the escape wheel, as it rotates clockwise about the escapement frame arbor axis. Beyond the illustrated position, gravity will oppose escapement impulse and pendulum deceleration will begin.

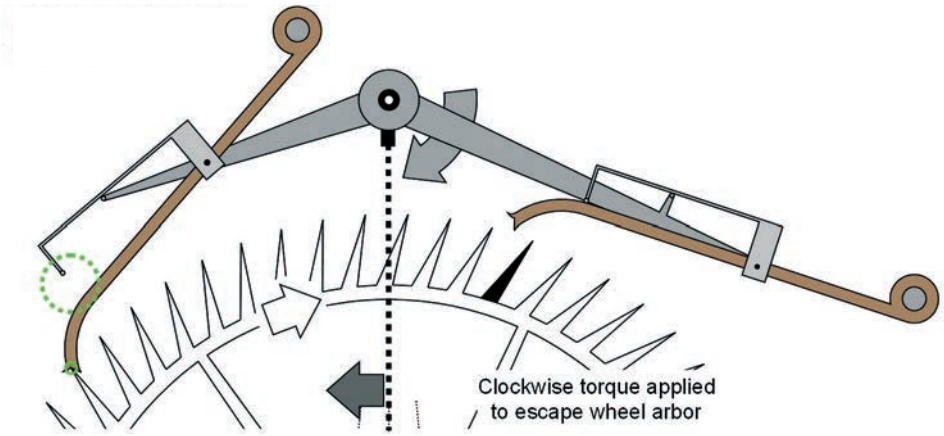

Figure 22 - Pendulum passing through mid swing. Entry pallet nib locking corner impulse continues.

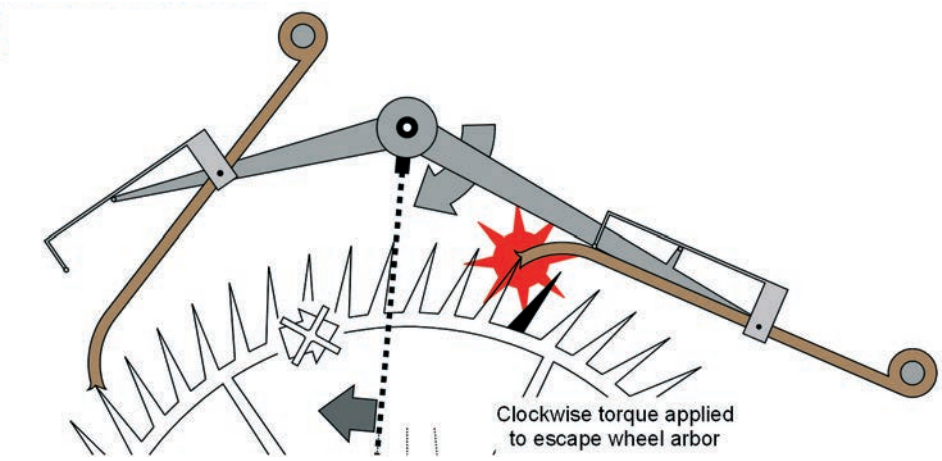

Figure 23 - Pendulum coincides with left-hand minimum displacement marker. Exit pallet nib locking corner contacts escape wheel tooth tip. Escape wheel halted. End of entry impulse.

Figures 23 (above) and Figure 24 (next page) - These separate figures represent numerous events occurring virtually simultaneously, but most clearly described in two separate stages.

Figure 23 (above) - Clockwise rotation of the exit nib about the escapement frame arbor axis has just induced contact with the escape wheel, as emphasised in red. The escapement geometry must be designed such that contact between the exit nib and an appropriate escape wheel tooth tip occurs precisely at the exit nib locking corner, at the exact instant the pendulum coincides with its left-hand minimum displacement marker. Subject to component materials and contact speed, a 'click' sound might be generated. The escape wheel is instantaneously halted and impulse to the entry pallet nib locking corner ceases. **Observe that the entry and exit pallet nib locking corners span eleven whole escape wheel tooth spaces.**

Figure 24 (below) - Virtually coincident with Figure 23, the pendulum has swung further to the left by an imperceptibly small amount. The exit nib locking corner is captured as the escape wheel is recoiled, the entry nib locking corner is thereby released and, after a brief period of free motion, the entry pallet arm is arrested by the entry composer. Subject to entry pallet arm tail weighting, inertia, travel and momentum, there may be an audible 'click' as the arm meets the composer. There may be further clicks if there is arm and/or composer bounce. The exit pallet arm and paired exit composer both begin to rotate imperceptibly clockwise about the exit pivot pin, lifting the exit composer away from the exit composer stop (illustrated exit composer changes from light grey to red). Escape wheel impulse applied to the exit nib locking corner generates anticlockwise torque about the escapement frame arbor axis, assisting gravity in decelerating the pendulum.

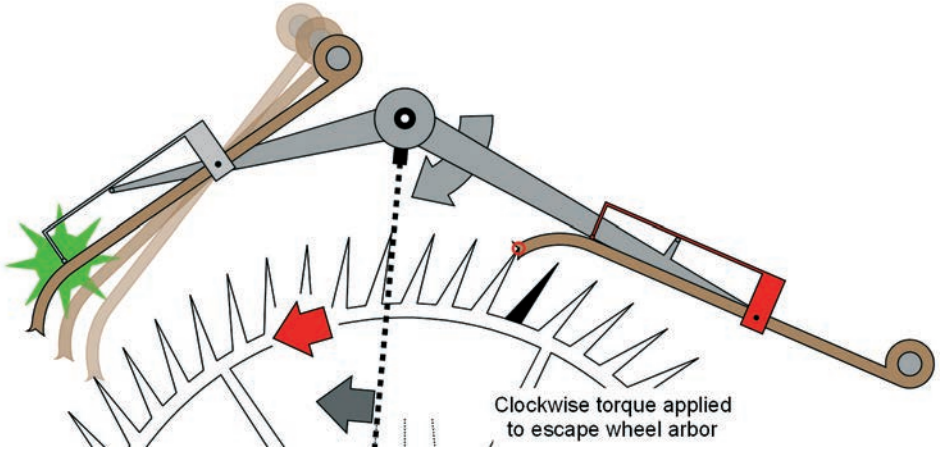

Figure 24 - Virtually coincident with Figure 23. Exit nib locking corner captured. Escape wheel recoil and exit composer lift begin. Entry pallet arm released and arrested by entry composer. Exit nib locking corner impulse and gravity decelerate the pendulum.

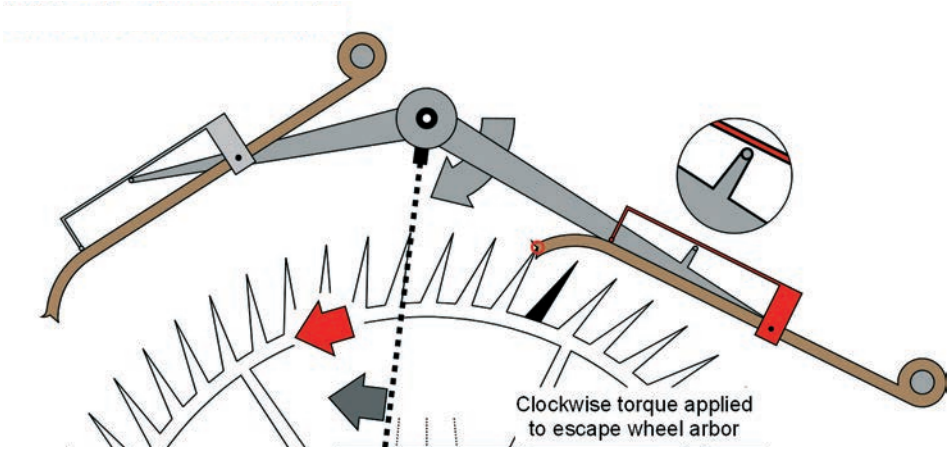

Figure 25 - Pendulum overswing to the left. Continued escape wheel recoil and exit composer lift (see inset). Exit pallet nib locking corner impulse and gravity continue pendulum deceleration.

Figure 25 (above) - Exit nib locking corner impulse and gravity continue to oppose diminishing pendulum momentum during increasing overswing to the left. Increasing exit composer lift is more clearly shown in the magnifying inset. All motions will eventually stop, for a brief instant, at the limit of overswing to the left (not illustrated, but would be adequately represented by removing all motion arrows from Figure 25). The extent of pendulum (and escapement) overswing may be adjusted by altering the driving weight (or spring), the most important objective being reliable escapement operation.

Figure 26 (next page) - Exit nib locking corner impulse and gravity combine to accelerate the pendulum to the right, as it returns from the limit of overswing to the left. The rigidly connected escapement frame therefore rotates anticlockwise about the escapement frame arbor axis. The captured exit pallet arm and the lifted exit composer rotate anticlockwise about the exit pivot pin, lowering the limb of the exit composer towards the exit composer stop, as shown in the magnifying inset.

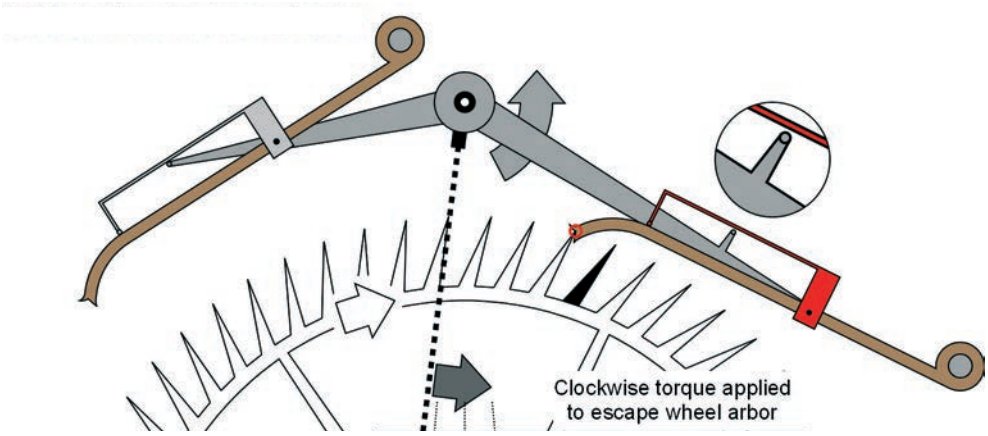

Figure 26 - Returning from overswing to the left. Normal, clockwise escape wheel rotation. Exit pallet nib locking corner impulse assists gravity in accelerating the pendulum from left to right. Lifted exit composer approaches the exit composer stop (see inset).

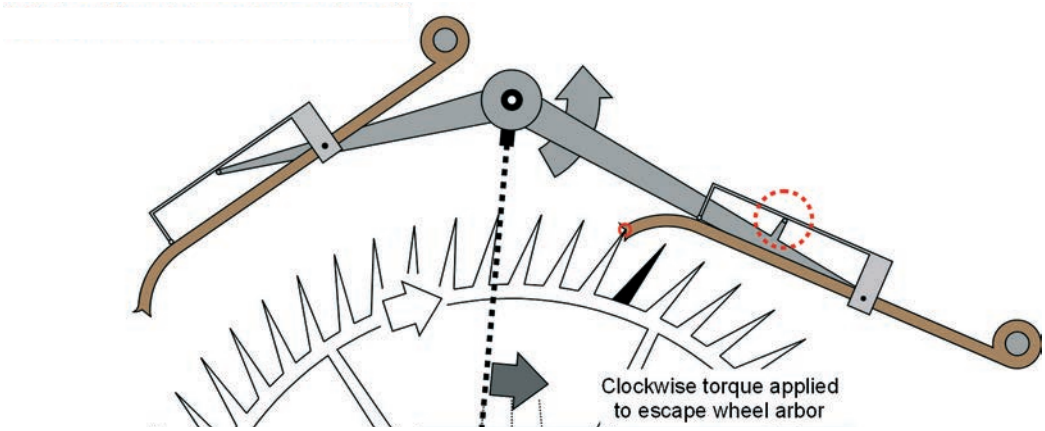

Figure 27 - Cessation of overswing to the left. Exit pallet nib locking corner impulse and gravity sustain pendulum acceleration to the right. Exit composer halted by exit composer stop.

Figure 27 (above) - The pendulum coincides with the left hand minimum displacement marker at the cessation of overswing to the left. At that exact instant, the anticlockwise rotations of the exit pallet arm and exit composer about the exit pivot pin have just reached the point at which the exit composer has contacted the exit composer stop (exit composer colour changes from red to light grey), as highlighted by the broken red circle. Exit composer arrest should be a gentle and, at most, barely audible event. The exit pallet nib locking corner is still receiving impulse from the escape wheel and is continuing to assist gravity in accelerating the pendulum to the right.

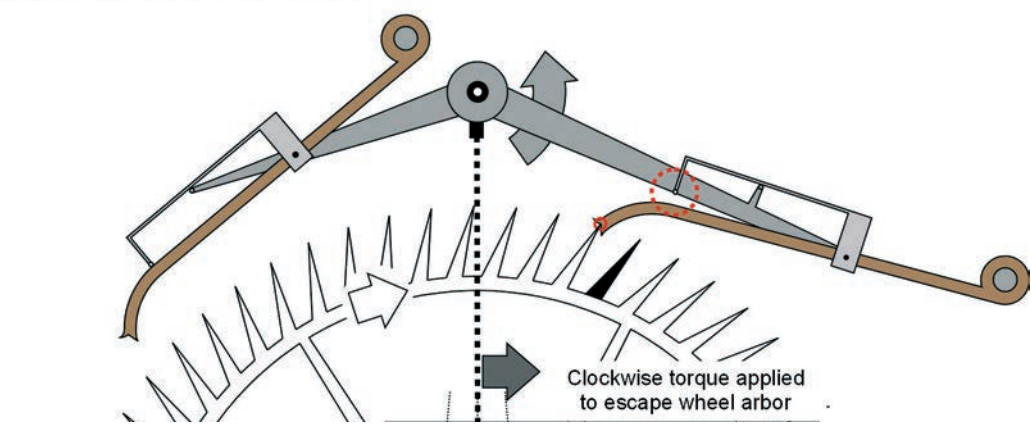

Figure 28 - Exit pallet nib locking corner impulse continues. Exit pallet arm detached from exit composer.

Figure 28 (previous page) - The exit pallet arm continues to rotate anticlockwise about the exit pivot pin, thereby breaking contact with the exit composer nose, as highlighted by the broken red circle. The exit composer is left behind, resting upon the exit composer stop. As illustrated, the pendulum is passing through mid-swing and the exit pallet arm is well clear of the composer. Observe that the nib of the resting entry pallet arm is swinging towards the escape wheel, as it rotates anticlockwise about the escapement frame arbor axis. Beyond the illustrated position, gravity will oppose escapement impulse and pendulum deceleration will begin.

Figures 29 and 30 (in sequence below) - These separate figures represent virtually simultaneous events.

Figure 29 (below) - Anticlockwise rotation of the entry nib about the escapement frame arbor axis has just induced contact with the escape wheel, as emphasised in green. The escapement geometry must be designed such that precise contact between the entry nib locking corner and an appropriate escape wheel tooth tip occurs at the exact instant the pendulum coincides with with its right-hand minimum displacement marker. Subject to component materials and speed of contact, a 'click' sound might be generated. The escape wheel is instantaneously halted and exit nib locking corner impulse ceases. **Observe that the pallet nib locking corners span twelve whole escape wheel tooth spaces.**

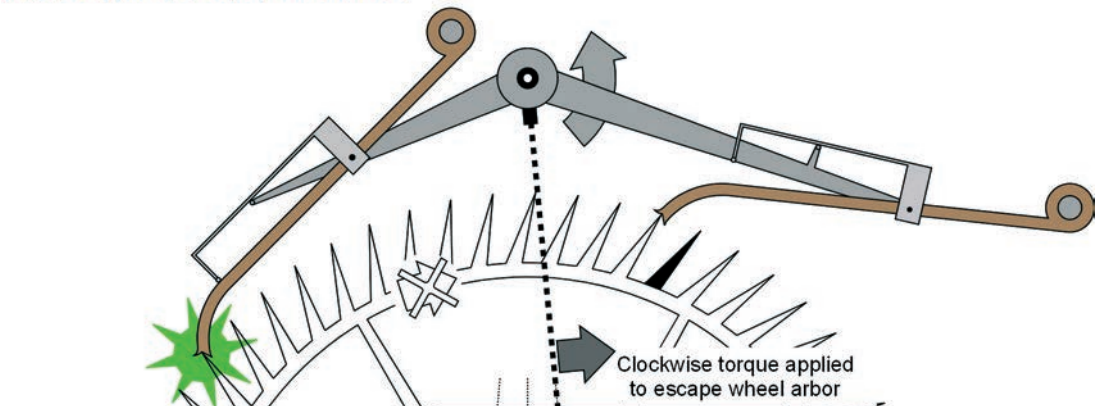

Figure 29 - Pendulum coincides with right-hand minimum displacement marker. Entry pallet nib locking corner contacts escape wheel tooth tip. Escape wheel halted. End of exit pallet nib locking corner impulse.

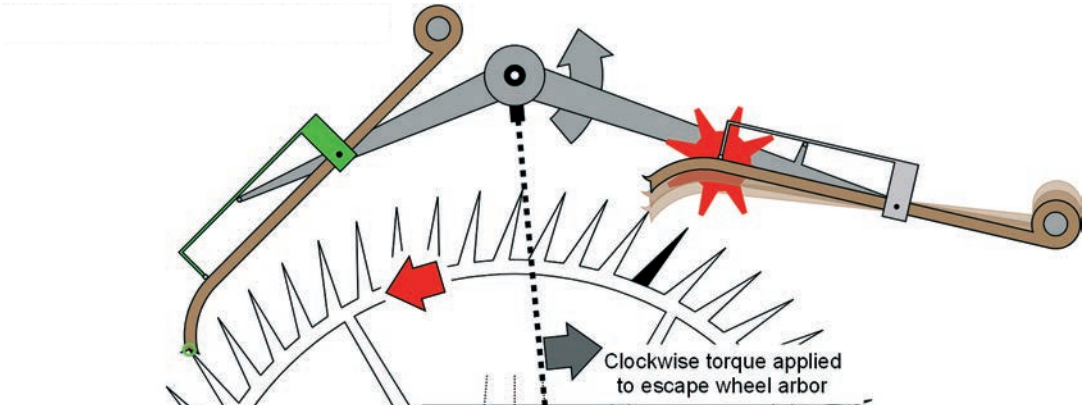

Figure 30 -Virtually coincident with Figure 29. Entry nib locking corner captured. Escape wheel recoil and entry composer lift begin. Exit pallet arm released and arrested by exit composer. Entry nib locking corner impulse and gravity combine to decelerate the pendulum.

Figure 30 (above) -Virtually coincident with Figure 29, the pendulum swings further to the right by an imperceptibly small amount. The entry nib locking corner is captured as the escape wheel is recoiled, the exit nib locking corner is thereby released and, after a brief period of free motion, the exit pallet arm is arrested by the exit composer. Subject to exit pallet arm tail weighting, inertia, travel and momentum, there may be an audible 'click' as the exit pallet arm meets the exit composer. There may be further clicks if there is arm and/or composer bounce. The entry pallet arm and paired composer begin to rotate imperceptibly clockwise about the entry pivot pin, lifting the entry composer away from the entry composer stop (entry composer colour changes from light grey to green). Escape wheel impulse to the entry nib locking corner generates clockwise torque about the escapement frame arbor axis, assisting gravity in decelerating the pendulum.

Figure 31 (below) - Entry nib locking corner impulse and gravity oppose diminishing pendulum momentum during increasing overswing to the right. Increasing entry composer lift is shown in the magnifying inset. All motions will eventually stop, for an instant, at the limit of overswing to the right (not illustrated, but would be adequately represented by removing all motion arrows from Figure 31).

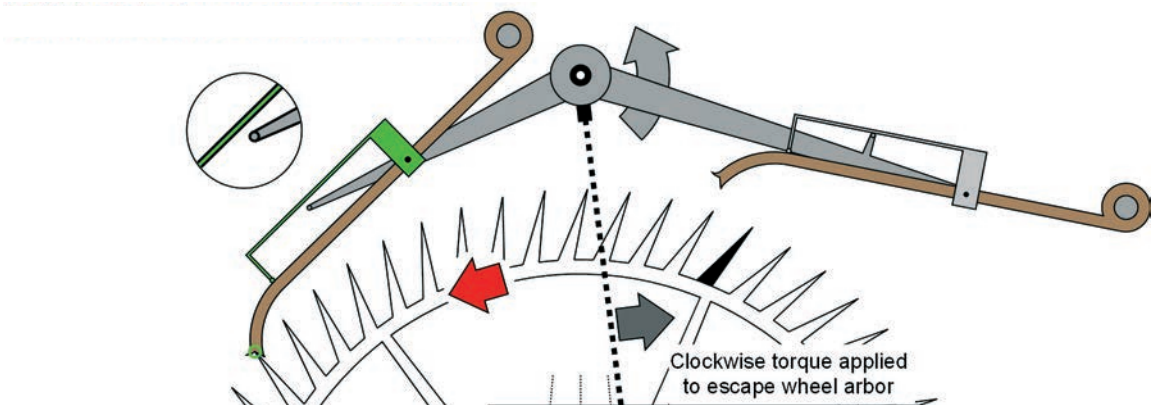

Figure 31 - Continuing overswing to the right and escape wheel recoil. Further entry composer lift. Pendulum deceleration sustained by a combination of entry pallet nib locking corner impulse and gravity.

TWO MINUTE ESCAPE WHEEL

Figures 20 to 31 inclusive illustrate one complete escapement cycle, during which the seconds beating pendulum has swung for exactly two seconds and the black escape wheel tooth has advanced clockwise by precisely one whole tooth space. The 60 tooth escape wheel has therefore rotated once in 2 x 60 = 120 seconds (i.e. two minutes).

NO SLIDING FRICTION, NO WEAR, NO LUBRICATION

A review of the described cycle of operation will confirm that at no point does sliding friction occur, apart from extremely limited rotations of the pallet arms and composers about their pivot pins. There is, therefore, no requirement that any part of the escapement be lubricated. In fact, lubrication of the pallet nibs would reduce vital static friction between captured nib locking corners and capturing escape wheel tooth tips, with potentially ruinous consequences. Furthermore, any lubricant at any of the pivots or nibs, be it modern or ancient, would suffer unavoidable alterations to its properties with age, use and exposure to its environment, with proven, potentially significant cumulative effects upon consistent timekeeping. Negligible sliding friction also generates negligible wear, which ensures negligible changes in performance. As was Harrison's bold, pioneering objective at the time of the Brocklesby Park commission, the twin pivot grasshopper escapement thereby entirely avoids all common (e.g. anchor or dead-beat) escapement problems in a typically direct and thorough fashion, by effectively eliminating their causes at source.

ESCAPEMENT MEAN SPAN

During one complete escapement cycle, the pallet nib locking corners span a minimum of eleven whole escape wheel tooth spaces (see Figure 23) and a maximum of twelve whole tooth spaces (see Figure 29). The **'mean span'** of the illustrated escapement is therefore (11 + 12) / 2 = 11.5 tooth spaces.

HARRISON'S STIPULATIONS

It is a sad and effectively universal truth that, despite almost two and a half centuries since Harrison's death, no grasshopper escapements have been described, drawn, designed or constructed in strict and simultaneous accordance with every one of his documented stipulations. As will be demonstrated shortly, however, detailed analyses of Harrison's final, 1775 manuscript and one of his surviving illustrations have revealed invaluable instructions, many of which are inarguably clear.

WRITTEN STIPULATIONS

In 1775, the year before his death, Harrison recorded many of his horological principles in a significant manuscript entitled: **'A DESCRIPTION CONCERNING SUCH MECHANISM AS WILL AFFORD A NICE, OR TRUE MENSURATION OF TIME; TOGETHER WITH SOME ACCOUNT OF THE ATTEMPTS FOR THE DISCOVERY OF THE LONGITUDE BY THE MOON: AS ALSO AN ACCOUNT OF THE DISCOVERY OF THE SCALE OF MUSICK'.** Commonly referred to as **'Concerning Such Mechanism'** or simply **'CSM'**, the manuscript includes many of Harrison's stipulations for the performance of his single pivot grasshopper escapement, relevant interpretations of which are listed below. Common sense suggests that these stipulations are no less valid for the twin pivot configuration. Stipulation numbering is arbitrary and unique to this publication.

■ **STIPULATION 1 - There must be no sliding friction and (therefore) no wear or requirement for lubrication.** This achievement was demonstrated during the earlier explanation of the twin pivot grasshopper escapement operating cycle. It is essential that variations in friction and resistance due to wear and lubricant degradation are eliminated, since they can generate significant cumulative inconsistencies in timekeeping performance.

■ **STIPULATION 2 - The mean torque arm should be one hundredth of the pendulum length.** Harrison's broad objective is that impulse be applied sensibly close to the centre of pendulum motion, thereby restricting the undesirable influence of the escapement. He is also encouraging higher impulse forces, whereby unavoidable variations are rendered a less significant proportion of the whole. Regrettably, Harrison fails to define his exact intentions for 'pendulum length', although the breadth of his objective suggests that precise implementation is by no means essential. The author considers idealised pendulum length to be a logical and sensible basis, if only because it defines a single mean torque arm for all timepieces with the same pendulum period (and, strictly speaking, the same local mean sea level acceleration due to gravity). Alternative interpretations generate illogical variations in escapement dimensions. Nevertheless, in an effort to avoid pointless and distracting controversy, the entirety of this publication will simply incorporate a mean torque arm of 10 mm (one hundredth of a metre) within final geometries, thereby complying with Harrison's broad intention. Fortunately, the incorporation of any alternative mean torque arm during the geometrical design process is extremely straightforward, as will be demonstrated in due course.

■ **STIPULATION 3 - The pendulum arc should be large, although fifteen degrees should not be exceeded.** The grasshopper escapement has an invaluable capacity to function efficiently at high escaping arcs. Put simply, Harrison's is demanding that the pendulum has 'velocity' (to borrow one of his terms), dominates the escapement and minimises the adverse effects of disturbances and variations.

■ **STIPULATION 4 - A 'long pendulum', beating seconds, should be incorporated.** See the above explanation of STIPULATION 3. Put simply, a long pendulum is more capable of meeting Harrison's demands than a short one.

■ **STIPULATION 5 - An escape wheel rotating once every four minutes should be used.** In combination with the seconds-beating pendulum of STIPULATION 4, this stipulation requires that an escape wheel of one hundred and twenty teeth be incorporated. Experience reveals that grasshopper escapement geometries are well suited to high tooth counts, whilst unavoidable, variable influences upon the necessarily high escape wheel torque are also rendered a less significant proportion of the whole

■ **STIPULATION 6 - For a summary of Harrison's instructions relating to the development of impulse during each grasshopper escapement cycle, see 'CONCLUSIONS - STIPULATION SIX' on page 29.**

CSM is ambiguous and incomplete: Harrison states: *'...let, as I order the Matter, the Force [from the Wheel] upon the Pendulum, as just before the interchanging of the Pallats, to be as by or from them the said Pallats supposed or taken as 3, then as just after their interchanging [and the Force to contrary Direction], it must be about as 2, that is, it must be so ordered [as may hereafter be observed by the Drawing] viz as that it be so by the taking, or supposing for the Purpose, a Mean betwixt the Actions of each Pallat…'.* Sadly, Harrison later declared that '…the Drawing…' and a more detailed explanation would no longer be offered, in response to poor treatment and incomplete reward by the Board of Longitude. It is considered fair to suggest that Harrison's deliberate exercise in self-sabotage committed his remarkable invention to almost two and a half centuries of effectively universal misrepresentation.

ILLUSTRATED STIPULATIONS

The following analysis will support a proposal that *'...the Drawing...'* promised in CSM (see STIPULATION SIX, above), but ultimately withheld, was created after all and that it still exists. **Figure 32** reproduces a scanned photocopy of the object in question, commonly referred to as **'MS3972/3'**. As will be demonstrated, Harrison's illustration incorporates a complete and unambiguous definition of his precise intentions for the delivery of impulse, together with invaluable clues relating to the manipulation of escaping arc.

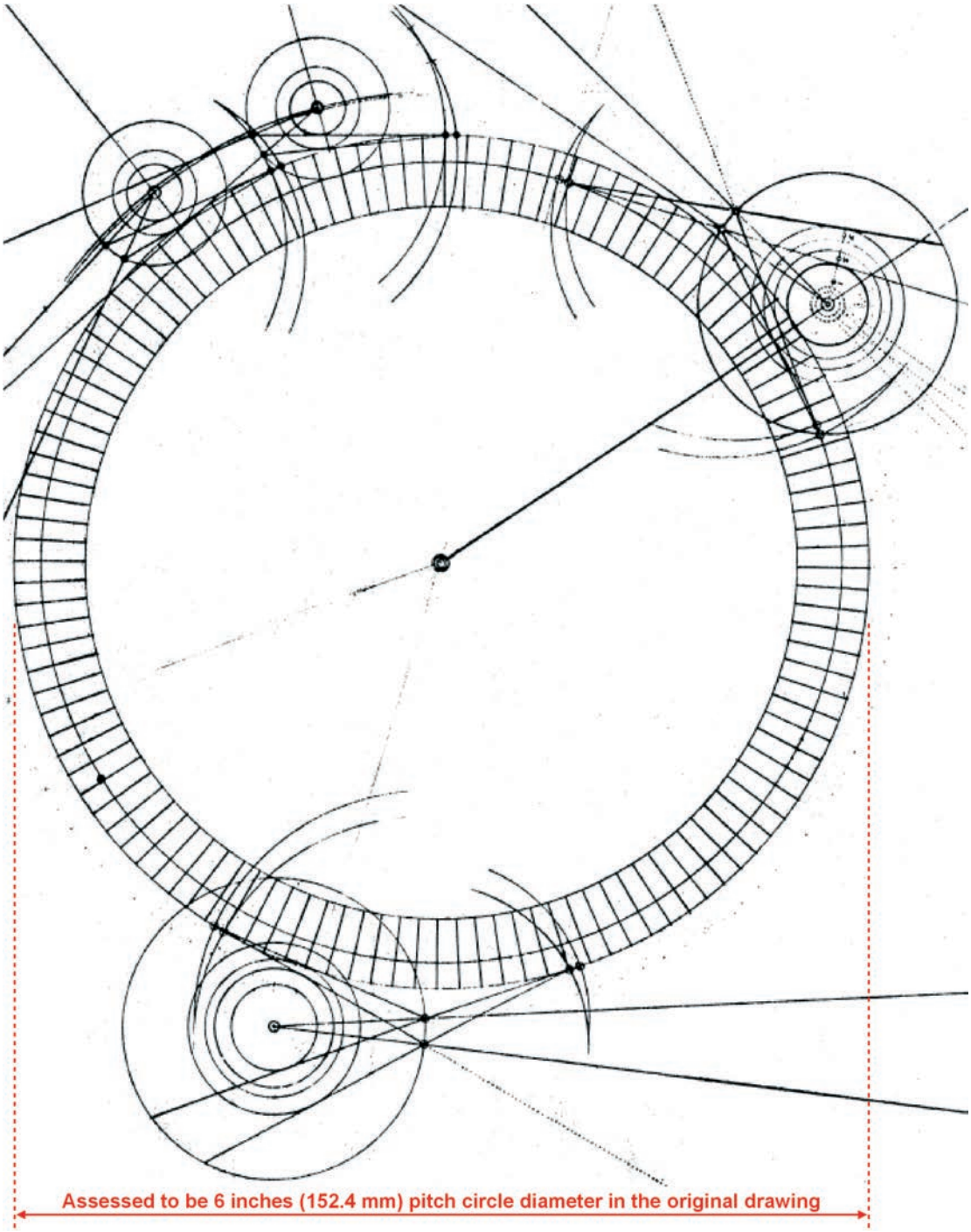

Figure 32 - MS3972/3, not to scale, edges cropped, lines and text added in red.

Alterations to MS3972/3 for the purposes of this publication are limited to scaling, slight cropping and an added dimension, in red, assessing the largest, clockwise rotating escape wheel teeth tips pitch circle diameter (PCD) to be six inches in Harrison's original illustration. A slightly smaller concentric circle defines the PCD of a second escape wheel. The innermost circle, assessed to be five inches in diameter, may be ignored. PCD intersections with one hundred and twenty equally spaced escape wheel radials define the teeth tips of either escape wheel. It is encouraging that, as stated earlier, CSM also stipulates a tooth count of one hundred and twenty (i.e. a ‘four-minute’ escape wheel, when associated with a seconds beating pendulum).

Three complete grasshopper escapement geometries are arranged around the two escape wheels. Each of the geometries simultaneously represents all start and end of impulse events during one complete cycle. Anticlockwise escape wheel recoil, overswing (supplementary arc) and instantaneous nib locking corner positions after release are irrelevant to clear definitions of any of the geometries and have not been illustrated.

■ - The closely grouped illustrations to the upper left are two compatible **'sub-geometries'**, which may be rearranged to form Harrison's **twin balance** escapement geometry, relevant to mechanically linked bar or circular balances swinging in opposition. PART TWO and part of the APPENDIX will identify Harrison's illustrated instructions and demonstrate how compatible sub-geometries may be created and combined.
■ - The illustration to the upper right is a **single pivot** grasshopper escapement geometry, spanning a mean of 17.5 escape wheel tooth spaces (17 tooth spaces minimum, 18 maximum, therefore 17.5 mean) of the smaller escape wheel. This configuration is analysed, explained and created from first principles in a separate publication, entitled 'Computer Aided Design of the Harrison Single Pivot Grasshopper Escapement Geometry' (see BIBLIOGRAPHY), modified extracts from which will be of considerable value shortly.
■ - The lower geometry is a **single pivot** grasshopper escapement geometry, spanning a mean of 16.5 escape wheel tooth spaces (16 tooth spaces minimum, 17 maximum, therefore 16.5 mean) of the larger escape wheel. It is considered likely that a comparison between this geometry and the 17.5 mean span geometry was Harrison's intended method of demonstrating how mean span and the lines of action influence the escaping arc and how mean torque arm may be controlled.

Before proceeding any further, it must be understood that MS3972/3 was almost certainly an explanatory illustration, not an accurate design drawing. Incorporated numbers and line styles (described shortly) add weight to that proposal, since they would have been of no value to Harrison, who obviously understood what he had drawn. The wide range of illustrated applications also suggests that the purpose was explanation. Not least, any competent 18th century designer faced with the task of creating accurate escapement geometries would, surely, have constructed them to a far greater scale than MS3972/3 and reduced all linear measurements arithmetically, in an effort to maximise precision. Unfortunately, all available copies of the original illustration have also, thus far, exhibited non-linear distortions. MS3972/3 measurements, be they from the original or a copy, must not, therefore, be trusted. It is, however, an inarguable certainty that *written numbers* are immune from such deficiencies, as will be demonstrated.

The **twin pivot** grasshopper escapement geometry is conspicuous by its absence from MS3972/3. The following analysis will therefore derive twin pivot stipulations from Harrison's 17.5 tooth spaces mean span **single pivot** geometry of MS3972/3, some of which are unique in their clarity, as demonstrated below.

THE 17.5 MEAN SPAN SINGLE PIVOT MS3972/3 GEOMETRY

Figure 33 reproduces the 17.5 mean tooth spaces spanned **single pivot** geometry from the upper right of Figure 32, rotated anticlockwise through approximately ninety degrees and greatly enlarged to no particular scale. Author alterations are limited to the addition of circled crosses at eleven points of intersection, Arial font labelling and a block of text, all in red. Normal escape wheel rotation is clockwise.

THE ANALYSIS AND RELEVANT GUIDANCE IS PRESENTED IN FOUR PARTS:

1 - PALLET ARMS LINES OF ACTION

Figure 33 includes four pallet arms lines of action, which define the directions of the start and end of impulse forces generated by supplied escape wheel energy during one complete cycle. Note that the magnitudes of those forces are not represented. The escapement frame arbor axis is labelled ‘Z’.

Relevant properties are as follows:

■ **(1)** - CJ represents the entry pallet arm line of action at the start of entry impulse. The compressive force, acting from J to C (and extending beyond L) at perpendicular torque arm LZ, will apply clockwise torque about Z.
■ **(2)** - DK represents the entry pallet arm line of action at the end of entry impulse. The compressive force, acting from K to D (and extending beyond M) at perpendicular torque arm MZ will apply clockwise torque about Z.
■ **(3)** - AD represents the exit pallet arm line of action at the start of exit impulse. The tensile force, acting from D to A at perpendicular torque arm FZ, will apply anticlockwise torque about Z.
■ **(4)** - BC represents the exit pallet arm line of action at the end of exit impulse. The tensile force, acting from C to B at perpendicular torque arm GZ, will apply anticlockwise torque about Z.

Ignoring recoil and pendulum overswing (which are irrelevant to this analysis), adequate torques, applied in a repeating sequence (1) - (2) - (3) - (4), would maintain the continuous motion of a pendulum.

Continues after Figure 33...

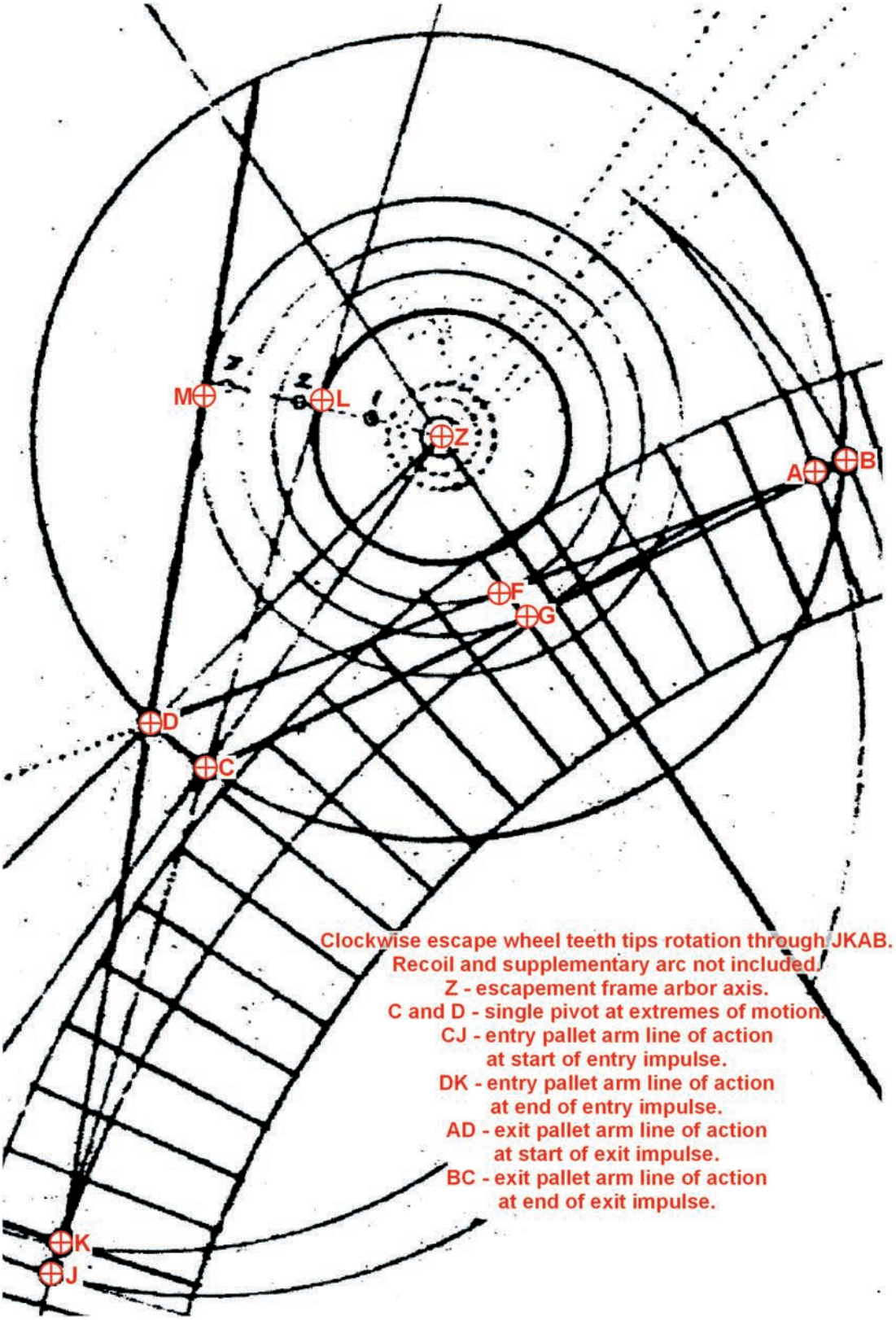

Figure 33 - MS3972/3 17.5 mean tooth spaces spanned, single pivot geometry illustration.

2 - HARRISON'S THREE NUMBERED POINTS

Harrison has inserted three separate, single-digit numbers '1', '2' and '3', arranged in that order. Each of those numbers is associated with a very small circle, all three of which lie along a common radial from the escapement frame arbor axis, Z. Very small circles such as these are a drawing convention consistently used by Harrison to define the positions of points, deemed to be located 'invisibly' at the centres of the very small circles. The three Harrison numbers are, therefore, each associated with defined points along the common radial.

With due regard for the deficiencies of the original or copied illustration, it is proposed that the adjacent separations of the points labelled 'Z', '1', '2', and '3' were intended to be equal. On that basis, if the distance from the point labelled 'Z' to the adjacent point labelled '1' is called 'd', then:

Distance Z to point 2 = 2d……... (1)

Distance Z to point 3 = 3d……... (2)

3 - TORQUE ARM CIRCLES

Harrison includes four concentric circles, referred to herein as **'torque arm circles'**, all centred at Z. The radii of the torque arm circles match the torque arms LZ, MZ, FZ and GZ, derived earlier. Their purpose is to illustrate the transference of the lengths of all four torque arms to Harrison's common radial from Z.

With due regard for the deficiencies of the original or copied illustration, it is proposed that the centre of the very small circle labelled '2' is equidistant from the two inner torque arm circles, of radii LZ and FZ, which represent the entry and exit start of impulse torque arms for one complete escapement cycle of operation. It is also proposed that the centre of the very small circle labelled '3' is equidistant from the two outer torque arm circles, of radii MZ and GZ, which represent the entry and exit end of impulse torque arms for one complete cycle.

Therefore: Distance Z to point 2 = 0.5 (LZ + FZ)……...(3)

and: Distance Z to point 3 = 0.5 (MZ + GZ)…….(4)

From (3) and (1): 0.5 (LZ + FZ) = 2d…….(5)

From (4) and (2): 0.5 (MZ + GZ) = 3d…….(6)

Therefore, from (5) and (6): (MZ + GZ) / (LZ + FZ) = 3 / 2……. (7)

4 - VARYING FORCES

The geometries of MS3972/3 are obviously incapable of representing the magnitudes of transmitted forces. Constant, equal forces are imposed, whereby torque is rendered equivalent to torque *arm*. In reality, forces within the grasshopper escapement are most certainly not constant (with the assumed exception, for the purposes of this analysis, of escape wheel delivery). An inspection of Figure 33 will confirm that, as a consequence of variations in the orientations of engaged pallet arms lines of action relative to the escape wheel, the transmitted components of force from the escape wheel inevitably alter during each complete cycle. The greater the divergence of any pallet arm line of action from tangential to the escape wheel, the greater will be the reduction in the transmitted component of *'...the Force [from the Wheel] upon the Pendulum...'*, as Harrison expresses it. Of academic interest, the force varies in proportion to the sine of the angle between the line of action and the corresponding escape wheel radial. For a geometry complying with equation (7), derived earlier, the practical consequence of such variations is that the ratio of mean end of impulse torque to mean start of impulse torque will differ from the 3 to 2 ratio of mean torque *arms* defined by that equation.

CONCLUSIONS - STIPULATION SIX

From equation (7), derived above, Harrison's stipulation, ingeniously incorporated within the MS3972/3, 17.5 mean span single pivot geometry, is that the ratio of the mean of the end of impulse torque arms to the mean of the start of impulse torque arms (referred to herein as the 'mean end/start ratio', T) should be exactly 3 to 2. This is a precise and unambiguous interpretation of the CSM statement *'...a Mean betwixt the Actions of each Pallat...'*.

CSM includes Harrison's honest acknowledgement of the influence of varying forces. By stipulating a ratio of 3 to *'about as 2'* for '*…the Force [from the Wheel] upon the Pendulum...'*, Harrison is acknowledging that there are differences between his drawn geometries and escapements constructed in accordance with them. In none of his known manuscripts or illustrations does Harrison propose that any allowances for varying forces be made. He was apparently content to design his escapement on the basis of forces assumed to be constant.

MS3972/3 SINGLE PIVOT GEOMETRIES ESCAPING ARC

Based upon measurement, with due regard for the identified deficiencies of the original or copied MS3972/3 escapement illustrations, it is estimated that both single pivot geometries incorporate an escaping arc of 9.75 degrees.

MS3972/3 SINGLE PIVOT GEOMETRIES LINES OF ACTION

With continuing regard for the identified deficiencies of Harrison's MS3972/3 escapement illustrations, it would appear that all single pivot geometry entry pallet arm lines of action at the start of impulse are tangential to the escape wheel PCD. It is, however, possible that the exit lines of action at the start of impulse deviate slightly from tangential in both geometries. It is considered especially relevant that Harrison highlighted long extensions to the exit lines of action at the start of exit impulse in both geometries, painstakingly drawing each as a series of closely spaced dots. It is, surely, unlikely that such emphasis and time consuming drawing effort would have been included and expended to no purpose. In support of that conclusion, investigations have confirmed that alterations to the orientation of the exit pallet arm line of action at the start of exit impulse may be used to manipulate the escaping arc of *any* configuration of Harrison's grasshopper escapement. Detailed guidance will be offered in the latter stages of the twin pivot grasshopper escapement geometry design process, presented shortly

CSM, MS3972/3 AND THE TWIN PIVOT GEOMETRY

To summarise earlier proposals before proceeding further, it will be assumed that Harrison's written and illustrated stipulations for the **single pivot** grasshopper escapement, now clearly identified within CSM and MS3972/3, may be applied to the **twin pivot** configuration. The remainder of PART ONE is offered on that basis.

GEOMETRICAL REPRESENTATION

Figure 34 overlays semi-transparent representations of physical twin pivot escapement components, in brown and grey, with a complete twin pivot escapement geometry and escape wheel PCD, in green, red and orange.

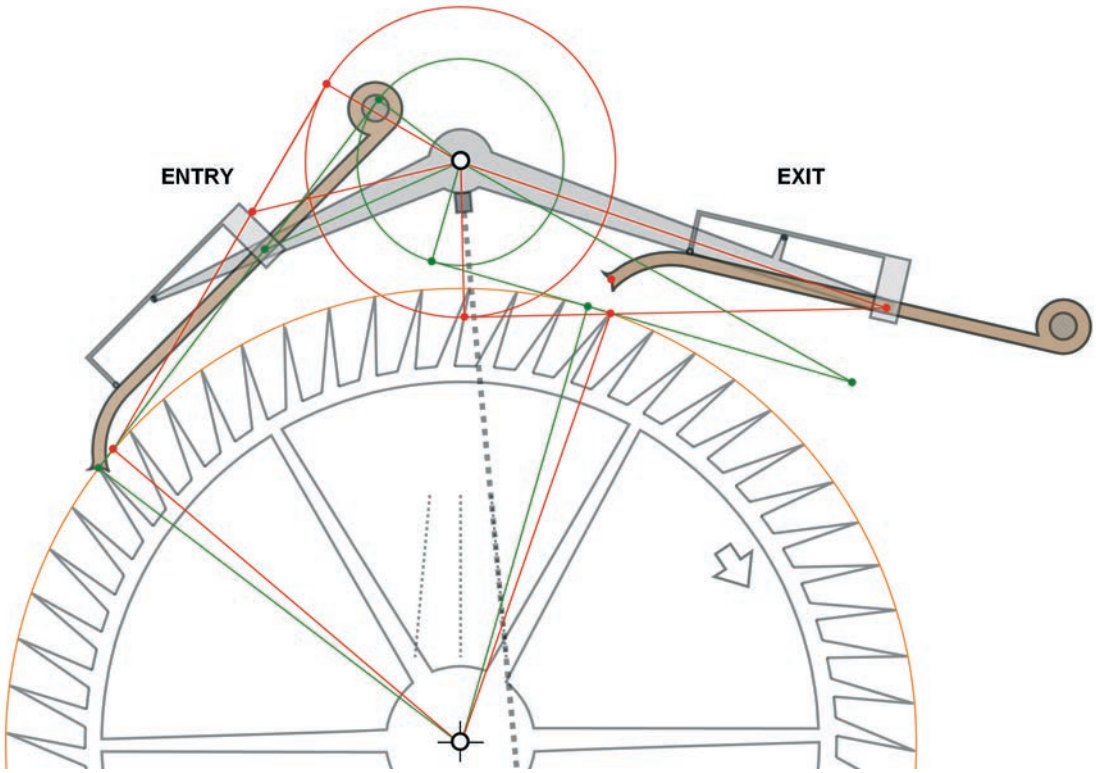

Figure 34 - Twin pivot grasshopper escapement geometry with an overlay of physical components.

A combination of every one of the situations depicted in Figures 20 to 31 is represented in the geometry of Figure 34, with the exceptions of pendulum overswing and escape wheel recoil, which are irrelevant to the creation or definition of a grasshopper escapement geometry. Green geometrical constructions represent start of impulse events and red geometrical constructions represent end of impulse events. The influence of the composers upon the pallet nib locking corners is not illustrated, but will be evaluated at the end of the geometrical design process, when instantaneous pallet nib lifts after release are determined.

SYMMETRICAL ENTRY VERSUS EXIT TORQUE ARMS

Intentional and extremely influential features of Figure 34 are two concentric **'torque arm circles'** (one green and one red) centred at the escapement frame arbor axis, to which appropriate pallet arm lines of action are tangential. Such an escapement geometry will generate perfectly symmetrical entry versus exit start and end of impulse torque arms during each complete escapement cycle. As will be appreciated shortly, the deliberate incorporation of only two torque arm circles is also an enabling feature of the devised twin pivot design technique. In contrast, Harrison's single pivot geometry, which (infinity aside) can only ever incorporate four separate torque arm circles, will always generate asymmetrical entry versus exit torque arms. Of considerable significance, in none of his manuscripts or illustrations does Harrison claim, or even suggest, that asymmetrical torque or torque arms are *essential*, or that symmetrical torque or torque arms *must be avoided*. Harrison merely states (without explanation or proof) that asymmetry is of no consequence. It may therefore be concluded that the incorporation of symmetrical entry versus exit torque arms is perfectly acceptable.

COMPUTER AIDED DESIGN OF THE TWIN PIVOT GEOMETRY

The devised twin pivot grasshopper escapement design technique is exceptionally well suited to the use of Computer Aided Design (CAD) software. Detailed instructions, explanations and illustrations enable the creation and verification of entire twin pivot grasshopper escapement geometries in simultaneous compliance with every one of Harrison's currently identified stipulations, or any chosen variations. Of particular value is a unique capacity to manipulate escaping arc whilst simultaneously maintaining any chosen end/start ratio. By virtue of that unequalled combination and superior flexibility, less capable mathematical methods are rendered entirely obsolete.

COMPUTER HARDWARE AND CAD SOFTWARE

Adequate drawing precision was assured by the use of inexpensive IMSI TurboCAD Deluxe 15 Computer Aided Design (CAD) software, nevertheless capable of claimed resolutions of ten decimal places. In practice, TurboCAD is slightly inconsistent at the higher decimal paces, although no meaningful consequences have been identified. The software includes a 'Help' function and tutorials, enabling advancement from CAD novice to the necessary level of competence within a few hours. A seven year old AMD Sempron 3000+ computer and twelve year old Windows 2000 Pro operating system completed all tasks at acceptable speeds. Expensive hardware and software is, therefore, clearly not essential. The only significant problem is a tendency for curves, circles, text and small circular points to distort and/or become displaced during transfer to *publishing* software. Despite extensive corrective effort, minor remnants remain.

DRAWING SEQUENCE OVERVIEW

■ The CAD design sequence largely consists of **'STEPS'**, numbered **ONE** to **SEVEN**, which simultaneously incorporate any designer-chosen end/start ratio, in addition to all other designer choices, apart from a chosen, balanced (entry = exit) escaping arc and a chosen mean torque arm.
■ Of particular relevance to STEPS FIVE and SIX, a separate APPENDIX describes invaluable properties of the twin pivot escapement geometry in far greater detail than could sensibly be incorporated within the CAD design sequence.
■ Near the end of the design process, the incorporation of a chosen, balanced escaping arc requires the construction of additional geometries and graphical interpolation.
■ The designer-chosen mean torque arm is then incorporated by adjusting all linear dimensions (but no angles) to a common scale, easily and speedily achieved using the CAD scaling function.
■ A determination of entry and exit pallet nib lifts after release (assumed to be instantaneous) completes the design process.

DESIGNER CHOICES

In preparation for the creation of a complete twin pivot geometry, the designer must choose the following:

■ **The CAD resoultion.** Subject to the software in use, CAD linear and angular resolutions may require selection by the designer. Maximum resolution is suggested. Ten decimal places will be used for the example.
■ **The total number of escape wheel teeth.** Directly or indirectly, MS3972/3 and CSM illustrate or stipulate 120 teeth for the single pivot geometry, which will be adopted for the twin pivot example.
■ **The mean number of tooth spaces spanned by the entry and exit pallet nib locking corners during each complete escapement cycle.** An escapement spanning a mean of 17.5 tooth spaces (17 minimum, 18 maximum, therefore 17.5 mean) will be created for the example. BALANCED ESCAPING ARC ADJUSTMENT (page 41) explains how the optimum mean span may be identified, using the CAD design sequence.
■ **The angle clockwise from the entry pallet arm line of action at the start of entry impulse to the escape wheel radial at the start of entry impulse.** This angle, illustrated in CAD STEP ONE (Figure 35 on page 33), will be referred to as the **'entry angle'** or **'an'**. In accordance with the assessment of MS3972/3 presented earlier, ninety degrees (entry start of impulse line of action tangential to the escape wheel) will be used for the example.
■ **The *initial* angle anticlockwise from the exit pallet arm line of action at the start of exit impulse to the escape wheel radial at the start of exit impulse.** This angle, illustrated in CAD STEP ONE (Figure 35 on page 33), will be referred to as the **'exit angle'** or **'ax'**. Prompted by MS3972/3, ninety degrees (exit start of impulse line of action tangential to the escape wheel) will initially be used for the example. The designer's initial choice of exit angle will almost certainly be altered slightly during the incorporation of the designer-chosen escaping arc.
■ **The target end/start ratio, 'T' of the geometry.** Although any designer-chosen end/start ratio may be incorporated, a ratio of 3 to 2 will be assumed, in compliance with Harrison's MS3972/3 instruction for his single pivot grasshopper escapement.
■ **The mean torque arm, 'M'.** A target of 10 mm will be adopted for the example. Regardless of all possible interpretations of Harrison's vague CSM stipulation for mean torque arm, 10 mm complies with his broad intention, as explained earlier. For the purposes of explanation, the choice is by no means critical. Alteration requires nothing more than an appropriate scaling of all linear dimensions (but no angles), using the CAD scaling function.
■ **The escaping arc.** For a pendulum centre of motion coincident with the escapement frame arbor axis, the minimum theoretical pendulum arc for correct functioning is equal to the escaping arc. For this example, an arc of 9.75 degrees will be the chosen target, in agreement with the assessed, apparently matching arcs of Harrison's two MS3972/3 single pivot geometries.
■ **The escaping arc resoultion.** To avoid unnecessary expenditure of time and effort, the designer should choose the minimum number of decimal places to which the balanced escaping arc should be determined.

DRAWING CONVENTIONS AND SUGGESTIONS

■ Numbers thus [NN] in the text refer to identical numbers [NN] in the illustrations.
■ **Essential CAD instructions are in bold font**. Most of the remaining text is mere amplification, explanation, suggestions or points of interest, all of which may be completely ignored, if so desired, without affecting the design process or the outcome.
■ Experience suggests that more straightforward CAD construction and fewer mistakes should result if a geometry is drawn 'lying on its side', rather than upright. All CAD illustrations herein are drawn thus. Upon completion of all CAD constructions and operations, the geometry may, if considered necessary, be rotated in its entirety until the escapement frame arbor axis is vertically above the escape wheel arbor axis, as it would be in a movement train.
■ In all relevant illustrations, **green indicates fresh start of impulse constructions, red indicates fresh end of impulse constructions and orange indicates fresh common (neither start nor end of impulse) constructions.** Other colours, **such as blue, will be used to emphasise especially relevant prior constructions,** with the exception of **various shades of grey, which are merely 'ghosts' of less relevant prior constructions**. Take care to avoid any confusion with an earlier PART ONE colour convention, which illustrated twin pivot entry and exit composers in green and red, respectively, whenever they were not in their resting positions.
■ Designers may wish to copy the labels used in the CAD sequence to their own CAD constructions, until sufficient familiarity with the geometry and design process renders them unnecessary.
■ Normal escape wheel advancement is clockwise.
■ Recoil and supplementary arc are irrelevant to the creation of a geometry and are not included.
■ Composers are, in the main, not represented. Their influence will be acknowledged near then end of the design process, when instantaneous entry and exit pallet nib locking corner lifts after release are determined.
■ All figures, CAD or otherwise, should be regarded as illustrative and not to scale.
■ All lines are straight and all curves are segments of circular arcs, unless stated otherwise.
■ All dimensions are millimetres or degrees.

STEP ONE - Figure 35

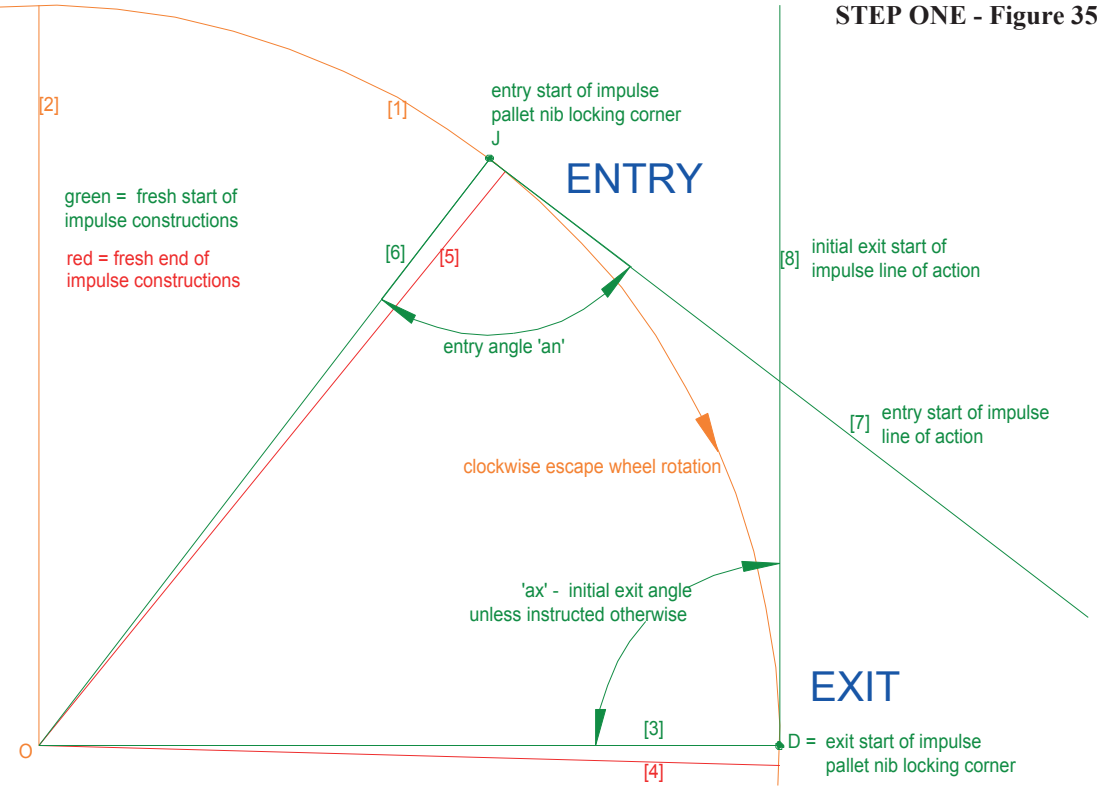

■ **[1] - Construct a circular arc (shown in orange) of an arbitrary radius, with an orientation and approximate extent as illustrated above.** Arc [1] is part of the escape wheel pitch circle, around which the tips of all escape wheel teeth must travel. A radius of 100 mm was chosen for this example.

■ **[2] - Construct a vertical line (shown in orange), of any convenient length, upwards from the centre of arc [1].** This line, in combination with the next construction, will emphasise the escape wheel arbor axis, O.

■ **[3] - Construct a horizontal line (shown in green) starting from the centre of arc [1], extending to the right as far as the arc.** The intersection of line [3] with arc [1] is labelled D. At the start of exit impulse, the exit pallet nib locking corner is captured by an escape wheel tooth tip located at point D.

■ **[4] - Construct a radial (shown in red) from the centre of arc [1], clockwise from line [3] by the angle subtended by half an escape wheel tooth space.** For the illustrated 120 tooth escape wheel, half an escape wheel tooth space between [3] and [4] subtends an angle of (360/120) / 2 = 1.5 degrees. The purpose of this construction will become clear in STEP THREE.

■ **[5] - Construct a radial (shown in red) from the the centre of arc [1], anticlockwise from line [3] by the angle subtended by the minimum span of the entry and exit pallet nib locking corners.** For the example, the minimum span is 17 tooth spaces, which subtends an angle of (17 x 360 / 120) = 51 degrees between lines [3] and [5]. The purpose of this construction will become clear in STEP THREE.

■ **[6] - Construct a radial (shown in green) from the the centre of arc [1], anticlockwise from line [4] by the angle subtended by the maximum span of the entry and exit pallet nib locking corners.** For the example, the maximum span is 18 tooth spaces, which subtends an angle of (18 x 360 / 120) = 54 degrees between lines [4] and [6]. The intersection of line [6] with arc [1] is labelled J. At the start of entry impulse, the entry pallet nib locking corner is captured by an escape wheel tooth tip located at point J.

■ **[7] - Construct a line (shown in green) from point J at the designer-chosen entry angle, 'an', to radial [6].** For this example, the entry angle is 90 degrees. Line [7] is the entry pallet arm line of action (i.e. direction of transmitted force) at the start of entry impulse.

■ **(8) - Construct a line (shown in green) from point D at the initial designer-chosen exit exit angle, 'ax', to line [3], unless a different exit angle is specified.** For this example, an initial exit angle of 90 degrees is illustrated. Line [8] is the initial exit pallet arm line of action at the start of exit impulse.

STEP TWO - Figure 36

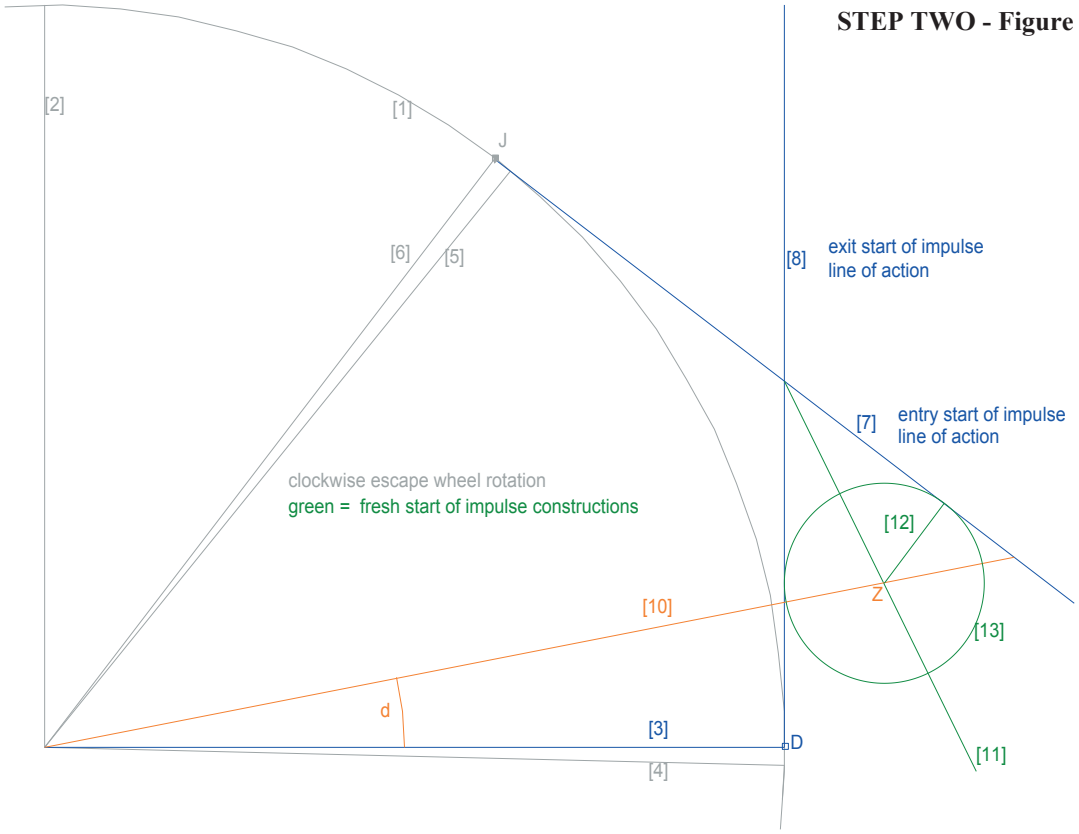

STEP TWO creates fresh start of impulse constructions in green and fresh general constructions in orange. Lines [7] and [8] from STEP ONE are emphasised in blue, rather than their original green, because they are especially relevant to STEP TWO and are therefore worthy of emphasis, but are not fresh constructions. Less relevant STEP ONE constructions are reproduced in grey. An understanding of this convention will be assumed throughout the remainder of this publication.

■ **[10] - Construct a radial (shown in orange) from the centre of arc [1], anticlockwise removed from the exit start of impulse radial [3] by angle 'd'. A first execution of STEP TWO will require that the choice of angle 'd' be arbitrary, provided that line [10] is clockwise removed from the intersection of the entry and exit start of impulse lines of action, labelled [7] and [8].** The latter condition should ensure that a twin pivot configuration emerges from the CAD design sequence. A first, arbitrary angle 'd' of eleven degrees is illustrated above. Later operations will identify and instruct the incorporation of specific values of angle 'd'.

■ **[11] - Construct a line (shown in green) from the intersection of lines [7] and [8], which bisects the acute angle between lines [7] and [8].** The intersection of line [11] and line [10] is labelled 'Z'. For the incorporated angle 'd', point Z is the corresponding location of the escapement frame arbor axis.

■ **[12] - Construct a perpendicular to line [7] (shown in green), terminating at Z.** Recall from STEP ONE that line [7] is the entry pallet arm line of action at the start of entry impulse. Line [12] is therefore the torque arm of the entry pallet arm at the start of entry impulse, acting about the escapement frame arbor axis, Z.

■ **[13] - Construct a circle (shown in green), centred at Z, of radius equal to the length of line [12].** For the constructed location of Z, circle [13] is the start of impulse torque arm circle, to which line [7] is tangential.

Since Z, at the centre of torque arm circle [13], lies along bisecting line [11], line [8] must also be tangential to circle [13]. Recall from STEP ONE that line [8] is the exit pallet arm line of action at the start of exit impulse. The torque arm of the exit pallet arm at the start of exit impulse is therefore identical to the torque arm of the entry pallet arm at the start of entry impulse. The constructed location of Z thereby satisfies the requirement, declared earlier in SYMMETRICAL ENTRY VERSUS EXIT TORQUE ARMS (page 31), that the escapement should incorporate symmetrical entry versus exit start of impulse torque arms.

OPTIONAL CHECKS FOR CARELESS ERRORS

The geometry could, if so desired, be checked for careless errors, before proceeding further. See CHECKING GEOMETRIES, offered on page 43, completing whichever checks are relevant to the constructions created thus far. Checking may be repeated any number of times, at any stage of the CAD design process. No further reminders will be offered.

STEP THREE - Figure 37

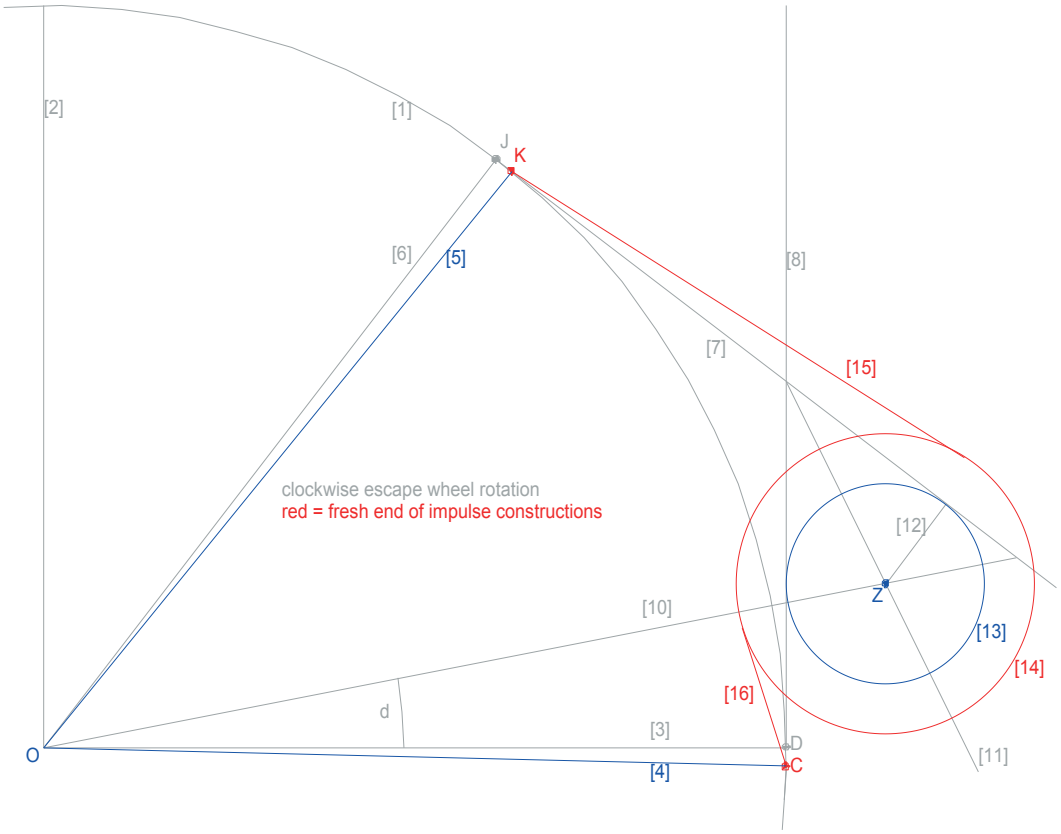

STEP THREE creates fresh entry and exit **end** of impulse constructions. all illustrated in red.

■ The intersection of arc [1] and radial [5] is labelled K. Point K is the location of the captured entry nib locking corner at the end of entry impulse, an immeasurably brief instant before release.

■ The intersection of arc [1] and radial [4] is labelled C. Point C is the location of the captured exit nib locking corner at the end of exit impulse, an immeasurably brief instant before release.

■ **[14] - Construct a circle (shown in red), centred at Z, of radius equal to the radius of circle [13] multiplied by the designer-chosen end/start ratio, T.** Circle [14] is the end of impulse torque arm circle. For this particular example T = 3 / 2. The radius of end of impulse torque arm circle [14] is therefore the radius of the start of impulse torque arm circle [13] multiplied by 3 / 2. As a CAD alternative to calculation for a ratio of 3 / 2, the radius of circle [14] is the length of radial [12] extended by half of its length.

■ **[15] - Construct a tangent to circle [14] (shown in red), from point K.** Line [15] defines the entry pallet arm line of action at the end of entry impulse an immeasurably brief instant before entry nib locking corner release.

■ **[16] - Construct a tangent to circle [14] (shown in red), from point C.** Line [16] defines the exit pallet arm line of action at the end of exit impulse an immeasurably brief instant before exit nib locking corner release.

Since the entry and exit end of impulse lines of action are both tangential to the end of impulse torque arm circle [14], the torque arm of the entry pallet arm at the end of entry impulse will be identical to the torque arm of the exit pallet arm at the end of exit impulse. This satisfies the requirement, declared earlier in SYMMETRICAL ENTRY VERSUS EXIT TORQUE ARMS (page 31), that the escapement should incorporate symmetrical entry versus exit end of impulse torque arms.

To summarise the combined outcome of STEPS TWO and THREE, it has been ensured that the constructed escapement will deliver equal entry versus exit start of impulse torque arms and equal entry versus exit end of impulse torque arms. The entry end/start ratio and mean torque arm will thereby be identical to the exit end/start ratio and mean torque arm, respectively.

STEP FOUR - Figure 38

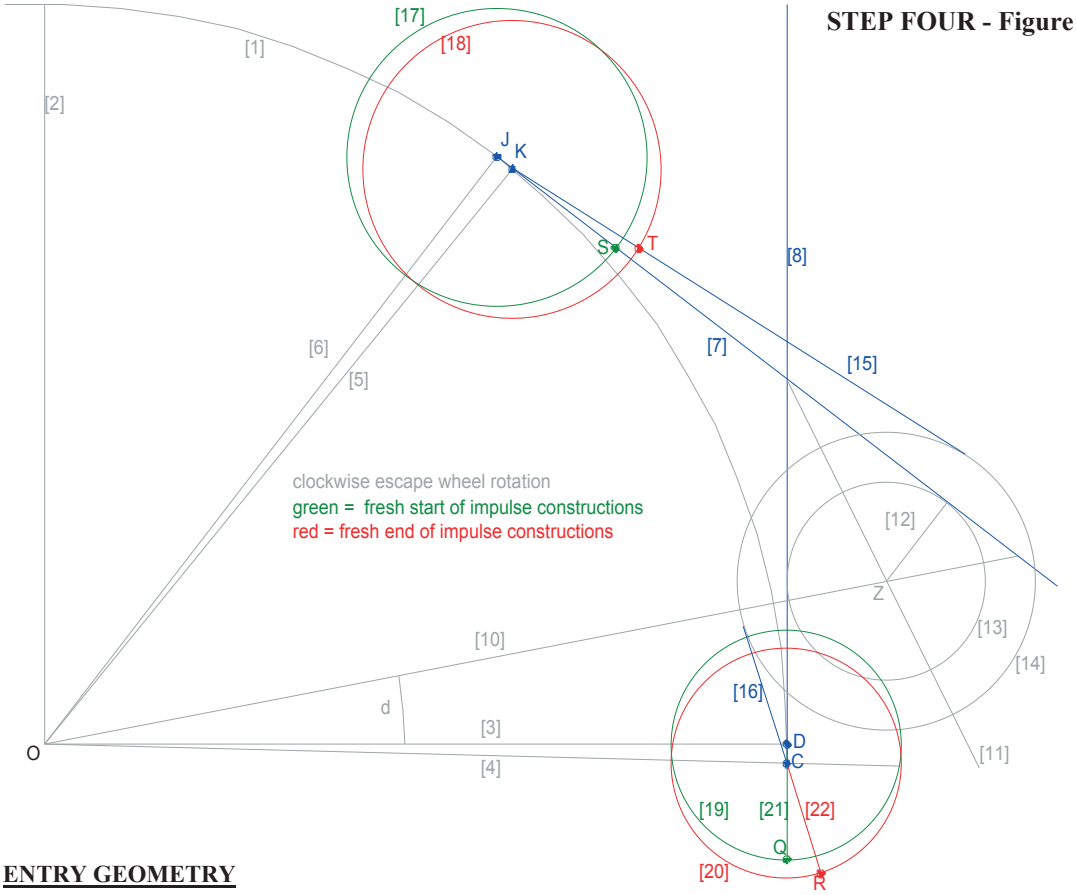

ENTRY GEOMETRY

■ **[17] - Construct a circle (shown in green), centred at J, of an arbitrary radius.** The radius of circle [17] is an arbitrary representation of the **'active length'** (between the pivot and the nib locking corner) of the entry pallet arm. Since point J is the position of the entry pallet nib locking corner at the start of entry impulse, potential locations of the arbitrary entry pallet arm pivot at the start of entry impulse lie along the circumference of circle [17]. The illustrated intersection of start of impulse circle [17] and start of impulse line of action [7] is labelled 'S'.
■ **[18] - Construct a circle (shown in red), centred at K, of the same radius as circle [17].** Since point K is the position of the entry pallet nib locking corner at the end of entry impulse, potential locations of the arbitrary entry pallet arm pivot at the end of entry impulse lie along the circumference of circle [18]. The illustrated intersection of end of entry impulse circle [18] and end of entry impulse line of action [15] is labelled 'T'.

For the arbitrary entry pallet arm active length and the established lines of action, the illustrated locations of S and T define the only physically representative and correctly functioning locations of the entry pallet arm pivot at the start and end of entry impulse, respectively.

EXIT GEOMETRY

■ **[19] - Construct a circle (shown in green), centred at D, of an arbitrary radius.** The radius of circle [19] is an arbitrary representation of the active length of the exit pallet arm. Since point D is the position of the exit pallet nib locking corner at the start of exit impulse, potential locations of the arbitrary exit pallet arm pivot at the start of exit impulse lie along the circumference of circle [19].
■ **[20] - Construct a circle (shown in red), centred at C, of the same radius as circle [19].** Since point C is the position of the exit pallet nib locking corner at the end of exit impulse, potential locations of the arbitrary exit pallet arm pivot at the end of exit impulse lie along the circumference of circle [20].
■ **[21] - Extend the start of exit impulse line of action [8] until it intersects the start of exit impulse circle [19] as illustrated.** The illustrated point of intersection is labelled 'Q'.
■ **[22] - Extend the end of exit impulse line of action [16] until it intersects the end of exit impulse circle [20] as illustrated.** The illustrated point of intersection is labelled 'R'.

For the arbitrary exit pallet arm active length and the established lines of action, the illustrated locations of Q and R define the only physically representative and correctly functioning locations of the exit pallet arm pivot at the start and end of exit impulse, respectively.

STEP FIVE - Figure 39

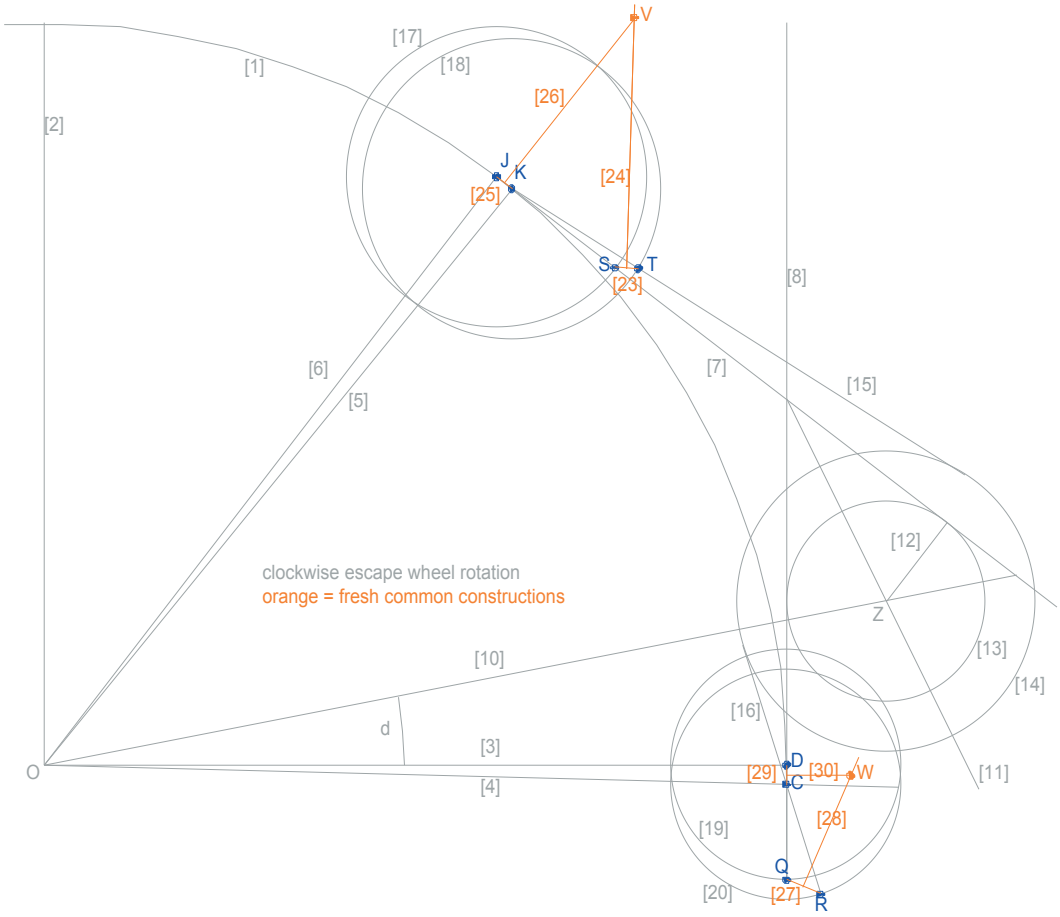

The above illustrates fresh constructions in **orange**, since none are specific to the start or end of impulse.

ENTRY GEOMETRY. The APPENDIX describes the basis of the following (orange) constructions.

- **[23] - Construct a straight line between points S and T.**
- **[24] - Construct a straight line from the mid point of ST, perpendicular to ST, in the direction shown.**
- **[25] - Construct a straight line between points J and K.**
- **[26] - Construct a straight line from the mid point of JK, perpendicular to JK, in the direction shown.** For drawing methods other than CAD, or as an alternative CAD construction, it will be useful to note that an extension of line [26] would pass through the escape wheel axis, O and bisect angle JOK.
- The intersection of lines [24] and [26] is labelled V. As described in the APPENDIX, for any arbitrary choice of the STEP FOUR entry pallet arm active length, constructions [23], [24], [25] and [26] will always define the same location of the entry geometry 'universal escapement frame arbor axis', V.

EXIT GEOMETRY. The APPENDIX describes the basis of the following (orange) constructions.

- **[27] - Construct a straight line between points Q and R.**
- **[28] - Construct a straight line from the mid point of QR, perpendicular to QR, in the direction shown.**
- **[29] - Construct a straight line between points C and D.**
- **[30] - Construct a straight line from the mid point of CD, perpendicular to CD, in the direction shown.** For drawing methods other than CAD, or as an alternative CAD construction, it will be useful to note that an extension of line [30] would pass through the escape wheel axis, O and bisect angle COD.
- The intersection of lines [28] and [30] is labelled W. As described in the APPENDIX, for any arbitrary choice of the STEP FOUR exit pallet arm active length, constructions [27], [28], [29] and [30] will always define the same location of the exit geometry 'universal escapement frame arbor axis', W.

STEP SIX - Figure 40

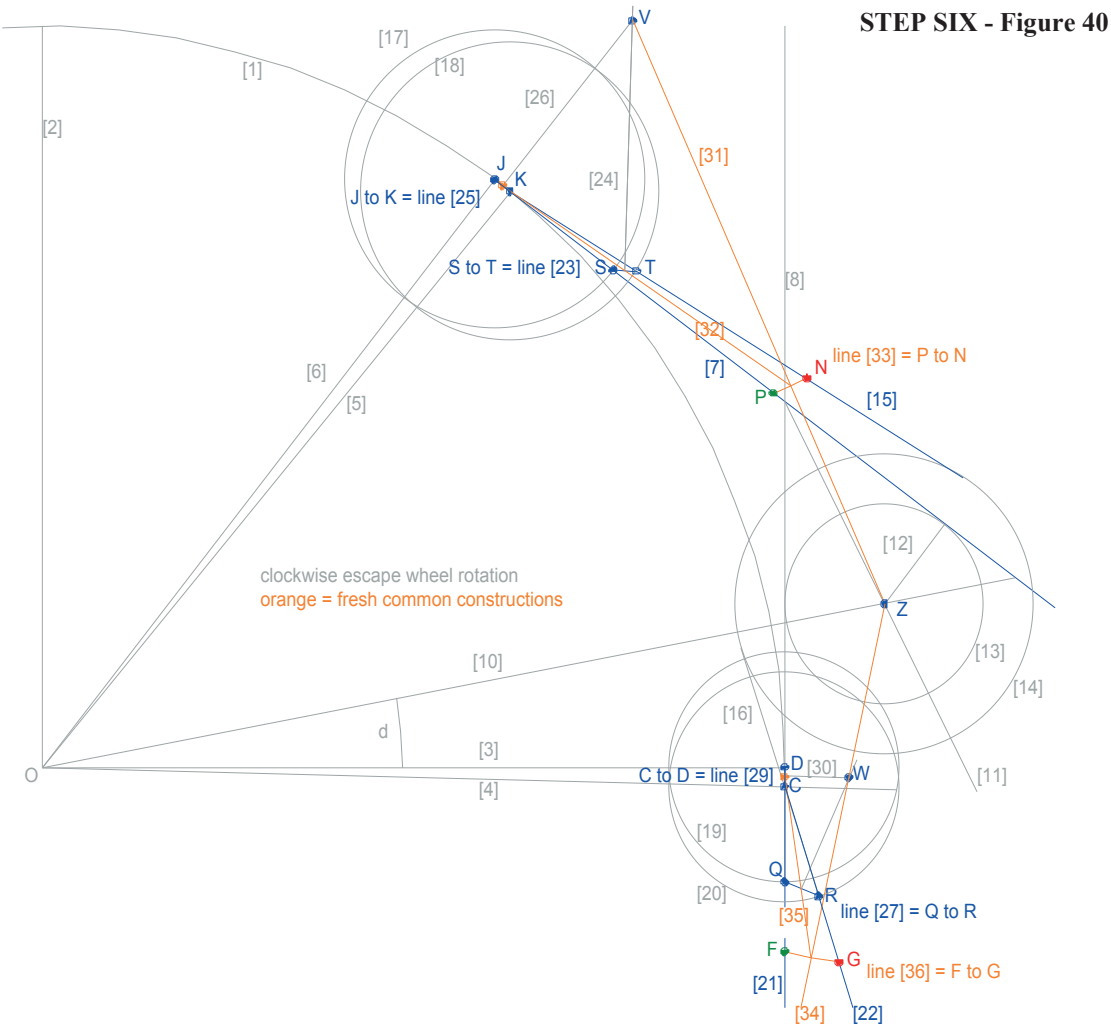

ENTRY GEOMETRY. The APPENDIX describes the basis of the following (orange) constructions.

■ **[31] - Construct a straight line between points V and Z.** Z is the STEP TWO escapement frame arbor axis.
■ **[32] - Construct a straight line from the mid point of line [25] (between J and K) to the mid point of line [23] (between S and T), extending as far as line [31].**
■ **[33] - At the intersection of lines [31] and [32], construct a perpendicular to line [31].**
■ The intersection of lines [7] and [33] is labelled P. For an escapement frame arbor axis at Z, point P is the entry pallet arm pivot location at the start of entry impulse and JP is the entry pallet arm active length.
■ The intersection of lines [15] and [33] is labelled N. For an escapement frame arbor axis at Z, point N is the entry pallet arm pivot location at the end of entry impulse and KN is the entry pallet arm active length.
■ By virtue of universal properties of V (see APPENDIX), JP will match KN, PV will match NV and (therefore) PZ will match NZ, thereby ensuring correct functioning of the entry geometry incorporating Z, J, K, N and P.

EXIT GEOMETRY. The APPENDIX describes the basis of the following (orange) constructions.

■ **[34] - Construct a straight line between points W and Z, extending as shown.**
■ **[35] - Construct a straight line from the mid point of line [29] (between C and D) to the mid point of line [27] (between Q and R), extending as far as line [34].**
■ **[36] - At the intersection of lines [34] and [35], construct a perpendicular to line [34].**
■ The intersection of line [21] (through D and Q, extended if necessary) and line [36] is labelled F. For an escapement frame arbor axis at Z , point F is the exit pallet arm pivot location at the start of exit impulse and DF is the exit pallet arm active length.
■ The intersection of line [22] (through C and R, extended if necessary) and line [36] is labelled G. For an escapement frame arbor axis at Z, point G is the exit pallet arm pivot location at the end of exit impulse and CG is the exit pallet arm active length.
■ By virtue of universal properties of W (see APPENDIX), DF will match CG, FW will match GW and (therefore) FZ will match GZ, thereby ensuring correct functioning of the exit geometry incorporating Z, D, C, F and G.

STEP SEVEN - Figure 41

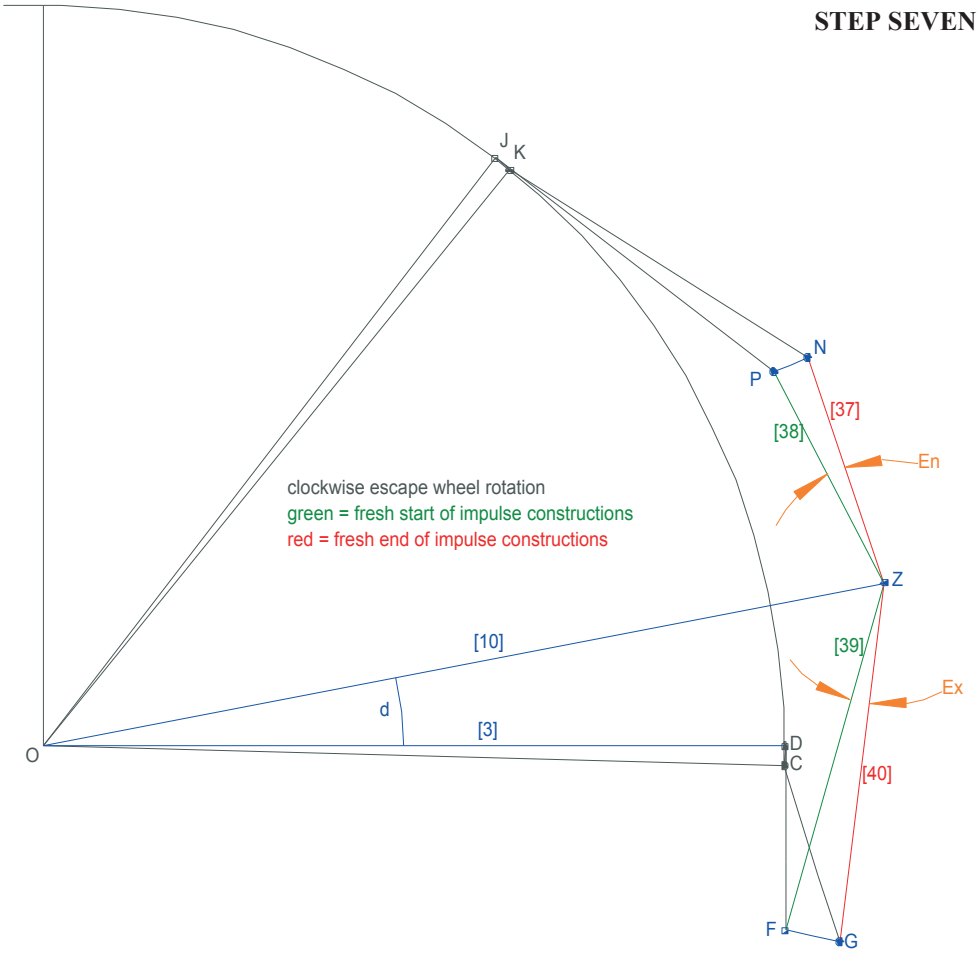

Many of the earlier constructions have been removed from the above illustration, leaving the arc of the escape wheel pitch circle (centred at O, passing through J, K, D and C), STEP TWO escapement frame arbor axis Z, compatible start and end of impulse entry pallet arm pivot locations P and N respectively, compatible start and end of impulse exit pallet arm pivot locations F and G respectively, compatible start and end of impulse entry pallet arm lines of action JP and KN respectively, compatible start and end of impulse exit pallet arm lines of action DF and CG respectively and all previous escape wheel radials.

■ **[37] - Construct a straight line from Z to N.** This line represents the physical connection between the escapement frame arbor axis and the entry pallet arm pivot at the end of entry impulse.
■ **[38] - Construct a straight line from Z to P.** This line, equal in length to line [37], represents the physical connection between the escapement frame arbor axis and the entry pallet arm pivot at the start of entry impulse.
■ **Measure angle 'En', between [37] and [38].** This is the escaping arc of the entry geometry.
■ **[39] - Construct a straight line from Z to F.** This line represents the physical connection between the escapement frame arbor axis and the exit pallet arm pivot at the start of exit impulse.
■ **[40] - Construct a straight line from Z to G.** This line, equal in length to line [39], represents the physical connection between the escapement frame arbor axis and the exit pallet arm pivot at the end of exit impulse.
■ **Measure angle 'Ex', between [39] and [40].** This is the escaping arc of the exit geometry.
■ **Balance the entry and exit escaping arcs. See BALANCING THE ESCAPING ARCS (page 40).** For correct escapement functioning, En and Ex must be balanced (i.e. equal).
■ **Incorporate the balanced, designer-chosen escaping arc, referred to as E*. See BALANCED ESCAPING ARC ADJUSTMENT (page 41).**
■ **Incorporate the designer-chosen mean torque arm, referred to as M*. See MEAN TORQUE ARM ADJUSTMENT (page 42).**
■ **Determine the instantaneous pallet nib locking corner lifts. See DETERMINING INSTANTANEOUS PALLET NIB LOCKING CORNER LIFTS (page 42).**
■ **Check the geometry. See CHECKING GEOMETRIES (page 43).**
■ **Upon successful completion of all of the above, a complete, correctly functioning, twin pivot grasshopper escapement geometry will have been created in accordance with all designer choices and inputs.**

BALANCING THE ESCAPING ARCS

For correct and efficient functioning, the escaping arc of the twin pivot entry geometry, referred to as **'En'**, must balance (i.e be equal to) the escaping arc of the exit geometry, referred to as **'Ex'**.

For a given combination of escape wheel tooth count, escapement mean span, end/start ratio, entry angle and exit angle, balanced escaping arcs may be achieved by altering STEP TWO angle 'd', between lines [3] and [10]. A proven technique is to construct at least three geometries, each incorporating a different angle d, by repeating STEP ONE to STEP SEVEN of the CAD sequence as far as, but not including, the STEP SEVEN instruction 'Balance the entry and exit escaping arcs'. As illustrated in **Figure 42**, accurate plots of d versus En and d versus Ex identify the angle d at which En equals Ex, at the 'black star' point of intersection of the two curves. It should speed the balancing process and avoid unnecessary expenditure of effort if at least one choice of d generates an En greater than the corresponding Ex and at least one other choice of d generates an En less than the corresponding Ex. The 'black star' intersection of the two curves will thereby be contained between those two choices. Experience suggests that CAD software set to a high resolution is suitable for the accurate plotting of points, whilst typical CAD software usually includes a convenient curve drawing tool (e.g. Bezier), which should be worthy of consideration.

A single execution of the above process may well suffice. If considered necessary, however, greater precision may be achieved by constructing at least two more geometries with angles d extremely close to and to either side of the last 'black star' intersection of the d versus En and d versus Ex curves. Plots of angle d versus escaping arc for those additional geometries (not illustrated) must be added to the existing plots and the d versus En and d versus Ex curves redrawn to include all plotted points. The curves are thereby refined in the region of their intersection, more precisely defining the 'black star' point and the corresponding angle d. The refinement process may be repeated as many times as considered necessary, limited only by the maximum resolution of the chosen CAD software and, of course, the adopted plotting and curve fitting techniques.

Although the outcome of the above process will be a balanced escaping arc, it is extremely unlikely that the arc will match the designer's choice. BALANCED ESCAPING ARC ADJUSTMENT (next page) will explain how nothing more than straightforward repetitions of the above process may be used to alter the magnitude of the escaping arc, whilst simultaneously preserving entry versus exit balance.

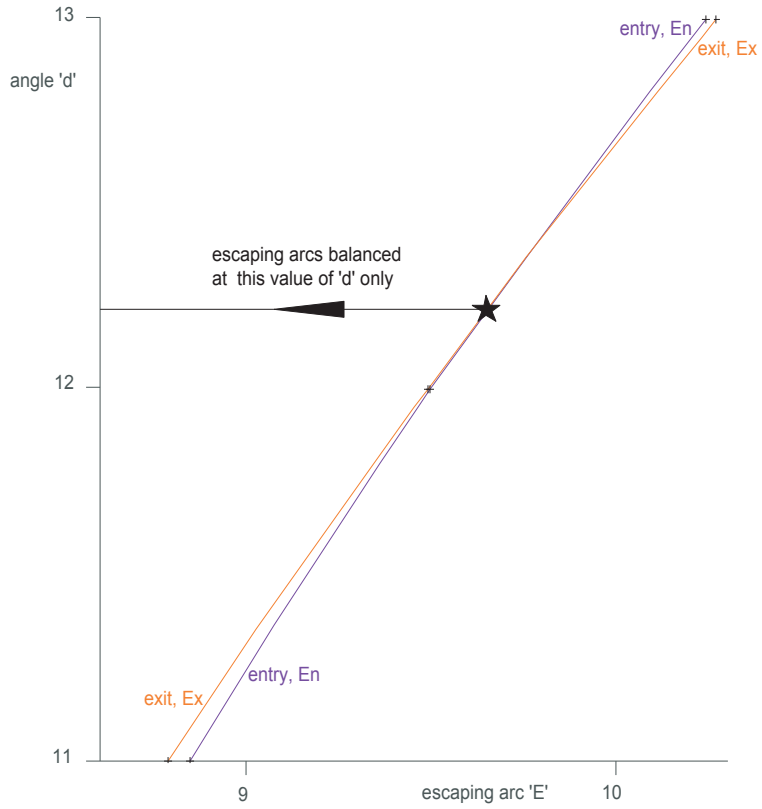

Figure 42 - Balancing the escaping arcs

BALANCED ESCAPING ARC ADJUSTMENT

A significant and (at the time of writing) unique advantage of the devised design technique is a capacity to simultaneously incorporate any or all of Harrison's stipulations or the designer's choices, most significantly amongst which is the formerly elusive magnitude of the balanced escaping arc.

For the designer-chosen escape wheel tooth count, end/start ratio, entry angle and initial exit angle, the mean number of escapement tooth spaces spanned should first be altered by integer multiples of one whole tooth space until the balanced escaping arc is as close to the designer's choice as possible. Although this adjustment unavoidably occurs in coarse steps, it will minimise deviations from the STEP ONE designer-chosen initial exit angle when the escaping arc is subsequently adjusted with greater precision.

Greater precision is achieved by altering the STEP ONE exit angle, 'ax'. The left-hand side of **Figure 43** illustrates three pairs of d versus En and d versus Ex curves, all created as described in BALANCING THE ESCAPING ARCS (page 40), for chosen exit angles ax of 89, 90 and 91 degrees. For each exit angle, the point at which the relevant d versus En curve intersects the d versus Ex curve is emphasised by a black star, as it was in Figure 42. Joining the three black stars is a black curve, which defines all points of balanced escaping arc within the plotted range of exit angles. The point at which the balanced escaping arc is equal to the designer-chosen escaping arc, E*, is emphasised by a blue star. The corresponding angle d* is determined by following the blue lines in the indicated directions. The corresponding exit angle, ax*, is determined by linear interpolation, as revealed in the greatly magnified inset on the right-hand side of Figure 43. An apparently adequate approximation is to construct the red line in the inset perpendicular to an estimated mean of the paired curves (for ax = 90 in this case) closest to the blue star. 'Blue star' angle d* and 'blue star' exit angle ax* are then input to CAD sequence STEPS ONE to SEVEN and the generated entry and exit escaping arcs, En and Ex, are checked for balance and agreement with E* to the chosen degree of precision. Of greatest importance, the CAD sequence preserves all other designer choices.

A single execution of the above process may well suffice. If necessary, however, greater precision may be achieved by constructing at least two more pairs of d versus En and d versus Ex curves for exit angles extremely close to and to either side of the previous 'blue star' exit angle, redrawing the black curve of balanced arcs to include the additional 'black star' points of intersection. The black curve is thereby refined in the region of the blue star intersection, more precisely establishing the 'blue star' angle d* and the corresponding 'blue star' exit angle ax*. More accurate entry and exit escaping arcs will thereby be generated when STEPS ONE to SEVEN are executed for the refined d* and ax*. The refinement process may be repeated as many times as necessary, limited only by the maximum resolution of the chosen CAD software and, of course, the adopted plotting and curve fitting techniques.

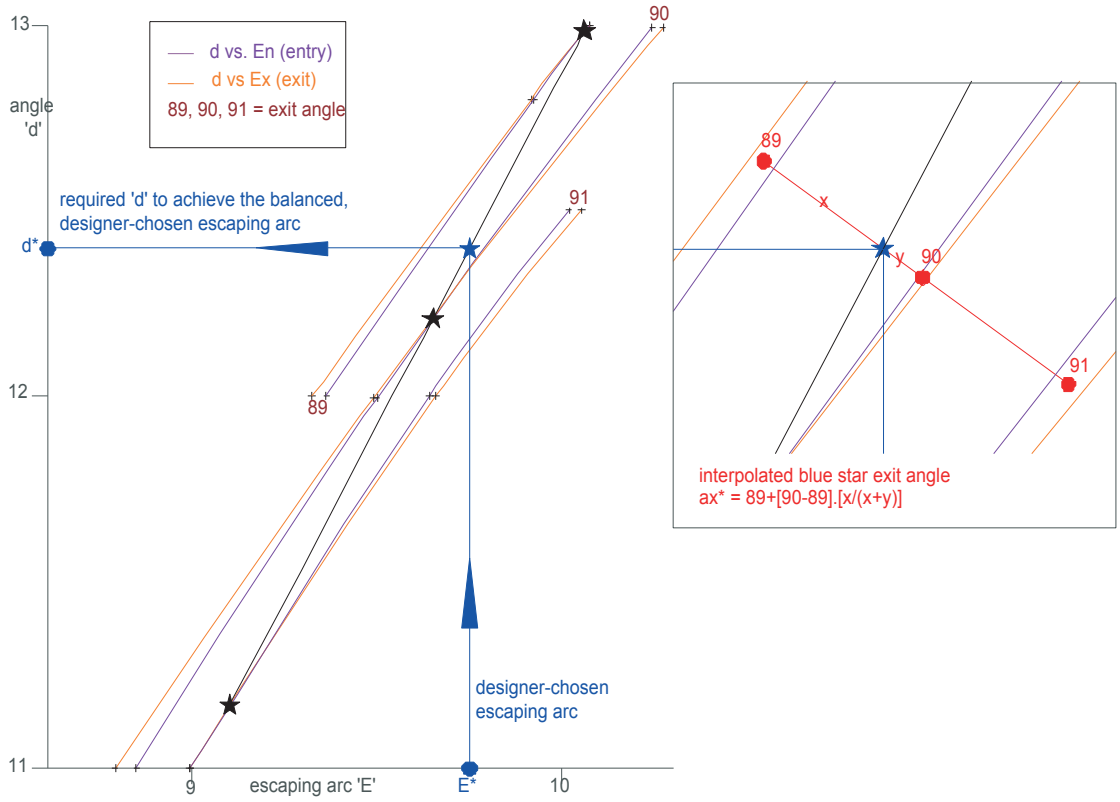

Figure 43 - Balanced escaping arc adjustment

MEAN TORQUE ARM ADJUSTMENT

The mean torque arm is linear dimension 'M' (not point M) in **Figure 46**, on page 43. The mean torque arm of any geometry may be determined by measuring the radii of the start and end of impulse torque arm circles and calculating the mean. As an entirely CAD alternative, construct any radial of both torque arm circles, bisect the portion of the radial between those circles and measure the radius of the bisecting point. The **designer-chosen mean torque arm**, which will be referred to as **M***, may be speedily incorporated using the CAD scaling function, altering every linear dimension (but no angles) of the geometry by the ratio M*/M. A designer-chosen mean torque arm of 10 mm has been incorporated within the geometry of **Figure 44**, below**.**

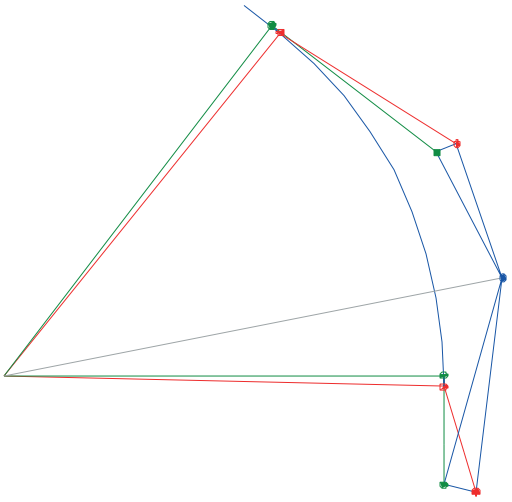

Figure 44 - Twin pivot grasshopper escapement geometry with a mean torque arm of 10 mm.

DETERMINING INSTANTANEOUS PALLET NIB LOCKING CORNER LIFTS

Of relevance to optimum trip protection, sound mechanical design and functionality, the instantaneous (zero travel time) entry and exit pallet nib locking corner **'lifts'** after release from the escape wheel, as illustrated in Fig. 24 (entry) and Fig. 30 (exit), are derived from circular arcs through J centred at Z, through K centred at N, through D centred at Z and through C centred at G. As illustrated in **Figure 45**, appropriate intersections define the instantaneous entry pallet nib locking corner lift, KK* and the instantaneous exit pallet nib locking corner lift, CC*.

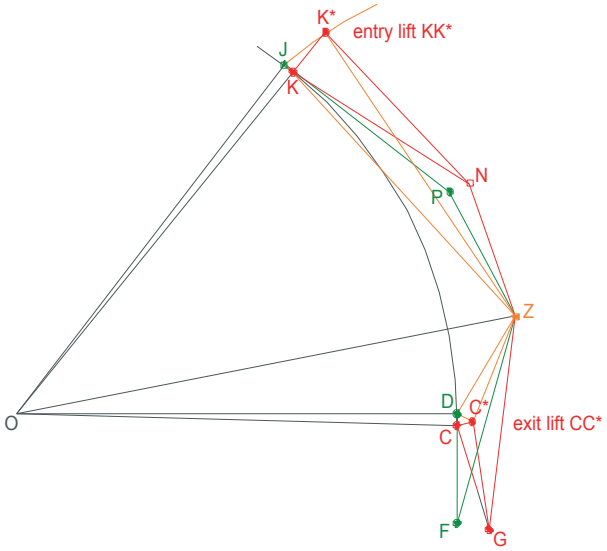

Figure 45 - Instantaneous entry and exit pallet nib locking corner lifts after release.

CHECKING GEOMETRIES

Upon completion (or at any time beforehand, if considered necessary), geometries should be checked. With reference to **Figure 46**, drawn to no particular scale, the following checklist is suggested:

Check (1) Angle COD should be the angle subtended by half an escape wheel tooth space.
Check (2) Angle DOK should be the angle subtended by the minimum tooth spaces spanned.
Check (3) Angle COJ should be the angle subtended by the maximum tooth spaces spanned.
Check (4) Angle JOK should be the angle subtended by half an escape wheel tooth space.
Check (5) JP should equal KN (equal entry pallet arm active lengths at the start and end of impulse).
Check (6) DF should equal CG (equal exit pallet arm active lengths at the start and end of impulse).
Check (7) PZ should equal NZ (entry pallet pivot to escapement frame axis at the start and end of impulse).
Check (8) FZ should equal GZ (exit pallet pivot to escapement frame axis at the start and end of impulse).
Check (9) Angle PJO should match the designer-chosen STEP ONE entry angle.
Check (10) Angle HDO should almost match the designer-chosen STEP ONE initial exit angle. Within two degrees is proposed, although opinions may differ. A greater deviation from the initial choice suggests that an alteration to the mean span should be investigated, as explained on page 41.
Check (11) Start of impulse lines of action JL and FH should be tangential to the smaller, green, start of impulse torque arm circle and end of impulse lines of action KM and GE should be tangential to the larger, red, end of impulse torque arm circle.
Check (10) EZ / HZ should match the designer-chosen end/start ratio, T. For Harrison compliant geometries, the ratio should be 3 / 2.
Check (12) In the final, scaled geometry, 0.5 (HZ + EZ) = dimension M in Fig. 46 should match the designer-chosen mean torque arm, M*.
Check (13) Escaping arcs NZP and FZG should both match the designer-chosen escaping arc, E*, with at least the designer-chosen degree of precision.

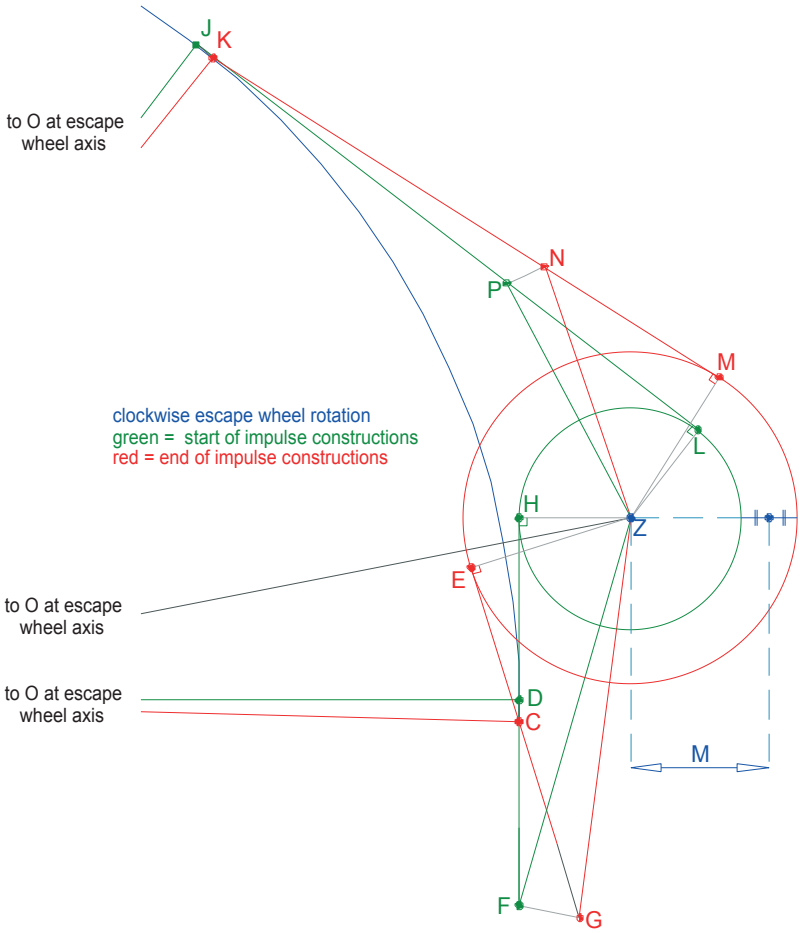

Figure 46

PART TWO

*

THE TWIN BALANCE GRASSHOPPER ESCAPEMENT

INTRODUCING THE TWIN BALANCE GRASSHOPPER ESCAPEMENT

The twin balance grasshopper escapement was almost certainly invented by John Harrison for his first, large marine timekeeper, commonly referred to as 'H1', created with the sole intention of accurately determining longitude at sea. **Figure 47** is a greatly simplified representation of the escapement and sixty tooth escape wheel of H1, maintaining the motions of two symmetrical, seconds-beating bar balances, proportionally much longer than schematically illustrated. **Figure 48** (overleaf) demonstrates how the balances are obliged to swing in opposition by two thin metal ribbons (emphasised in green and red), guided by circular arcs (in grey). In most respects, the cycle of operation is sufficiently similar to that of the twin pivot escapement of PART ONE to require no further explanation, except to mention that fine spring steel composer wires are incorporated instead of nose-heavy composers. Within each balance hub, a markedly curved spring composer ensures precise pallet arm nib locking corner capture and absorbs balance overswing. Upon release, each nib locking corner is withdrawn from the escape wheel by a separate spring composer arrangement. Composer springs and wooden pallet arms (illustrated in brown) are formed, balanced, pivoted and attached such that they are unaffected by externally imposed accelerations and generate no sliding friction, apart from inconsequential rotations of the pallet arms about their pivots. In combination with anti-friction balance and movement arbor supports, the unpredictable consequences of sliding friction, wear and lubrication are thereby, in effect, entirely eliminated.

Of passing interest, fine helical springs between the balance extremities of H1 are influenced by increases and decreases in ambient temperature, which induce the expansion and contraction of multiple brass and steel 'gridiron' rods, amplified and transmitted to the springs by an array of levers and linkages (not illustrated).

A similar escapement and bar balance arrangement, in combination with an escape wheel of one hundred and twenty teeth, was installed within Harrison's second large sea clock, H2. In an effort to eliminate a subsequently identified source of error, the third and last of his large longitude timekeepers, H3, incorporated circular balance wheels, disposed above and below an escape wheel of one hundred and twenty teeth.

Harrison's objective was the creation of a timekeeper with immunity from atmospheric variations, the inconsistencies of friction, wear and lubrication and the unpredictable accelerations encountered on board an eighteenth century sailing ship at sea. He eventually concluded, however, that *'...Velocity was very much wanting in my three large Machines ... notwithstanding their Weightiness of Ballances'* and was forced to abandon them. Sadly, the twin balance grasshopper escapement was an innocent casualty, being unsuited to size and pace of Harrison's subsequent, considerably more capable *'...Watch, or Time-Keeper for the Longitude...'*, referred to as 'H4'.

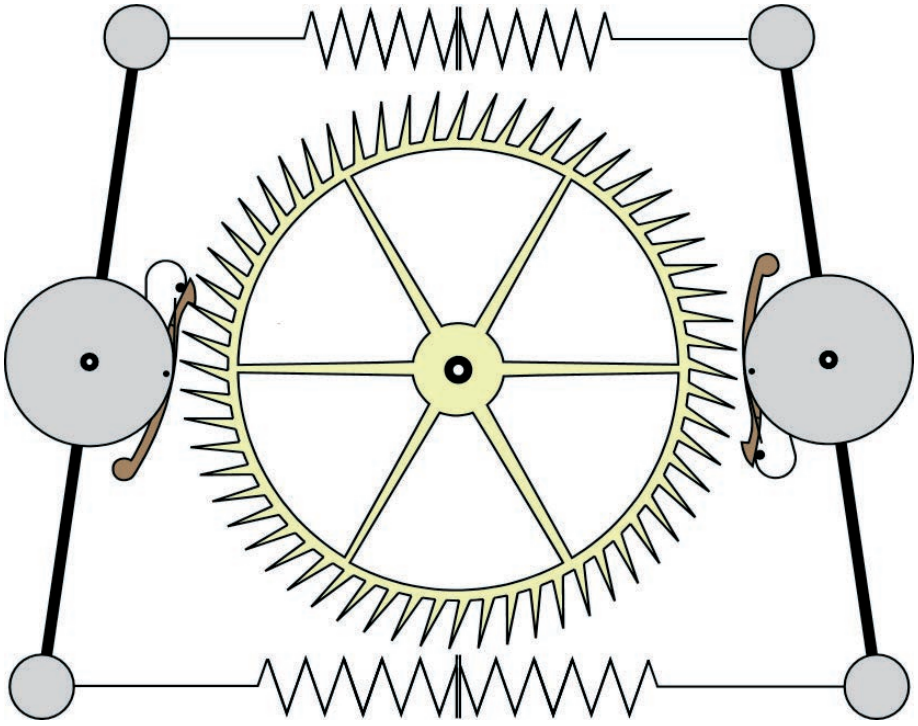

Figure 47 - Greatly simplified escapement, escape wheel and balances of Harrison's first sea clock, H1

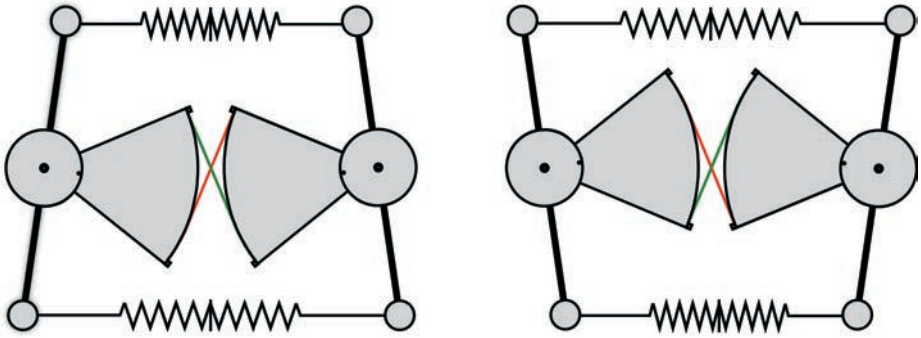

Figure 48 - Twin balances obliged to swing in opposition by two thin metal ribbons (in green and red).

TWO AND FOUR MINUTE ESCAPE WHEELS

One complete twin balance grasshopper cycle, during which an entire escape wheel tooth space passes through the escapement, occupies two seconds when associated with seconds beating balances. The sixty tooth escape wheel of H1 therefore completes one full rotation in 2 x 60 = 120 seconds (two minutes). The escape wheels of H2 and H3, both incorporating one hundred and twenty teeth, rotate once every four minutes.

NO SLIDING FRICTION, NO WEAR, NO LUBRICATION

A review of the mechanical arrangement of the twin balance grasshopper escapement will confirm that at no point does sliding friction occur, apart from limited, inconsequential rotations of the pallet arms about their pivot pins. In addition, the balance and movement arbors of Harrison's large sea clocks roll with extremely low resistance upon circular arcs and wheels, respectively. There is, therefore, no requirement that the escapement or balance pivots be lubricated. In fact, lubrication of the pallet nibs would reduce essential static friction between captured nib locking corners and capturing escape wheel teeth tips, with potentially ruinous consequences. Furthermore, any lubricant at any of the pivots or nibs, be it modern or ancient, would suffer unavoidable alterations to its properties with age, use and exposure to its environment, with proven, potentially significant cumulative effects upon consistent timekeeping.

Negligible sliding friction generates negligible wear and negligible variations in performance. Harrison's twin balance grasshopper escapement thereby entirely avoids all common escapement problems in a typically direct and thorough fashion, by effectively eliminating their causes at source.

HARRISON'S STIPULATIONS

Detailed analyses of Harrison's final, 1775 manuscript (CSM) and an associated escapement illustration (MS3972/3) reveal invaluable instructions for the design of twin balance geometries. The following analysis will identify those instructions, including relevant observations from the PART ONE twin pivot and associated single pivot studies, for ease of reference.

WRITTEN (CSM) STIPULATIONS

Although Harrison's 1775 manuscript, CSM, relates (amongst other topics) to the single pivot grasshopper escapement, common sense suggests that some of it may be applied to the twin balance configuration. The following stipulations are listed on that basis. Stipulation numbering is arbitrary and unique to this publication.

■ **STIPULATION 1 - There must be no sliding friction and (therefore) no wear or requirement for lubrication.** It has already been demonstrated that the grasshopper escapement complies with STIPULATION 1.

■ **STIPULATION 2 - An escape wheel rotating once every four minutes should be used.** An escape wheel of one hundred and twenty teeth in association with seconds beating balances satisfies this stipulation. Experience reveals that grasshopper escapement geometries are well suited to such high tooth counts, whilst unavoidable, variable influences upon the necessarily high escape wheel torque are also rendered a less significant proportion of the whole.

Of interest, Harrison's first sea clock, H1, incorporates seconds beating balances and an escape wheel of sixty teeth, whilst his later sea clocks, H2 and H3, incorporate seconds beating balances and escape wheels of one hundred and twenty teeth. It may therefore be that Harrison identified STIPULATION 2 before the creation of H2.

■ **STIPULATION 3 - Harrison's CSM instructions for the development of escapement impulse during each ingle pivot grasshopper escapement cycle are ambiguous and incomplete.** Harrison states: *'…let, as I order the Matter, the Force [from the Wheel] upon the Pendulum, as just before the interchanging of the Pallats, to be as by or from them the said Pallats supposed or taken as 3, then as just after their interchanging [and the Force to contrary Direction], it must be about as 2, that is, it must be so ordered [as may hereafter be observed by the Drawing] viz as that it be so by the taking, or supposing for the Purpose, a Mean betwixt the Actions of each Pallat…'*. Sadly, Harrison later declared that *'…the Drawing…'* and a more detailed explanation would no longer be offered, in response to poor treatment and incomplete reward by the Board of Longitude.

STIPULATION 4 - Harrison's only CSM guidance relating to balance amplitude and frequency of oscillation is specific to his fourth longitude timekeeper, H4. He declares that the single balance wheel of H4 changes direction five times every second and describes an arc of two hundred and fifty five degrees, well beyond the capabilities of any grasshopper escapement. The only instructions specific to a grasshopper escapement require that the escaping arc of *simple pendulums* driven by the *single pivot* configuration should be large, but should not exceed fifteen degrees. Put simply, Harrison's is demanding that simple pendulums have 'velocity' (to borrow one of his terms), dominate the escapement and minimise the adverse effects of disturbances and variations. The 255 degree arc of H4 does, however, suggest that the 15 degrees maximum for simple pendulums is inadequate for balances.

ILLUSTRATED STIPULATIONS

A PART ONE analysis entitled ILLUSTRATED STIPULATIONS supported a proposal that *'…the Drawing…'* promised in CSM, but ultimately withheld, was created after all and that it still exists. **Figure 32** on page 26 reproduced a scanned photocopy of the object in question, commonly referred to as '**MS3972/3'**. Two separate single pivot grasshopper escapement geometries and a potentially misleading arrangement of two twin balance grasshopper escapement **'sub-geometries'** (as they will be referred to herein) simultaneously display all start and end of impulse events, with the exception of irrelevant escape wheel recoil, balance overswing and instantaneous pallet nib locking corner resting positions after release. MS3972/3 also incorporates a complete and unambiguous definition of Harrison's precise intentions for the delivery of single pivot grasshopper escapement impulse, together with invaluable clues relating to the manipulation of escaping arc. Those features aside, it must at all times be bourne in mind that MS3972/3 is a small illustration, almost certainly created as an accompaniment to a written explanation, quite possibly CSM, published in 1775. It is unlikely that it was an intentionally accurate design drawing.

ESCAPE WHEEL TOOTH COUNT

In reassuring agreement with CSM, a total of one hundred and twenty escape wheel teeth are incorporated within Figure 32. The tips of those teeth are defined by the intersections of one hundred and twenty short black radials with the largest black escape wheel pitch circle. Two slightly smaller black circles may be ignored. In association with seconds beating balances, such an escape wheel will rotate once every four minutes during normal operation.

MECHANICAL ARRANGEMENTS

Figure 49 (overleaf) superimposes semi-transparent masks and greatly simplified representations of only the most relevant mechanical escapement components upon two identical copies of Harrison's twin balance illustration, placed side-by-side. All composer springs have been omitted. Recall that the escape wheel normally advances in a clockwise direction and that overswing and recoil are not represented.

■ **The left-hand illustration of Figure 49** emphasises one of the two sub-geometries, which is labelled '**A'** and will henceforth be referred to as '**geometry A'**. Superimposed upon geometry A are a representation of a physical pallet arm, shown in brown and a straight mechanical link, illustrated in **green**. The green link is a greatly simplified representation of the rigid physical connection between the balance arbor and the pallet arm pivot pin, both of which are, in reality, incorporated within the entire hub of the balance (not illustrated, to avoid clutter). The physical pallet nib locking corner is aligned with Harrison's **start** of impulse tooth tip, whilst the physical pallet arm pivot and the co-located physical pivot at the upper end of the straight link are both aligned with Harrison's **start** of impulse pallet arm pivot location. The physical pivot at the lower end of the link is aligned with Harrison's balance arbor axis.

■ **The right-hand illustration of Figure 49** emphasises the other sub-geometry, labelled 'B', henceforth referred to as '**geometry B'**. The physical, brown pallet arm is shorter than in geometry A and the greatly simplified, straight mechanical link is illustrated in **red**. In correctly functioning opposite phase to the physical components of geometry A, the physical pallet nib locking corner of geometry B is aligned with Harrison's **end** of impulse tooth tip location, which is half a tooth space clockwise from the start of impulse tooth tip. The physical pallet arm pivot and the co-located physical pivot at the upper end of the straight link are aligned with Harrison's **end** of impulse pallet arm pivot location, whilst the physical pivot at the lower end of the link is aligned with Harrison's balance arbor axis.

■ Half an escapement cycle after the above situations, Harrison's currently unoccupied pivot locations, each of which are emphasised by a small black dot, would be occupied by the applicable physical pallet arm pivot and the co-located upper link pivot at the **end** of geometry A impulse and the **start** of geometry B impulse.

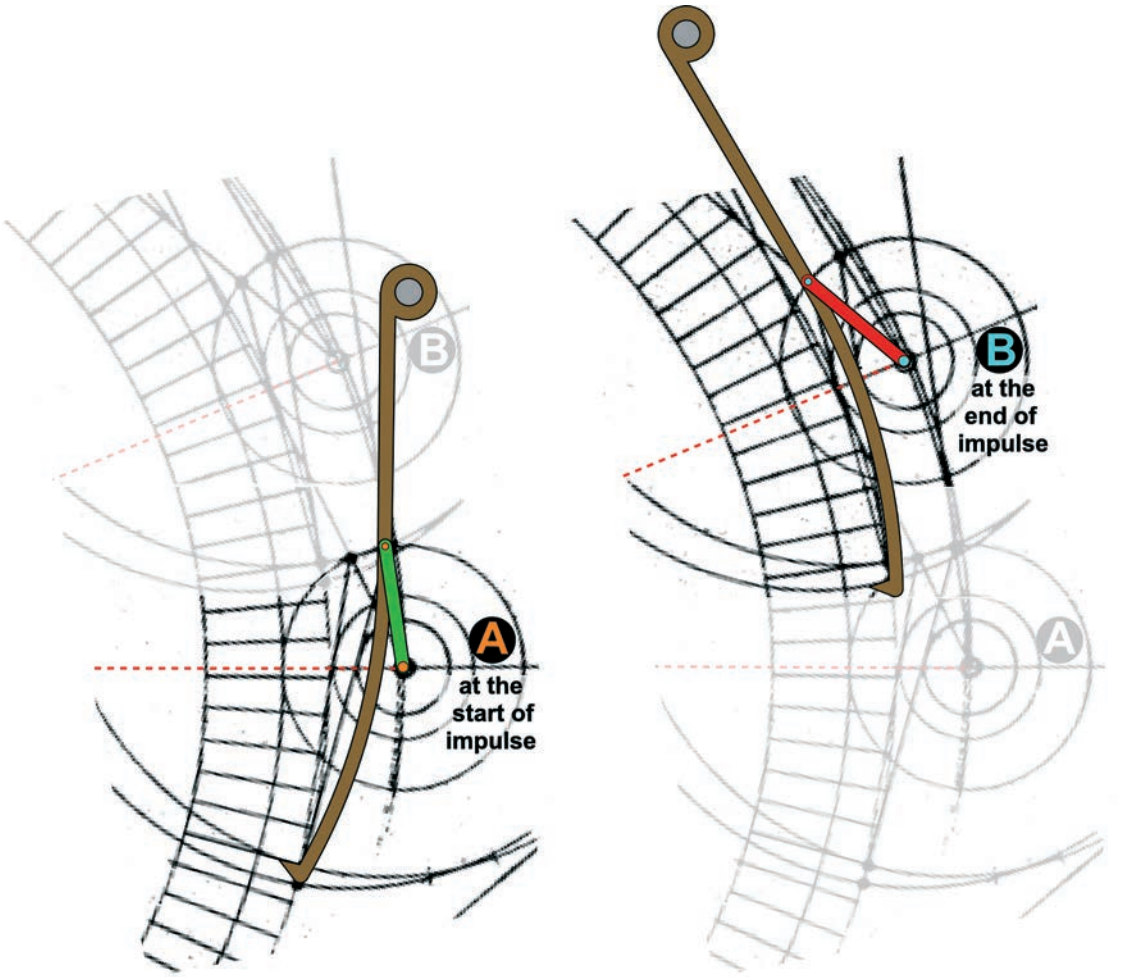

Figure 49 - Simplified mechanical arrangements of Harrison's MS3972/3 twin balance sub-geometries. Geometry A at the start of impulse and geometry B at the end of impulse (ignoring overswing).

MS3972/3 ANALYSIS IN EIGHT PARTS

Figure 50 (overleaf) reproduces the small, black and white twin balance grasshopper escapement illustration of MS3972/3, greatly enlarged to no particular scale and orientated to suit the proportions of the page. Coloured lines, labels and circled crosses have been added for the purposes of the following analysis and must not be attributed to Harrison. Circled crosses and associated labels exclusive to geometry A are coloured light orange and circled crosses and associated labels exclusive to geometry B are coloured light blue. Overswing is not incorporated.

1 - PALLET ARMS LINES OF ACTION

In Figure 50, geometries A and B each include two pallet arm lines of action, in each case defining the paths of the start and end of impulse forces generated within each sub-geometry by supplied escape wheel energy during one complete cycle. Note that the magnitudes of those impulse forces are not represented.

The lines of action function as follows:

■ **(i) -** At the start of geometry A impulse, F is the location of the pallet arm pivot, D is the location of the captured pallet nib locking corner and DF is the pallet arm active length along the start of impulse line of action. A tensile force, acting from F to D at perpendicular torque arm HZ, will apply anticlockwise torque about the balance axis, Z. Based upon measurement, bearing in mind the identified deficiencies of MS3972/3, the angle anticlockwise from DF to escape wheel radial OD is either 90 degrees (i.e. DF tangential to the escape wheel PCD), or is very close to 90 degrees. For reasons to be be explained in due course, geometry A will also be described as the **'entry geometry'** and the angle anticlockwise from DF to OD will be referred to as the **'entry angle'**, abbreviated '**an**'.

Continues after Figure 50...

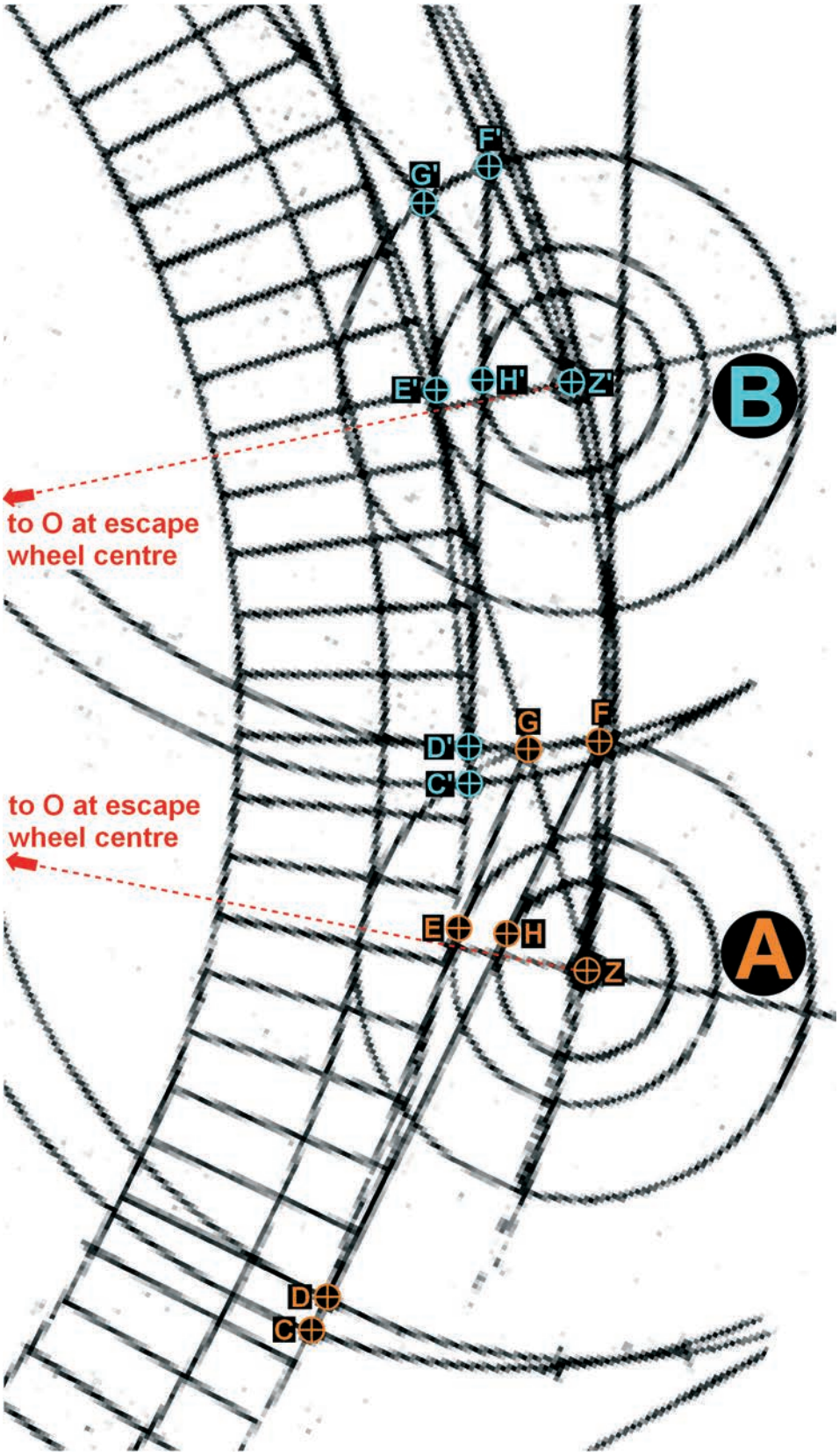

Figure 50 - Pair of MS3972/3 twin balance grasshopper escapement sub-geometries

■ **(ii) -** At the end of geometry A impulse, G is the location of the pallet arm pivot, C is the location of the pallet nib locking corner an immeasurably brief instant before release and CG is the pallet arm active length along the end of impulse line of action. A tensile force, acting from G to C at perpendicular torque arm EZ, will apply anticlockwise torque about the balance axis, Z.

■ **(iii) -** At the start of geometry B impulse, F' is the location of the pallet arm pivot, D' is the location of the captured pallet nib locking corner and D'F' is the active length along the start of impulse line of action. A tensile force, acting from F' to D' at perpendicular torque arm H'Z', will apply anticlockwise torque about the balance axis, Z'. Based upon measurement, bearing in mind the deficiencies of MS3972/3, the angle anticlockwise from D'F' to OD' is either 90 degrees (i.e. D'F' tangential to the escape wheel PCD), or is very close to 90 degrees. For reasons to be explained in due course, geometry B will also be described as the **'exit geometry'** and the angle anticlockwise from D'F' to OD' will be referred to as the **'exit angle'**, abbreviated '**ax**'.

■ **(iv) -** At the end of geometry B impulse, G' is the location of the pallet arm pivot, C' is the location of the pallet nib locking corner an immeasurably small instant before release and C'G' is the pallet arm active length along the end of impulse line of action. A tensile force, acting from G' to C' at perpendicular torque arm E'Z', will apply anticlockwise torque about the balance axis, Z'.

2 - TORQUE ARM CIRCLES

As explained during the earlier twin pivot analysis, the 17.5 mean tooth spaces span single pivot geometry of MS3972/3 instructs that the mean end/start ratio of torque arms should be precisely 3 to 2. Encouragingly, Harrison has also incorporated torque arm circles within his twin balance illustration. In Figure 50, the torque arm circle radii of geometry A increase from HZ to EZ from the start to the end of geometry A impulse, whilst the torque arm circle radii of geometry B increase from H'Z' to E'Z' from the start to the end of geometry B impulse.

Despite the deficiencies of the original or copied MS3972/3, the absence of numerical guidance within the twin balance illustration and a complete lack of specific instructions in any of Harrison's manuscripts, measurement of the two sets of twin balance torque arm circles suggests that Harrison has applied the 3 to 2 ratio of his single pivot geometry to each of the twin balance sub-geometries. The remainder of PART TWO will therefore assume that the ratio of the end of impulse torque arm to the start of impulse torque arm is precisely 3 to 2 for geometries A and B. Thus EZ / HZ = 3/2 and E'Z' / H'Z' = 3/2. Future revision of the ratio, if so desired, would be extremely straightforward.

In the absence of any instructions, evidence or logical arguments to the contrary, it is also considered sensible that geometries A and B should each deliver the same mean torque arm to the linked balances during each escapement cycle. Therefore, if M is the mean torque arm, (EZ + HZ) / 2 = M and (E'Z' + H'Z') / 2 = M.

As a consequence of the above conditions, the torque arm circles of geometry A will match the corresponding torque arm circles of geometry B in every respect.

3 - VARYING FORCES

The geometries of MS3972/3 are obviously incapable of representing the magnitudes of transmitted forces. Constant, equal forces are imposed, whereby torque is rendered equivalent to torque *arm*. In reality, forces within the twin balance grasshopper escapement are most certainly not constant (with the assumed exception, for the purposes of this analysis, of escape wheel delivery). An inspection of Figure 50 will confirm that, as a consequence of alterations to the orientations of engaged pallet arms lines of action relative to the escape wheel during each escapement cycle, the transmitted components of force from the escape wheel will alter. The greater the divergence of any pallet arm line of action from tangential to the escape wheel, the greater will be the reduction in the transmitted component of *'…the Force [from the Wheel] upon the Pendulum…'*, as Harrison expresses it in CSM. Of academic interest, the force varies in proportion to the sine of the angle between the line of action and the corresponding escape wheel radial. A consequence of such variations is that the ratio of end of impulse torque to start of impulse torque will differ from the 3 to 2 ratio of torque *arms* defined by the torque arm circles identified earlier. Nowhere in his written or illustrated work does Harrison propose that any correction for varying forces be made, whilst CSM merely acknowledges the existence of variation by including the condition *'about as'*.

4 - ESCAPING ARC

In Figure 50, angle FZG represents the escaping arc of geometry A and angle F'Z'G' represents the escaping arc of geometry B. For correct and efficient functioning of the twin balance escapement, those two escaping arcs should be equal. With continuing allowances for the deficiencies of the original or copied MS3972/3 illustration, the escaping arc is either 18.5 degrees, or is close to 18.5 degrees in both sub-geometries. For the purposes of this publication, exactly 18.5 degrees will be assumed. Future revision of the arc, if so desired, would be extremely straightforward.

5 - PALLET NIB LOCKING CORNER LOCATIONS

■ In Figure 50, geometry A start of impulse pallet nib locking corner D coincides with one of Harrison's illustrated escape wheel tooth tips.
■ Between each geometry A capture and subsequent release event, the escape wheel must advance clockwise by half a tooth space if it is to function correctly. C must therefore be half a tooth space clockwise from D.
■ In Figure 50, geometry B start of impulse pallet nib locking corner D' coincides with one of Harrison's illustrated escape wheel tooth tips.
■ Between each geometry B capture and subsequent release event, the escape wheel must advance clockwise by half a tooth space if it is to function correctly. C' must therefore be half a tooth space clockwise from D'.

6 - BALANCE PIVOT LOCATIONS

■ **(i) -** With continuing allowances for the deficiencies of the original or copied MS3972/3 illustration, it would appear from Figure 50 that the broken red escape wheel radial through the balance pivot, Z, of geometry A is displaced anticlockwise from the closest escape wheel tooth tip by 0.25 of a tooth space.
■ **(ii) -** With continuing allowances for the deficiencies of the original or copied MS3972/3 illustration, it would appear from Figure 50 that the broken red escape wheel radial through the balance pivot, Z', of geometry B is displaced clockwise from the closest escape wheel tooth tip by 0.25 of a tooth space.

7 - ENCOMPASSED TOOTH SPACES

■ At the start of geometry A impulse, escape wheel radials through D and Z encompass 5.25 tooth spaces. At the end of geometry A impulse, escape wheel radials through C and Z encompass 5.75 tooth spaces. The difference in encompassed tooth spaces is 0.5 of a tooth space.
■ At the start of geometry B impulse, escape wheel radials through D' and Z' encompass 4.75 tooth spaces. At the end of geometry B impulse, escape wheel radials through C' and Z' encompass 5.25 tooth spaces. The difference in encompassed tooth spaces is 0.5 of a tooth space.

As is necessary for correct functioning, the encompassed tooth spaces differ by 0.5 of a tooth space in either sub-geometry, supporting observations (i) and (ii) in '6 - BALANCE PIVOT LOCATIONS', above.

8 - ENTIRELY SEPARATE SUB-GEOMETRIES

■ **(a) -** Ignoring recoil, the Figure 50 geometry A start of impulse event (nib locking corner capture at D) must occur at the same instant as the geometry B end of impulse event (an immeasurably brief instant before nib locking corner release from C'). At that instant, the nib locking corners at D and C' are separated by an illustrated 7.5 tooth spaces.
■ **(b) -** Ignoring recoil, the geometry A end of impulse event (an immeasurably brief instant before nib locking corner release from C) must occur at the same instant as the geometry B start of impulse event (nib locking corner capture at D'). At that instant, the nib locking corners at C and D' are separated by an illustrated 8.5 tooth spaces.
■ **(c) -** From (a) and (b), the mean separation of the nib locking corners of geometries A and B during one complete cycle of the MS3972/3 twin balance grasshopper illustration is (7.5 + 8.5) / 2 = 8 tooth spaces.
■ A significant conclusion arises from (c), above. As demonstrated in PART ONE for the single and twin pivot configurations, the mean span of any grasshopper escapement during one complete cycle must differ from a whole number of tooth spaces by half a tooth space if the escapement is to function correctly. Calculation (c) reveals that the twin balance illustration of MS3972/3 fails to satisfy that condition. It can only be concluded that Harrison has deliberately illustrated two *entirely separate* sub-geometries, rather than a correctly functioning (albeit unrealistically closely grouped) combination.

It is revealingly likely that Harrison would have chosen the adopted approach if his original intention for MS3972/3 was as an accompaniment a written explanation, such as a (subsequently withheld) part of CSM. In support of that proposal (in addition to the observations offered in PART ONE of this publication), the pallet nib locking corners of geometries A and B are aligned with clearly defined, easily identified features (i.e. escape wheel teeth tips and the mid points of adjacent teeth tips). On that basis, Harrison would have assessed the quarter tooth space misalignments of radials OZ and OZ' from their nearest escape wheel teeth tip radials to be the more easily explained consequences.

It is unfortunate that Harrison's subsequent decision to withhold an accompanying, written explanation actually rendered the orphaned illustration more difficult to understand than it would otherwise have been, had it been created for isolated publication from the outset.

It should, of course, be bourne in mind that Harrison may have decided to withhold his written explanation after he had started, but before he had entirely completed, the surviving illustration. It is all too easily forgotten, in this age of straightforward, computerised editing, that the correct coordination of a particularly time consuming, hand-drawn illustration and a accompanying, explanatory text of some complexity, perhaps hand-written within a bound notebook (as was the original CSM), might have demanded that the illustration be created in cautious stages.

COMPUTER AIDED DESIGN OF THE TWIN BALANCE GEOMETRY

Computer Aided Design (CAD) software is exceptionally well suited to the devised design technique, which creates twin balance grasshopper escapement geometries complying with every one of Harrison's currently identified stipulations or any designer-chosen variations. Of particular value is a unique capacity to manipulate escaping arc whilst simultaneously maintaining any chosen end/start ratio and mean torque arm.

COMPUTER HARDWARE AND CAD SOFTWARE

As described in PART ONE, precision was assured by the use of inexpensive IMSI TurboCAD Deluxe 15 Computer Aided Design (CAD) software, nevertheless capable of claimed resolutions to ten decimal places. Although TurboCAD is slightly inconsistent at the higher decimal paces, no meaningful consequences arise. The software includes a 'Help' function and tutorials, enabling advancement from CAD novice to the required level of competence within a few hours. A seven year old AMD Sempron 3000+ computer and twelve year old Windows 2000 Pro operating system completed all tasks at acceptable speeds. Expensive hardware and software is, therefore, clearly not essential. A significant TurboCad 15 deficiency is an inclination to distort and/or displace curves, circles, text and small circular points during transfer to *publishing* software. Despite extensive corrective effort, minor remnants remain.

DRAWING SEQUENCE OVERVIEW

The greater part of the design technique is a numbered sequence of ten CAD 'STEPS', which creates two separate, but entirely compatible sub-geometries, referred to earlier as geometry A and geometry B.
■ **First executions of CAD sequence STEPS ONE to SEVEN create geometry A**, which should encompass an odd integer multiple of half a tooth space more than geometry B at the start (or any other matching stage) of impulse. The designer-chosen end/start ratio is incorporated during STEP TWO. Of particular relevance to STEPS THREE and FOUR, the APPENDIX describes invaluable properties of the twin balance escapement sub-geometry in far greater detail than could sensibly be included within the CAD sequence. The designer-chosen escaping arc is incorporated in STEPS SIX and SEVEN, which involves further executions of STEPS ONE to FIVE.
■ **CAD sequence STEPS EIGHT to TEN are exclusive to the creation of geometry B**. Further executions of STEPS ONE to FIVE are instructed, taking particular care to incorporate the encompassed tooth spaces of geometry B. Of greatest importance, the compatibility of geometry 'B with geometry A is assured by imposing the end/start ratio, escaping arc and mean torque arm of geometry A upon geometry B.

Upon completion of the CAD sequence, simple scaling of all linear dimensions (but no angles) of geometries A and B, easily and speedily achieved using the CAD scaling function, incorporates the common, designer-chosen mean torque arm. Instantaneous pallet nib lifts after release from the escape wheel may then be determined.

A correctly functioning, fully compliant twin balance grasshopper escapement is finally created by placing correctly orientated geometries A and B at or extremely close to any desired locations around a common escape wheel of the chosen tooth count.

DESIGNER CHOICES

In preparation for the design process, the following must be chosen:

■ **The CAD resolution.** Subject to the CAD software in use, linear and angular resolutions may require selection by the designer. The highest resolution is strongly recommended. The example will use a resolution of ten decimal places.

■ **The total number of escape wheel teeth.** MS3972/3 illustrates 120 teeth for the twin balance geometry, which will be adopted for the example.

■ **The number of tooth spaces encompassed by geometry A at the start of geometry A impulse.** The earlier MS3972/3 analysis identified 5.25 tooth spaces, which will be adopted for the example.

■ **The number of tooth spaces encompassed by geometry B at the start of geometry B impulse.** Any odd integer multiple of half a tooth space less than geometry A could be chosen, if so desired. The earlier MS3972/3 analysis identified 4.75 tooth spaces (0.5 of a tooth space less than the 5.25 tooth spaces of geometry A) which will be adopted for the example.

■ **The angle anticlockwise from the geometry A start of impulse pallet arm line of action, to the escape wheel radial through the captured pallet nib locking corner.** That angle is ODF in Figure 50, referred to earlier as the 'entry angle' or 'an'. Based upon an earlier Figure 50 observation, supported by a measure of common sense, an entry angle of 90 degrees (start of impulse line of action tangential to the escape wheel) will be adopted for the example, although the devised CAD technique will accommodate any sensible alternative.

■ **The *initial* angle anticlockwise from the geometry B start of impulse pallet arm line of action, to the escape wheel radial through the captured pallet nib locking corner.** That angle is OD'F' in Figure 50, referred to earlier as the 'exit angle' or 'ax'. Based upon the earlier MS3972/3 analysis, supported by a measure of common sense, an exit angle of 90 degrees (start of impulse line of action tangential to the escape wheel) will *initially* be incorporated within the example, although the devised CAD technique will accommodate any sensible alternative. The initial choice of geometry B exit angle will almost certainly be altered during the design process, when the escaping arc of geometry B is matched to the designer-chosen escaping arc of geometry A.

■ **The target end/start ratio, 'T', for both geometries.** Although any designer-chosen end/start ratio may be incorporated, a ratio of 3 to 2 will be adopted for the example, in agreement with earlier assumptions derived from Harrison's MS3972/3 single pivot and twin balance illustrations.

■ **The desired mean torque arm, M*.** For the purposes of explanation, an arbitrary target of 10 mm will suffice. Subsequent scaling of all linear dimensions (but no angles) using the speedy CAD scaling function will incorporate any mean torque arm, including those of MS3972/3, H1, H2 or H3 (although, in such cases, incorporation of the relevant escape wheel PCD would almost certainly be a more accurate, indirect means of generating the intended mean torque arm).

■ **The desired escaping arc, E*.** Any realistic arc may be chosen. In the earlier analysis, the escaping arc of MS3972/3 geometries A and B was assumed to be 18.5 degrees, which will be adopted for the example.

■ **The escaping arc resoultion.** To avoid unnecessary expenditure of time and effort, the designer should specify the minimum number of decimal places to which escaping arc must be determined. The CAD design technique will accomodate any realistic choice.

■ **The desired balance configuration.** Although geometrical constraints might enforce slight alterations, the designer must decide where the two balance axes should preferably be located. For the example, balance axes on horizontally opposite sides of the escape wheel axis will be the preferred arrangement, if only in the interests of consistent illustration and clear explanation. A vertical arrangement will also be considered.

DRAWING CONVENTIONS AND SUGGESTIONS

■ Numbers thus [NN] in the text refer to identical numbers [NN] in the illustrations.
■ **Essential CAD instructions are in bold font**. Most of the remaining text is mere amplification, explanation, suggestions or points of interest, all of which may be ignored, if so desired, without influencing the design process or altering the outcome.
■ Experience suggests that more straightforward execution and fewer mistakes should result if all geometries are created with the start of impulse escape wheel tooth tip located along a horizontal line through the escape wheel axis. For consistency, all CAD illustrations will locate the start of impulse tooth tip horizontally to the right of the escape wheel axis. Geometries A and/or B will eventually be relocated around a common escape wheel, such that they transmit their impulse to the designer-chosen balance configuration, or a configuration extremely close to the designer's choice, in a continuous, correctly functioning cycle.
■ In all relevant illustrations, **green indicates fresh start of impulse constructions, red indicates fresh end of impulse constructions and orange indicates fresh common (neither start nor end of impulse) constructions.** Other colours, **such as blue, will be used to emphasise especially relevant prior constructions,** with the exception of **various shades of grey, which are merely 'ghosts' of less relevant prior constructions**.
■ To avoid confusion, designers may wish to copy the labels used in the CAD sequence to their own CAD drawings, until sufficient familiarity with the geometry renders them unnecessary.
■ Normal escape wheel advancement is clockwise.
■ Recoil and supplementary arc are irrelevant to the creation of the geometries and are not included.
■ Composers are not represented. Their influence will only be acknowledged near then end of the design process, when determining instantaneous pallet nib lifts after release.
■ All drawings, CAD or otherwise, should be regarded as illustrative and not to scale. Of particular relevance, as warned earlier, transfer of TurboCAD Delux 15 drawings to *publishing* software has introduced unavoidable distortions and/or slight displacements of curves, circles, text and small circular points.
■ All lines are straight and all curves are segments of circular arcs, unless stated otherwise.
■ All dimensions are millimetres or degrees.

STEP ONE - Figure 51 - Applicable to geometry A, until instructed otherwise.

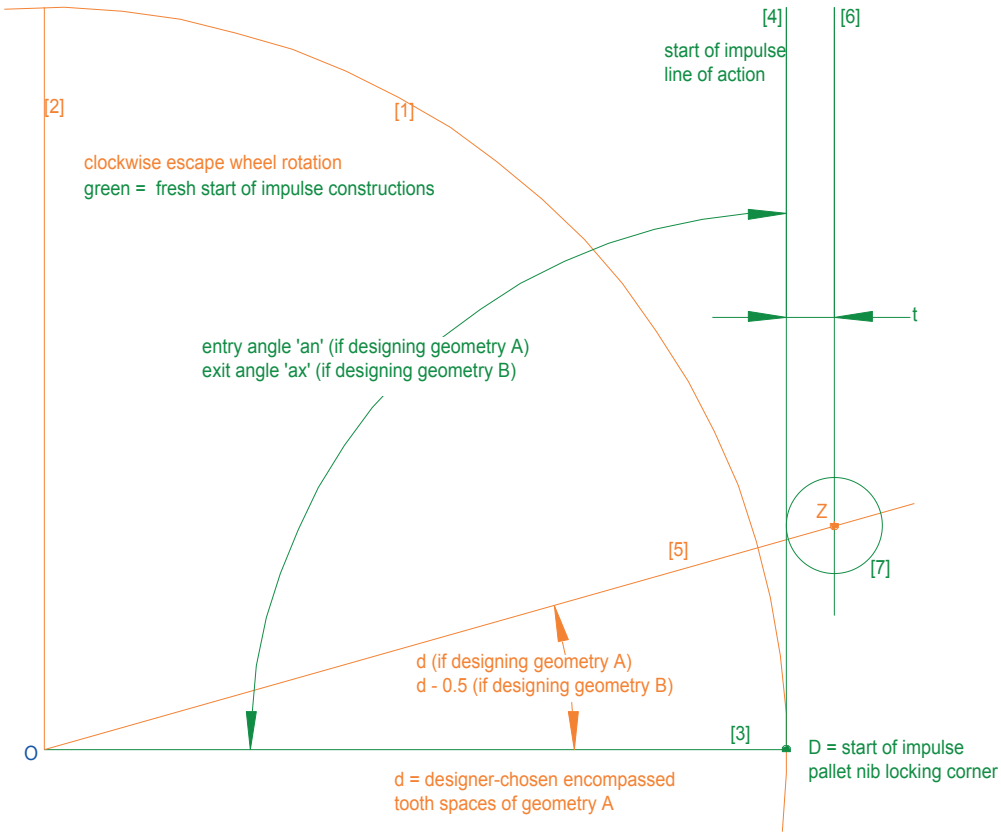

Apply all instructions to geometry A, until directed otherwise. Labelling is for geometry A, unless stated.

STEP ONE will include fresh **start** of impulse constructions, all in **green**.

■ **[1] - Construct a circular arc (shown in orange) of an arbitrary radius until instructed otherwise, with orientation and approximate extent as shown.** Arc [1] is part of the escape wheel teeth tips pitch circle, around which all teeth tips must travel. A radius of 100 mm was chosen for this example.
■ **[2] - Construct a vertical line (shown in orange), of any convenient length, upwards from the centre of arc [1].** This line, in combination with the next construction, will emphasise the escape wheel arbor axis, O.
■ **[3] - Construct a line (shown in green) starting from the centre of arc [1], extending horizontally to the right until it intersects arc [1].** The intersection of line [3] and arc [1] is labelled D. At the start of impulse, the pallet nib locking corner is captured by an escape wheel tooth tip located at point D.
■ **[4] - Until instructed otherwise, construct a line (shown in green) from point D, at the designer-chosen geometry A entry angle, 'an', to radial [3].** Line [4] defines the pallet arm line of action (i.e. direction of applied force) at the start of impulse. The chosen, illustrated angle between lines [3] and [4] is 90 degrees.
■ **[5] - Construct an extended escape wheel radial (shown in orange). Until instructed otherwise, the angle between radials [5] and [3] must be 'd', equivalent to the designer-chosen number of encompassed tooth spaces of geometry A, at the start of geometry A impulse.** As listed in DESIGNER CHOICES, the 5.25 encompassed tooth spaces of MS3972/3 geometry A at its start of impulse are incorporated and illustrated above. The illustrated angle 'd' is therefore 5.25 x 360 / 120 = 15.75 degrees.
■ **[6] - Construct a line (shown in green) parallel to line [4], separated from line [4] by the start of impulse torque arm, 't'. Until instructed otherwise, an arbitrary first choice of 't' for geometry A must be made.** An arbitrary 't' of 6.5 mm is incorporated within the illustrated geometry. The point of intersection of line [6] and line [5] defines a location of point Z, which represents the balance arbor axis. Until the incorporation of a specific start of impulse torque arm is instructed, the arbitrary choice of 't' is not critical, although pronounced deviations from the proportions of the above illustration are likely to demand greater corrective effort at a later stage in the design process.
■ **[7] - Construct a circle (shown in green), centred at Z, to which line [4] is tangential.** The radius of circle [7] is the start of impulse torque arm, 't', incorporated earlier. Circle [7] is therefore the start of impulse 'torque arm circle'.

STEP TWO - Figure 52 - Applicable to geometry A, until instructed otherwise.

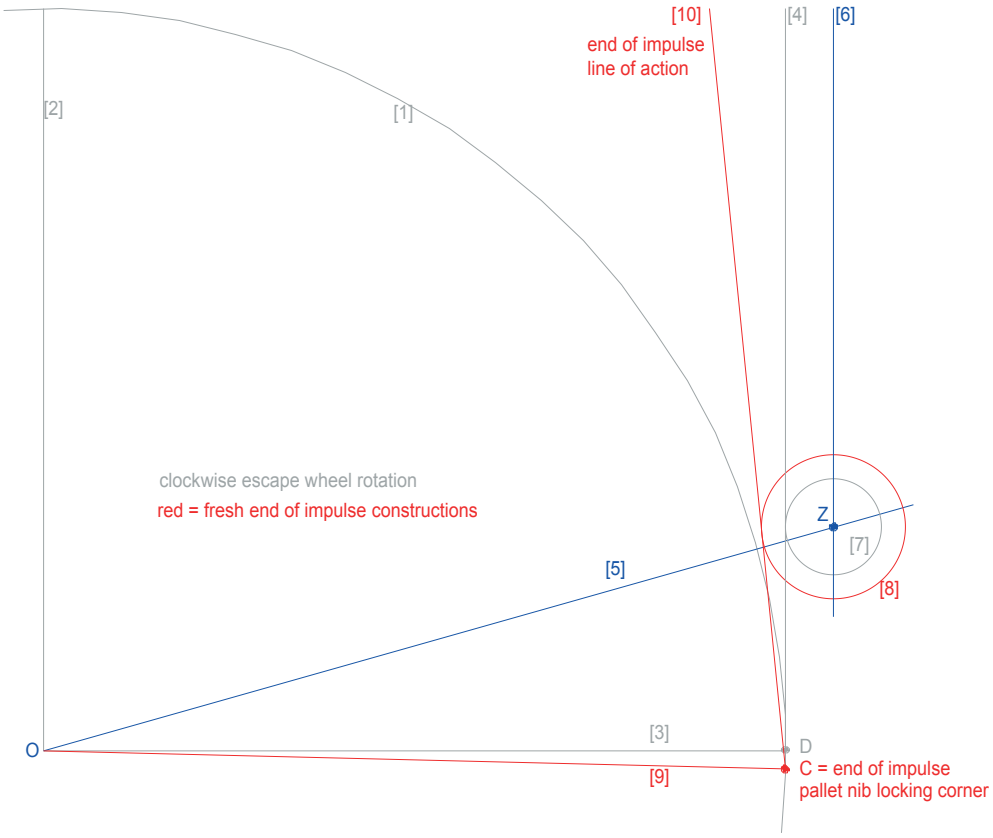

Apply all instructions to geometry A, until directed otherwise. All labelling is for geometry A.

STEP TWO will include fresh **end** of impulse constructions, all in **red**. Any constructions from STEP ONE (which are, therefore, not fresh) are reproduced in grey or emphasised in blue, regardless of their state of impulse (if any).

■ **[8] - Construct a circle (shown in red), centred at Z, of radius equal to the radius of the start of impulse torque arm circle, [7], multiplied by the designer-chosen end/start ratio, T.** Circle [8] is thereby the end of impulse torque arm circle. In the above illustration the STEP ONE radius of the start of impulse torque arm circle [7] was 6.5 mm and the designer-chosen end/start ratio T is 3 / 2 (as listed in DESIGNER CHOICES). The radius of the illustrated end of impulse torque arm circle [8] is therefore 6.5 x 3 / 2 = 9.75 mm. As a straightforward drawing alternative for T = 3 / 2, extend any radius of [7] by half of its length, whence the total length of the extended radial is the required radius of [8].

Note that the achieved mean torque arm is (6.5 + 9.75) / 2 = 8.125 mm, which fails to match the designer-chosen mean torque arm of 10 mm for this example. To avoid any risk of confusion during the CAD sequence, the achieved mean torque arm must **not** be altered until instructed.

■ **[9] - Construct a radial (shown in red) from the escape wheel axis O, clockwise removed from line [3] by half an escape wheel tooth space subtended angle.** For a 120 tooth escape wheel, half of the space between adjacent teeth tips subtends an angle of 0.5 (360 / 120) = 1.5 degrees between radials [3] and [9]. The point of intersection of line [9] with arc [1] is labelled C. Point C is the location of the captured pallet nib locking corner at the end of impulse, an immeasurably brief instant before release.

■ **[10] - Construct a straight line (shown in red) from point C, tangential to circle [8] as shown.** Line [10] defines the pallet arm line of action at the end of impulse, which correctly incorporates a torque arm about the balance axis, Z, equal to the radius of the end of impulse torque arm circle, [8].

OPTIONAL CHECKS FOR CARELESS ERRORS

The geometry could, if so desired, be checked for careless errors, before proceeding further. See CHECKING GEOMETRIES (page 67), completing whichever checks are relevant to the constructions created thus far. Checking may be repeated any number of times, at any stage of the CAD design process. No further reminders will be offered.

STEP THREE - Figure 53 - Applicable to geometry A, until instructed otherwise.

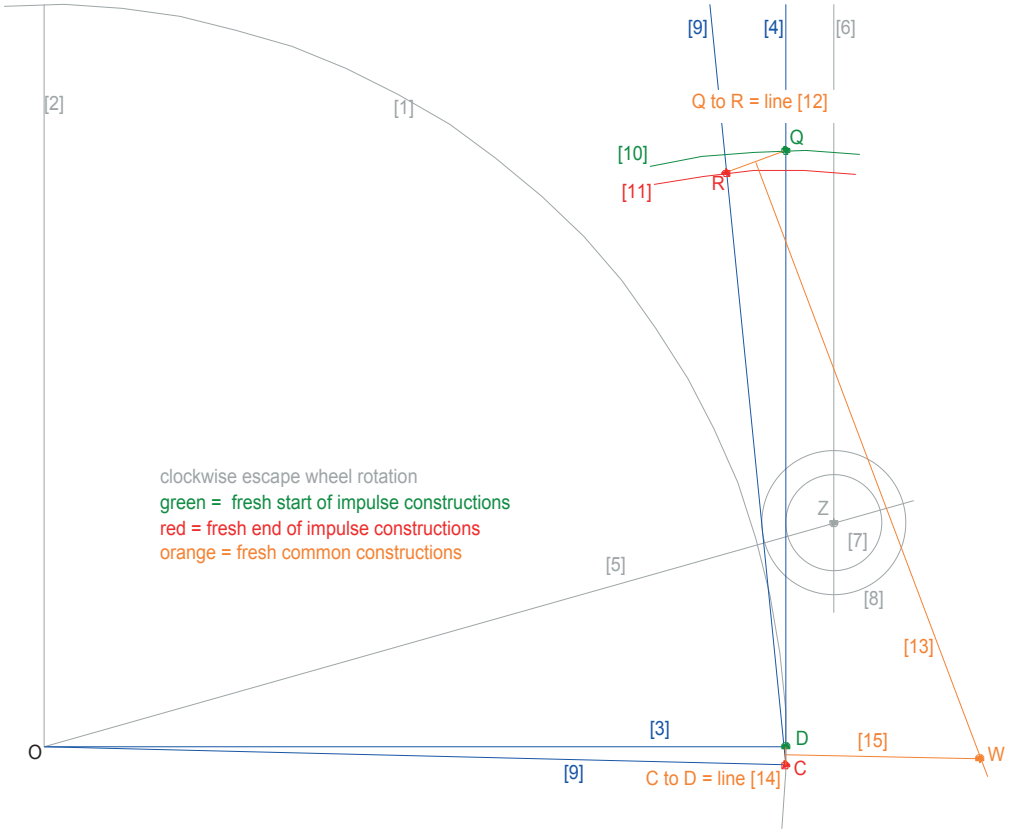

Apply all instructions to geometry A, until directed otherwise. All labelling is for geometry A.

■ **[10] - Construct a circular arc (shown in green), centred at D, of an arbitrary radius.** The radius of arc [10] is a first, arbitrary representation of the active length of the pallet arm. Since point D is the position of the pallet nib locking corner at the start of impulse, all potential pivot pin locations of the arbitrary pallet arm at the start of impulse lie along arc [10], or any sensible extensions of arc [10].
■ **[11] - Construct a circular arc (shown in red), centred at C, of the same radius as arc [10].** Since point C is the position of the pallet nib locking corner at the end of impulse, all potential pivot pin locations of the arbitrary pallet arm at the end of impulse lie along arc [11], or any sensible extensions of arc [11].
■ The intersection of start of impulse arc [10] and start of impulse line of action [4] is labelled Q. The intersection of end of impulse arc [11] and end of impulse line of action [9] is labelled R. For the matching, arbitrary radii of [10] and [11] and the illustrated lines of action, points Q and R define the locations of the pallet arm pivot at the start and end of impulse, respectively. DQ and CR are the corresponding start and end of impulse pallet arm active lengths, created equal in length by the above constructions.
■ **[12] - Construct a straight line (shown in orange) between point Q and point R.** Necessary for [13], next.
■ **[13] - Construct a straight line (shown in orange) from the mid point of line [12], perpendicular to line [12], extending as shown.** Any balance arbor axis located anywhere along perpendicular bisector [13] will be equidistant from points Q and R. The rigid connection between any chosen balance arbor and the pallet arm pivot will thereby be properly represented, which is essential for correct mechanical functioning of any escapement incorporating equal start and end of impulse pallet arm active lengths DQ and CR. It is, however, extremely unlikely that line [13] will be aligned with the chosen STEP ONE balance arbor axis, Z. Constructions [14] to [18] inclusive will resolve that misalignment, without altering the location of Z.
■ **The APPENDIX describes the basis of constructions [14] and [15] and point W.**
■ **[14] - Construct a straight line (shown in orange) from C to D.** As explained in the APPENDIX, *theoretically* valid pallet arms of zero active length are represented by points C and D.
■ **[15] - Construct a straight line (shown in orange) from the mid point of line [14], perpendicular to line [14], extending as far as line [13].** For methods other than CAD, or as an alternative CAD construction, it will be useful to note that an extension of line [15] (not illustrated) would pass through axis, O and bisect angle COD.
■ The intersection of lines [13] and [15] is labelled W. As concluded in the APPENDIX, for any pallet arm active length, line [15] and the appropriate construction of line [13] will define precisely the same location of point W.

STEP FOUR - Figure 54 - Applicable to geometry A, until instructed otherwise.

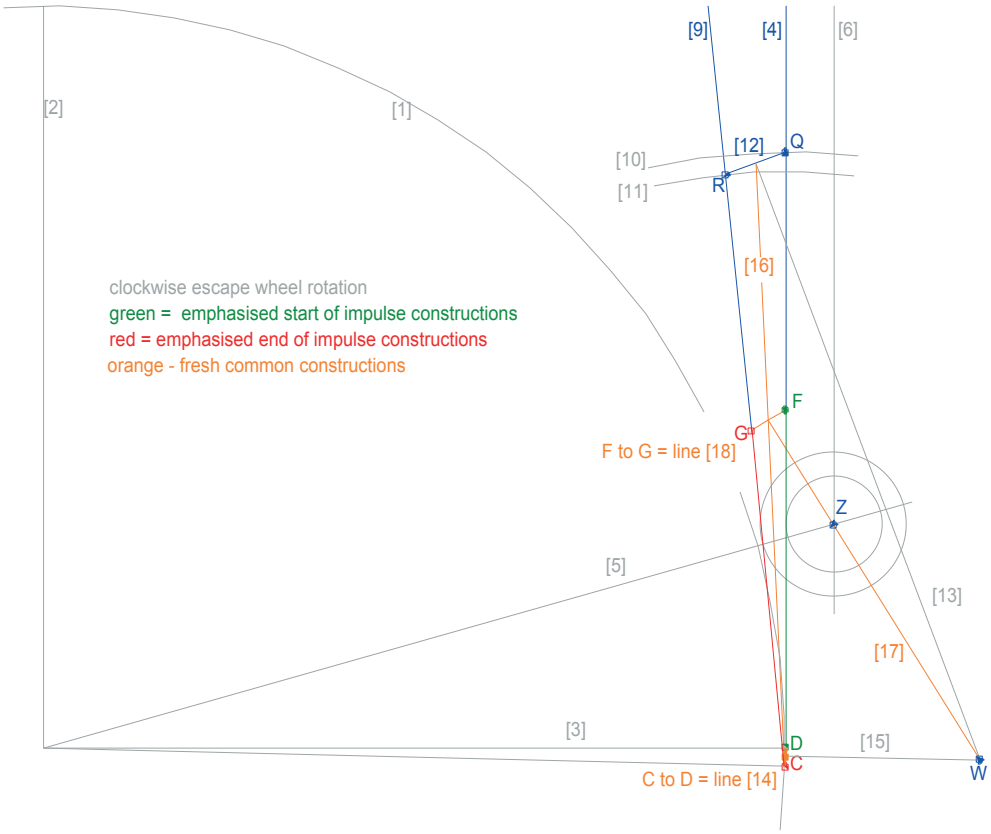

Apply all instructions to geometry A, until directed otherwise. All labelling is for geometry A.

■ The APPENDIX describes the basis of constructions [16], [17], [18], point F and point G.

■ [16] - Construct a straight line (shown in orange) from the mid point of orange line [14] (between C and D) to the mid point of line QR. The mid point of [14] is defined by a small orange dot and the mid point of QR is at the intersection of line [12] (from Q to R) and line [13]. Line [16] is the straight 'universal line of intersections', the invaluable properties of which are described in detail in the APPENDIX.
■ [17] - Construct a straight line (shown in orange) from point W, passing through point Z and extending beyond Z until it intersects the 'universal line of intersections' [16].
■ [18] - Construct a straight perpendicular to line [17] (shown in orange), passing through the point of intersection of lines [16] and [17] and extending to the lines of action [4] and [9]. By virtue of the properties of the 'universal line of intersections', line [18] is simultaneously valid for axis Z and axis W,
■ The intersection of lines [4] and [18] is labelled F. For a balance arbor axis located at Z or W, point F is the pallet arm pivot location at the start of impulse and DF is the pallet arm active length at the start of impulse.
■ The intersection of lines [9] and [18] is labelled G. For a balance arbor axis located at Z or W, point G is the pallet arm pivot location at the end of impulse and CG is the pallet arm active length at the end of impulse.

By virtue of the universal properties of point W, explained in detail in the APPENDIX, the distance from C to G will be identical to the distance from D to F. Representations of the pallet arm active lengths of the geometry at the start and end of impulse are thereby equal, as necessary (amongst other things) for correct functioning. Furthermore, since line [17] is a perpendicular bisector of line [18] (from F to G), the distance from F to Z will be identical to the distance from G to Z. Representations of the rigid connection between STEP ONE axis Z and the pallet arm pivot positions at the start and end of impulse are thereby equal, as necessary (amongst other things) for correct functioning.

Since the location of STEP ONE axis Z and the directions of the start and end of impulse lines of action have been entirely unaffected by constructions [14] to [18], the STEP TWO designer-chosen end/start ratio and the mean torque arm generated by STEPS ONE and TWO (calculated in STEP TWO to be 8.125 mm for this example) have been preserved.

STEP FIVE - Figure 55 - Applicable to geometry A, until instructed otherwise.

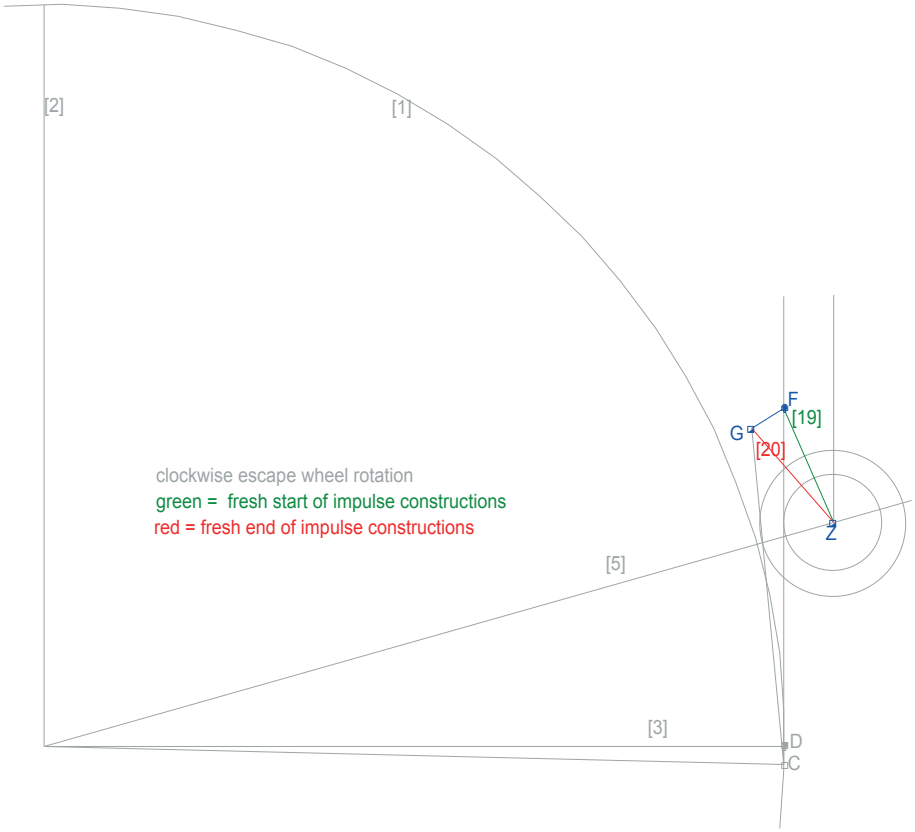

Apply all instructions to geometry A, until directed otherwise. All labelling is for geometry A.

Redundant prior constructions have been removed.

■ **[19] - Construct a straight line (shown in green) from point Z to point F.** Line [19] represents the connection between the balance arbor axis and the pallet arm pivot at the start of impulse.

■ **[20] - Construct a straight line (shown in red) from point Z to point G.** Line [20] represents the connection between the balance arbor axis and the pallet arm pivot at the end of impulse.

■ **Measure angle FZG -** This angle, between the start of impulse line [19] and the end of impulse line [20], is the escaping arc of the constructed geometry. In the above illustration, the measured escaping arc is slightly less than 18.5 degrees, which fails to match the designer-chosen arc of 18.5 degrees. A proven method of adjustment is explained in STEP SIX.

STEP SIX - Figure 56 - Only applicable to geometry A, *never* to geometry B

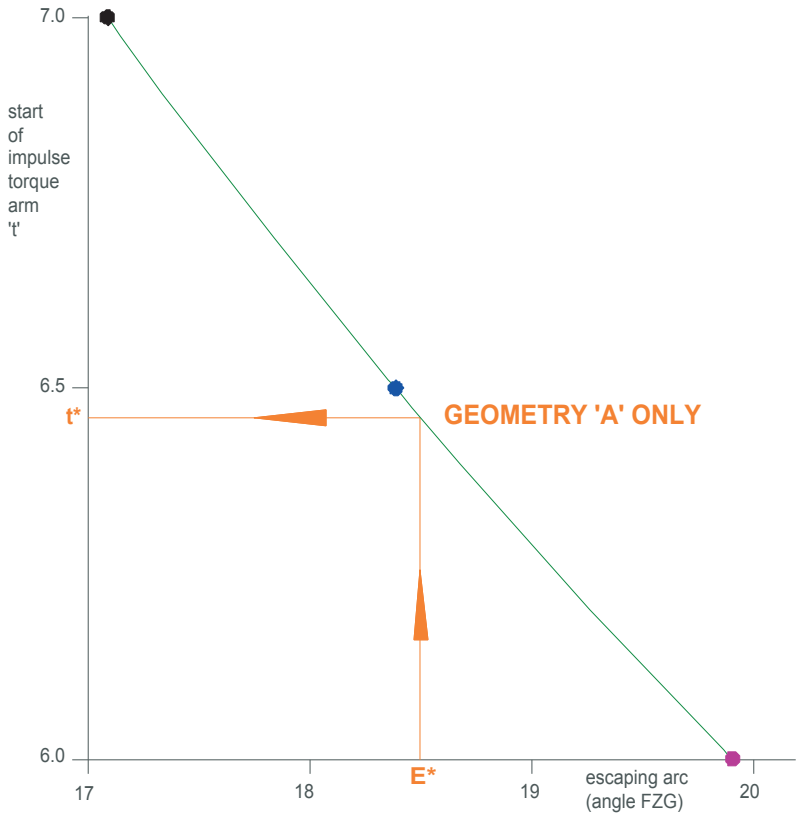

STEP SIX is only applicable to geometry A, *never* to geometry B. All labelling is for geometry A.

■ **- If the STEP FIVE escaping arc, FZG, fails to match the designer-chosen target with the desired degree of precision, create a plot of the STEP ONE start of impulse torque arm, 't', versus the corresponding STEP FIVE escaping arc, FZG.** Experience suggests that CAD software set to a resolution of ten decimal places is suitable for the accurate plotting of points. In the above illustration, only the blue point may thereby be created at this stage, representing (for this example) a STEP ONE dimension 't' of 6.5 mm and a corresponding STEP FIVE escaping arc, FZG, of slightly less than the designer-chosen target of 18.5 degrees.

■ **- Repeat CAD design STEPS ONE to FIVE for at least two more arbitrary choices of geometry A STEP ONE start of impulse torque arm, 't'.** This enables two further plots of STEP ONE 't' versus the corresponding STEP FIVE escaping arc, FZG, to be added to the above. Intelligent choices of STEP ONE 't' could minimise the expenditure of time and effort, the objective being to determine the single value of FZG matching the designer-chosen escaping arc. For this example, since the first, blue point is already very close to the designer-chosen escaping arc target of 18.5 degrees, two arguably sensible choices of STEP ONE 't' are 6.0 mm and 7.0 mm, since they encompass and are quite close to the target region. Those choices of 't' and the corresponding STEP FIVE outputs of escaping arc FZG are represented by the violet and black points in the above plot.

■ **- Fit an accurate curve to the plotted points.** Typical CAD software usually includes a convenient curve drawing tool (e.g. Bezier), which should be worthy of consideration.

■ **- Input the designer-chosen escaping arc, E*, represented in the above illustration by the vertical orange line.** For this example, the designer-chosen escaping arc, E*, of 18.5 degrees has been input.

■ **- Extract the geometry A start of impulse torque arm, t*, corresponding to the designer-chosen escaping arc, E*.** In the above illustration, a horizontal orange line is constructed from the point of intersection of the vertical orange line through E* with the green curve, thereby identifying the corresponding start of impulse torque arm, illustrated and referred to as t*. For this example t* is slightly less than 6.5 mm.

STEP SEVEN - Figure 57 - Only applicable to geometry A, *never* to geometry B

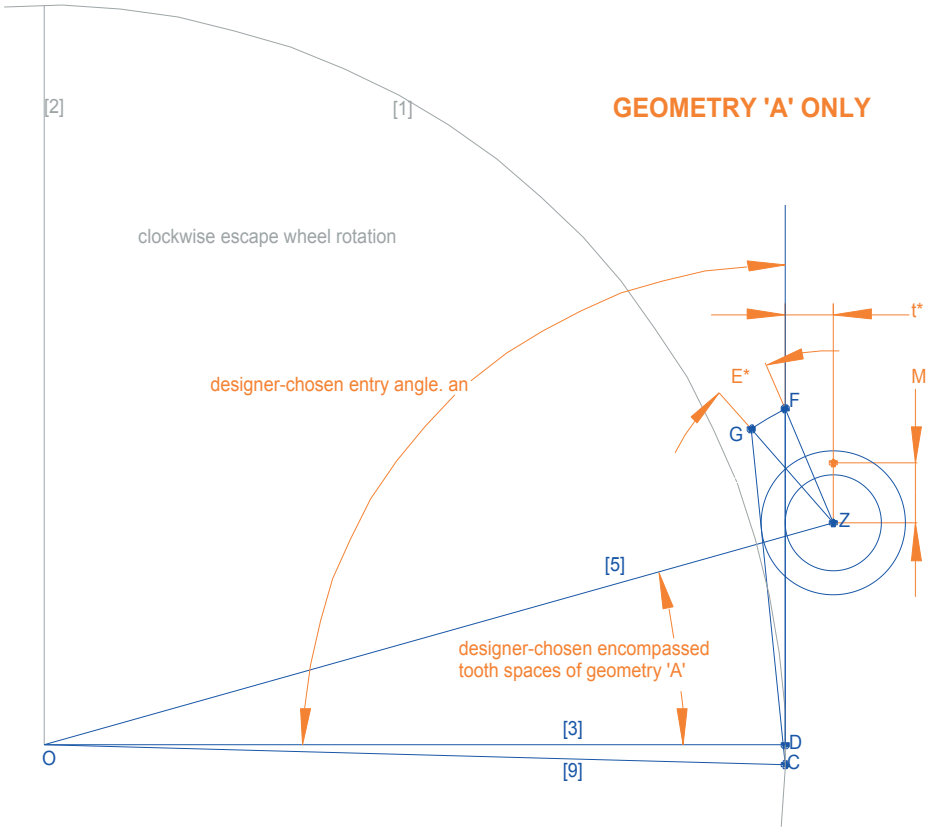

STEP SEVEN is only applicable to geometry A, *never* to geometry B. All labelling is for geometry A.

■ **(i) Repeat STEPS ONE to FIVE, incorporating start of impulse torque arm, t*, whilst maintaining all other chosen dimensions and counts, except (of course) escaping arc.** The designer-chosen escaping arc, E* (which, for this example, should be 18.5 degrees), will automatically emerge, with an accuracy related to the precision with which t* was determined in STEP SIX. The original choices of (for this example) escape wheel tooth count (120), escape wheel pitch circle radius (100 mm), number of encompassed tooth spaces at the start of impulse (5.25), entry angle (90 degrees between DF and OD) and end/start ratio (3 / 2) will all be preserved.

■ **(ii) Refine the geometry, if considered necessary.** Although a single completion of STEP SIX and instruction (i), above, may well be adequate, greater precision may be achieved by repeating STEP SIX and (i) for at least two more geometries with STEP ONE start of impulse torque arms extremely close to and to either side of t*. Plots of 't' versus escaping arc for those two additional geometries (not illustrated) should be added to the existing STEP SIX plots and the green STEP SIX curve redrawn to include all plotted points. The curve is thereby refined in the target region, more precisely defining the value of t* corresponding to E*. A repetition of instruction (i), above, for the more precisely determined t* will determine the exact value of the more precisely generated escaping arc, E*. The refinement process may be repeated as many times as considered necessary, limited only by the maximum resolution of the chosen CAD software and, of course, the adopted plotting and curve fitting techniques.

■ **(iii) Determine and record the mean torque arm, M, of the geometry.** For any twin balance grasshopper escapement geometry, the mean torque arm is the mean of the start of impulse torque arm and the end of impulse torque arm. Either measure the radii of the start and end of impulse torque arm circles and calculate the mean, or, as an entirely CAD alternative, construct any radial to both torque arm circles, bisect the portion of the radial between those circles and measure the radius of the bisecting point. The mean torque arm is dimension M in the above illustration.

To avoid any risk of confusion, the designer-chosen mean torque arm (10 mm for this example) will not be incorporated until the end of the design process. That aside, **the above illustration represents the optimised, designer-chosen form of geometry A.**

STEP EIGHT - Figure 58 - Only applicable to geometry B, *never* to geometry A

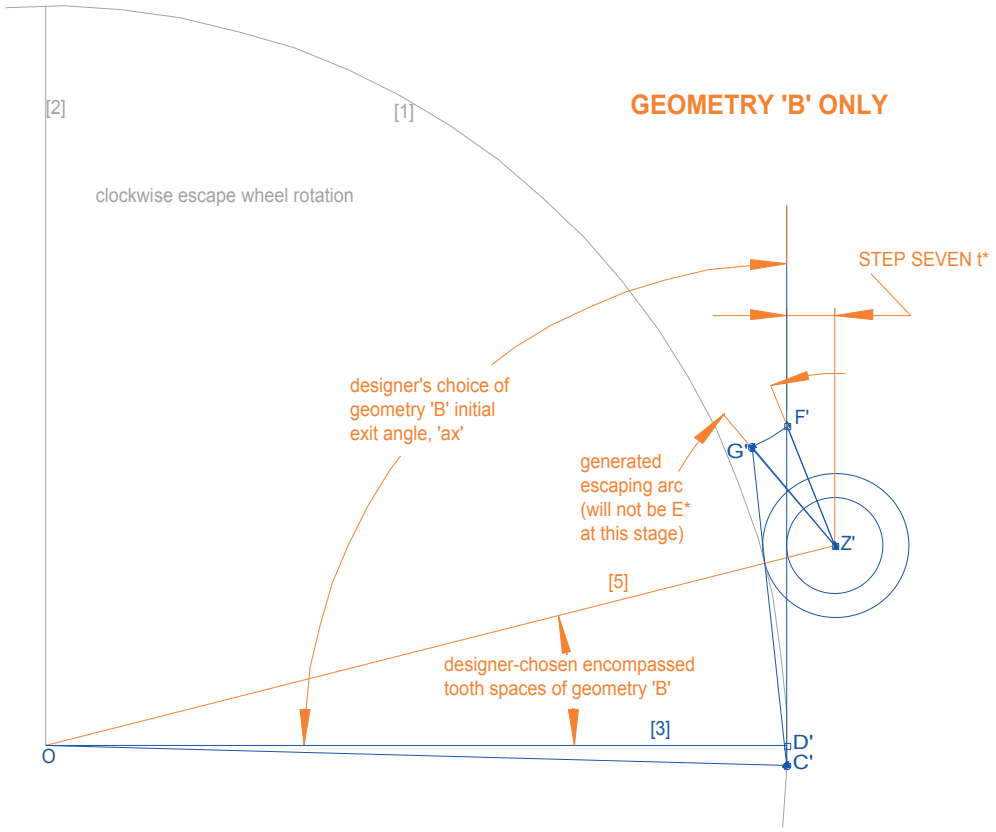

STEP EIGHT is only applicable to geometry B, *never* to geometry A. All labelling is for geometry B.

Designer-chosen mean torque arm aside, STEPS EIGHT to TEN will create an optimised geometry B, which is entirely compatible with the optimised geometry A defined in STEP SEVEN.

■ - Repeat STEPS ONE to FIVE, incorporating the designer's initial choice of geometry B exit angle, 'ax' until instructed otherwise and the designer's choice of start of impulse encompassed tooth spaces for geometry B. All other STEP SEVEN geometry A dimensions and counts must otherwise be incorporated, including the optimised STEP SEVEN geometry A start of impulse torque arm, t*.

For this example, the illustrated geometry B is the outcome of STEPS ONE to FIVE of the CAD sequence, incorporating the initial, designer-chosen geometry B exit angle, 'ax', of 90 degrees and the designer-chosen encompassed tooth spaces of 4.75 tooth spaces at the start of geometry B impulse. Those 4.75 encompassed tooth spaces subtend an angle of 4.75 x (360 / 120) = 14.25 degrees between lines [3] and [5].

The designer must also incorporate the designer-chosen STEP SEVEN, geometry A escape wheel tooth count (120 for this example), escape wheel pitch circle radius (100 mm for this example), end/start ratio (3 / 2 for this example) and optimised start of impulse torque arm, t* (slightly less than 6.5 mm from STEP SIX, for this example).

To avoid any risk of confusion, the designer-chosen mean torque arm will not be incorporated until the end of the design process.

MISMATCHED ESCAPING ARCS

As a consequence of the difference between the encompassed tooth spaces of geometries A and B, together with any differences between the designer's choices of entry angle, 'an' and initial exit angle, 'ax', the escaping arc of geometry B, illustrated above as F'Z'G', will (except by extremely unlikely chance) fail to match the designer-chosen escaping arc, E*, already successfully incorporated within optimised STEP SEVEN geometry A. For this example, the geometry B escaping arc illustrated above is slightly less than 18.505 degress, which fails (albeit by an extremely small margin in this case) to match the designer-chosen and achieved STEP SEVEN geometry A escaping arc of 18.5 degrees. A proven method of correcting the mismatch is offered in STEP NINE.

STEP NINE - Figure 59 - Only applicable to geometry B, *never* to geometry A

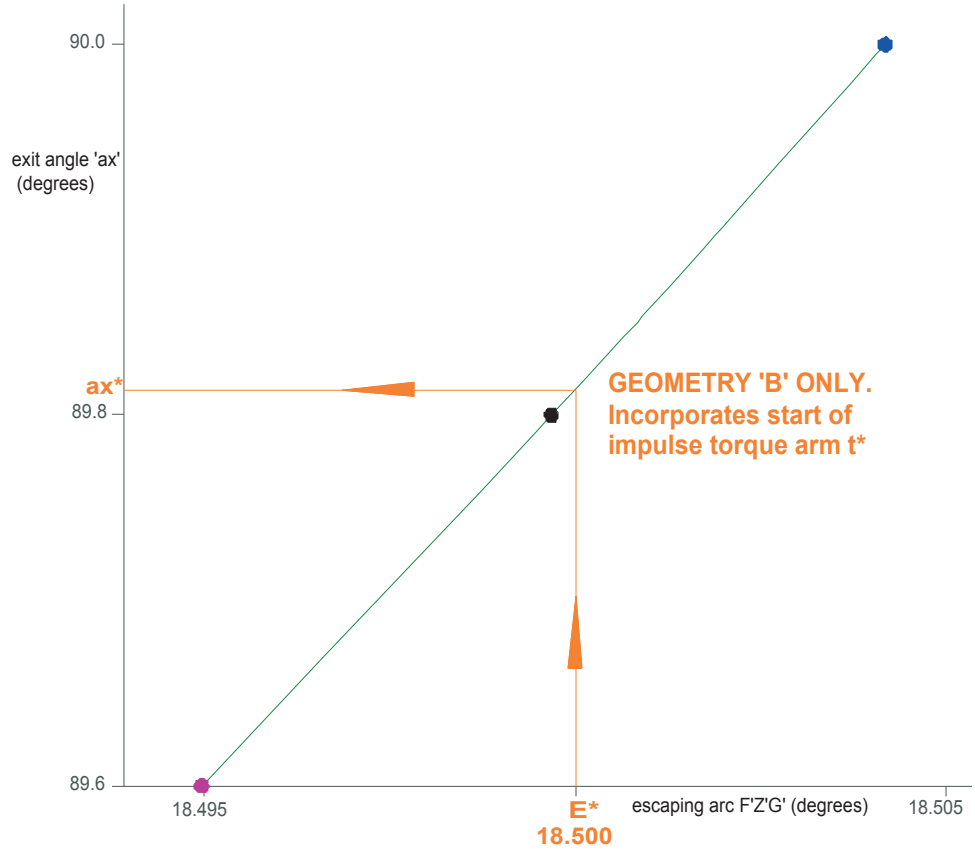

STEP NINE is only applicable to geometry B, *never* to geometry A. All labelling is for geometry B.

■ **- If the generated STEP EIGHT geometry B escaping arc, angle F'Z'G', fails to match the designer-chosen target, E*, create a plot of the STEP EIGHT exit angle, 'ax', versus the corresponding escaping arc, F'Z'G'.** Experience suggests that CAD software set to a resolution of ten decimal places is suitable for the accurate plotting of points. For this example, only the blue point in the above illustration may thereby be created at this stage, representing a STEP EIGHT designer-chosen initial exit angle, 'ax', of 90 degrees and a corresponding STEP EIGHT escaping arc, F'Z'G', of slightly less than 18.505 degrees. The designer-chosen target, E*, of 18.5 degrees has therefore *not* been achieved.

■ **- Repeat STEP EIGHT for at least two more choices of exit angle, enabling further plots of exit angle versus the corresponding STEP EIGHT escaping arc.** Sensible choices of exit angle could minimise the expenditure of effort, the objective being to determine the single exit angle corresponding to the designer-chosen escaping arc, E*. For this example, since the escaping arc of the blue point is greater than the designer-chosen target of 18.5 degrees, two arguably sensible choices of exit angle are 89.8 and 89.6 degrees, which direct the two additional plots (illustrated as black and violet dots) in the direction of the target escaping arc of 18.5 degrees.

■ **- Fit an accurate curve to the plotted points.** Typical CAD software usually includes a convenient curve drawing tool (e.g. Bezier), which should be worthy of consideration.

■ **- Input the designer-chosen escaping arc, E*, represented in the above illustration by the vertical orange line.** For this example, the designer-chosen escaping arc, E*, of 18.5 degrees is input.

■ **- Extract the geometry B exit angle corresponding to the designer-chosen escaping arc, E*, illustrated above as ax*.** In the above illustration, a horizontal orange line is constructed from the point of intersection of the vertical orange line through E* with the green curve, thereby identifying the corresponding exit angle, ax*. For this example ax* is slightly greater than 89.8 degrees.

■ **- Refine the geometry, if considered necessary.** A single execution of the above process may well suffice. If considered necessary, however, greater precision may be achieved by repeating STEP NINE for at least two more choices of exit angle extremely close to ax*. Those further choices and the existing plot of exit angle versus escaping arc will enable a more refined curve fit in the target region and a more accurate determination of ax*. The process of refinement may be repeated as many times as considered necessary, limited only by the maximum resolution of the chosen CAD software and, of course, the adopted plotting and curve fitting techniques.

STEP TEN - Figure 60 - Only applicable to geometry B, *never* to geometry A

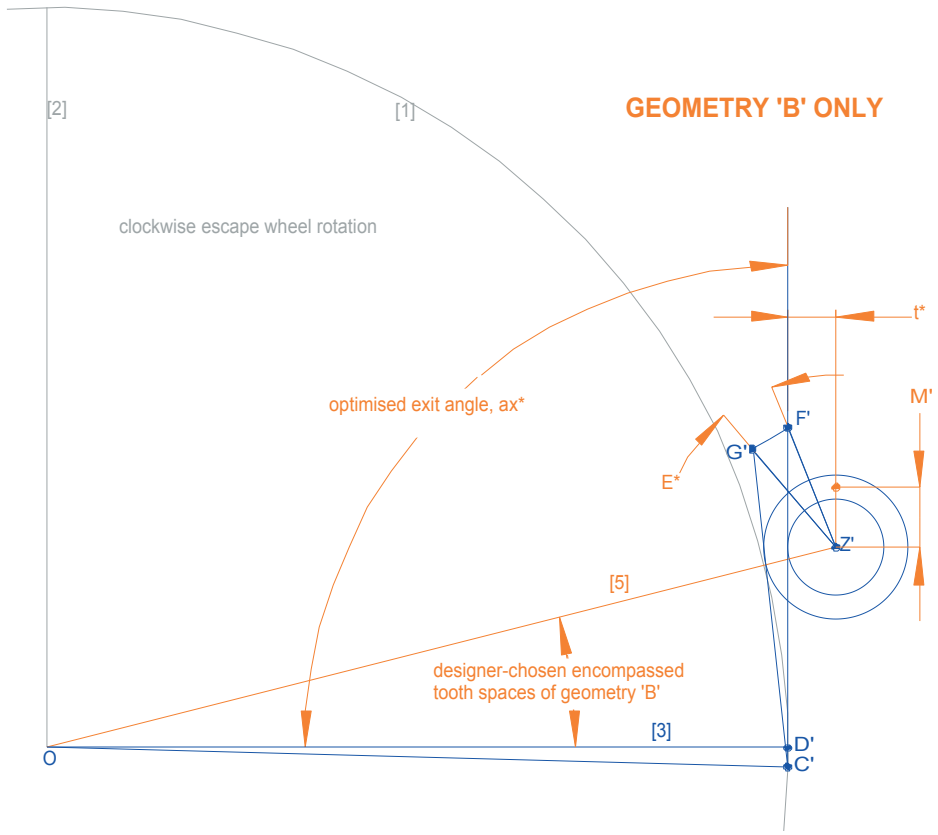

STEP TEN is only applicable to geometry B, *never* to geometry A. All labelling is for geometry B.

■ **- Evaluate ax*** - Despite the deficiencies of MS3972/3, identified earlier, it is apparent that Harrison's geometry B exit angle is at least extremely close to ninety degrees. Should compliance with the intentions of MS3972/3 be the objective (as it was for this example), it is proposed that an arbitrary maximum exit angle deviation of two degrees from ninety degrees be observed, although opinions may differ.

Should the optimised geometry B exit angle, ax*, deviate from the initial designer choice by more than the proposed two degrees, it will be necessary to impose a higher or lower number of geometry B encompassed tooth spaces. In the interests of simplicity, the encompassed tooth spaces of geometry B should always be **less** than the encompassed tooth spaces of geometry A by an odd integer multiple of half a tooth space. To satisfy that condition following an increase in the encompassed tooth spaces of geometry B, an increase in the encompassed tooth spaces of geometry A might be necessary. Although alternative methods of correction (not described) may be more efficient, they may complicate the CAD design process to an unacceptable extent and should, in the author's opinion, be avoided.

■ **- When the deviation of ax* from the designer's intial choice of exit angle is within the proposed two degrees, repeat STEPS ONE to FIVE, incorporating the STEP NINE exit angle, ax*, whilst preserving all other dimensions and counts.** The above geometry B is the outcome for the chosen example. Take care to input the designer's choices of escape wheel tooth count (120 for this example), escape wheel pitch circle radius (100 mm for this example), end/start ratio (Harrison's 3 / 2 for this example), STEP SEVEN geometry A start of impulse torque arm, t* and the geometry B encompassed tooth spaces at the start of impulse (4.75 for this example). By incorporating the end/start ratio from STEP TWO and the geometry A start of impulse torque arm, t*, from STEP SEVEN, the mean torque arm of the the above geometry B (illustrated as dimension M') will match the mean torque arm, M, of STEP SEVEN geometry A. The designer-chosen escaping arc, E* (18.5 degrees) will be automatically generated, with a precision related to the accuracy with which ax* was determined in STEP NINE.

The designer-chosen mean torque arm (10 mm for this example) will be incorporated next. That aside, **the above illustration represents the optimised, designer-chosen form of geometry B.**

MEAN TORQUE ARM ADJUSTMENT

Upon completion of the CAD sequence, the mean torque arm, M, of STEP SEVEN geometry A will match the mean torque arm, M', of STEP TEN geometry B. Except by extremely unlikely chance, however, those mean torque arms will fail to match the target, designer-chosen mean torque arm, referred to as M*. All linear dimensions (but no angles) of both sub-geometries must therefore be scaled, using the speedy and convenient CAD scaling function set to a ratio of M* / M. Since the geometry A and geometry B escape wheel PCD were created equal during the CAD sequence, the scaling of both of those PCD by the ratio M* / M will preserve their equality. A twin balance grasshopper escapement combining scaled geometries A and B will therby function as intended in combination with a common escape wheel of the scaled PCD.

Figure 61 illustrates optimised STEP SEVEN geometry A in blue and optimised STEP TEN geometry B in violet, after both have been scaled to deliver the designer-chosen mean torque arm, M* (10 mm for this example).

As a consequence of the necessary differences between geometries A and B, the separation of the balance arbor axis and the escape wheel arbor axis of geometry A is slightly greater than the separation of the balance arbor axis and the escape wheel arbor axis of geometry B, as emphasised in Figure 61 by two orange arcs centred at the escape wheel axis.

Despite the deficiencies of the original or copied MS3972/3 (identified in PART ONE), the two orange arcs in Figure 61 match two black arcs in Harrison's illustration (see Figure 50, page 49). It is, of course, quite likely that Harrison took some care to at least ensure the correct relative proportions of those arcs. It is also not entirely impossible that he could have directly manipulated their radii, in order to adjust his sub-geometries in a controlled manner, although the MS3972/3 single pivot analysis in PART ONE demonstrated that direct manipulation of the exit angle was a favoured and clearly emphasised method of alteration. Based upon such conclusions, the sole intention of Harrison's arcs would have been identical to their only purpose in Figure 61, which is to reveal and emphasise the slight (and otherwise inconspicuous) difference between the separations of the balance arbor axis and the two escape wheel arbor axes. Such observations add further support to an earlier proposal that Harrison's original intention for MS3972/3 was as an accompanying illustration to a separate, written explanation.

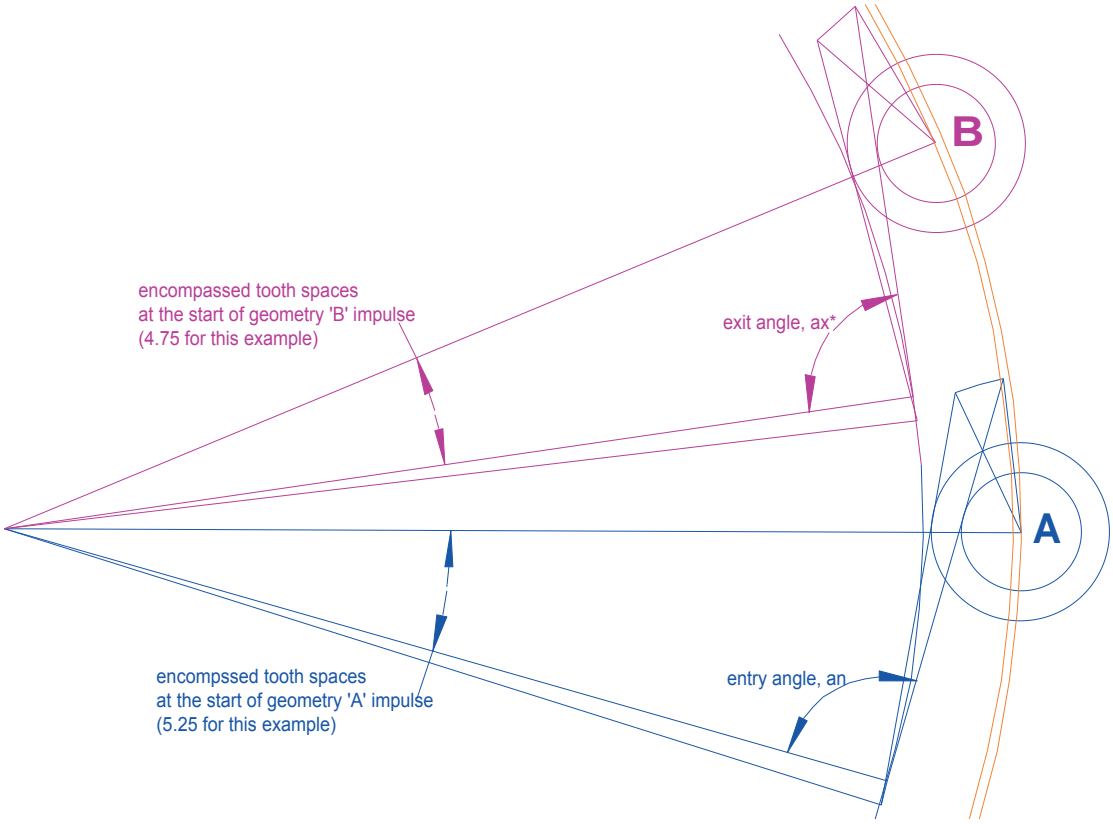

Figure 61 - Final designer-chosen geometries A and B, scaled to the designer-chosen mean torque arm (10 mm for this example) and arranged as per MS3972/3

DETERMINING INSTANTANEOUS PALLET NIB LOCKING CORNER LIFTS

Of relevance to optimum trip protection, sound mechanical design and functionality, the instantaneous (zero travel time) entry geometry A and exit geometry B pallet nib locking corner **'lifts'** after release from the escape wheel should be determined. Excessive nib lift might, for example, offer less than ideal trip protection by restricting nib length, whilst the lower extremes of lift are less forgiving of slight errors in adjustment, leading to unreliable operation and a tendency to trip, permitting escape wheel runaway.

Figure 62 reproduces geometries A and B of Figure 61, separated vertically to avoid confusion. Recall that both sub-geometries were scaled to deliver the designer-chosen mean torque arm, M*, which is essential preparation. CAD sequence labelling is used.

Pallet nib locking corner lift may be determined for entry geometry A (lower illustration) by constructing circular arcs through D centred at Z (shown in black) and through C centred at the end of impulse pallet arm pivot location G (in red). For exit geometry B (upper illustration) equivalent circular arcs through D' centred at Z' (shown in black) and through C' centred at the end of impulse pallet arm pivot location G' (in red) are appropriate. Assuming instantaneous (zero travel time) free motions after release, points Q and Q' represent the positions of the nib locking corners when the pallet arms are halted by their composer springs. The instantaneous pallet nib locking corner lifts are therefore defined by the straight-line separations of D and Q in geometry A and of D' and Q' in geometry B.

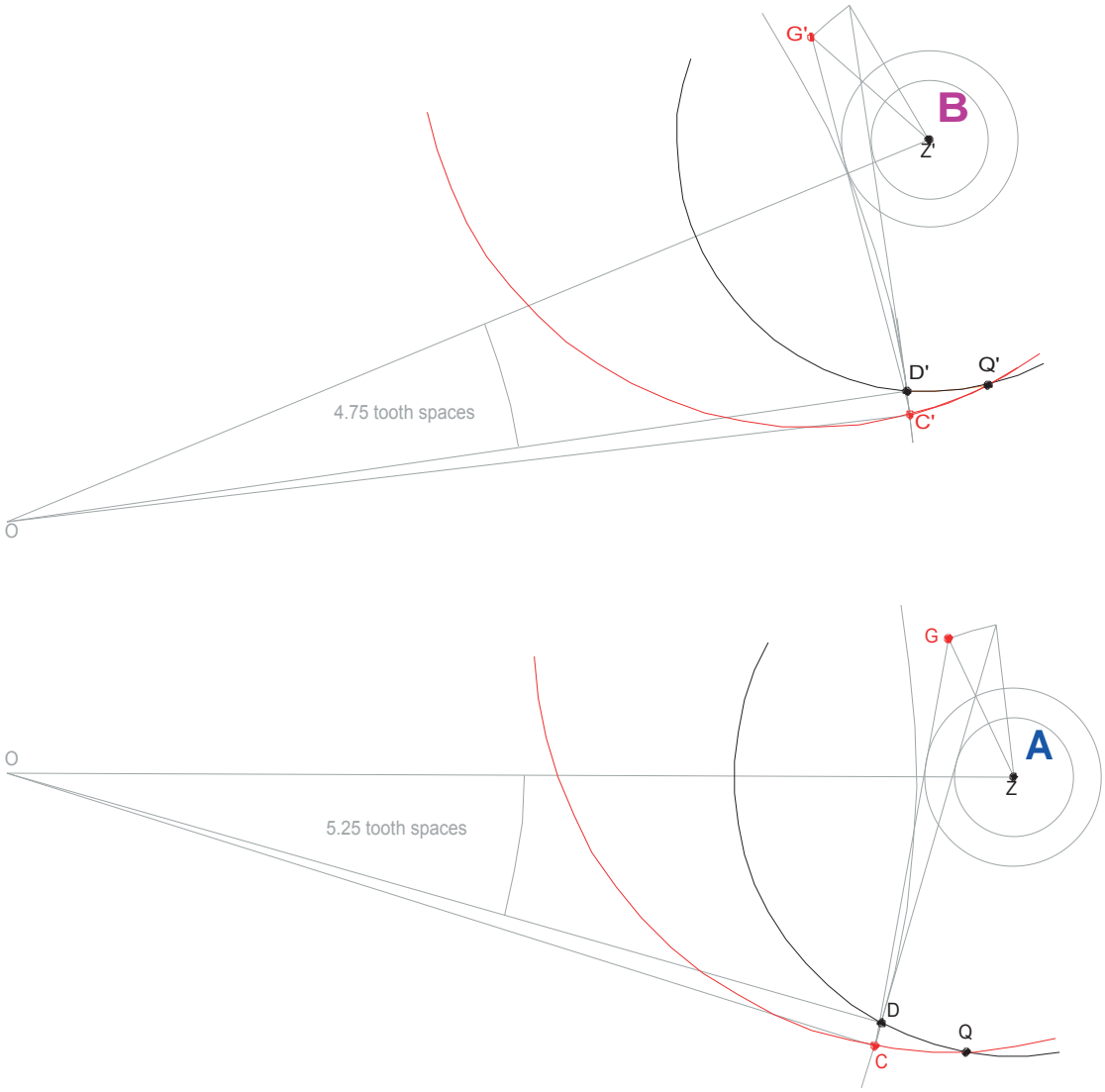

Figure 62 - Determining instantaneous pallet nib lifts DQ (geometry A) and D'Q' (geometry B)

UNITING GEOMETRIES A and B

Figure 63, drawn to a smaller scale than Figure 61 to suit the page width, places geometries A and B in correctly functioning positions around a common escape wheel, the irrelevant upper and lower segments of which are not illustrated. One hundred and twenty equally spaced teeth tips are represented by the intersections of **dark grey** radials with the escape wheel pitch circle, except for single blue, orange and violet escape wheel radials, each emphasised by three small dots. **Green** text, lines and labels represent **start** of impulse features and **red** text, lines and labels represent **end** of impulse features. The escape wheel normally advances clockwise.

Recall that, for the designer-chosen CAD example, the encompassed tooth spaces at the **start** of impulse are **5.25** for geometry A and **4.75** for geometry B. The **end** of impulse encompassed tooth spaces are therefore (**5.25** + 0.5) = **5.75** for geometry A and (**4.75** + 0.5) = **5.25** for geometry B. Those tooth counts may be verified by counting clockwise from a straight horizontal through the balance arbor axes, Z and Z', noting that ZZ' passes through the escape wheel arbor axis, O and (by virtue of deliberate rotation of the escape wheel) through diametrically opposite escape wheel teeth tips. In accordance with the above encompassed tooth spaces, radials DO, D'O, CO and C'O are each displaced 0.25 of a tooth space from their nearest escape wheel tooth tip radial.

If the escape wheel is rotated 0.25 of a tooth space clockwise from the illustrated position, the escape wheel tooth tip defined by the short blue radial will align with D, which is the location of the pallet nib locking corner at the **start** of geometry A impulse. In addition, the escape wheel tooth tip defined by the short orange radial will align with C', which is the location of the pallet nib locking corner at the **end** of geometry B impulse. A correctly functioning coincidence of those two impulse events is thereby confirmed. At that instant, the span of the escapement pallet nib locking corners, measured clockwise from D to C', is (120/2 - **5.25** + **5.25**) = **60 whole tooth spaces**.

If the escape wheel is rotated *further* clockwise by 0.5 of a tooth space (i.e. a total of 0.25 + 0.5 = 0.75 of a tooth space clockwise from the *illustrated* position), the escape wheel tooth tip defined by the short blue radial will coincide with C, which is the location of the pallet nib locking corner at the **end** of geometry A impulse. In addition, the escape wheel tooth tip defined by the short violet radial will align with D', which is the location of the pallet nib locking corner at the **start** of geometry B impulse. A correctly functioning coincidence of those two impulse events is thereby confirmed. At that instant, the span of the escapement pallet nib locking corners, measured clockwise from C to D', is (120/2 - **5.75** + **4.75**) = **59 whole tooth spaces**.

From a combination of the above, the mean span of the escapement is **0.5 (60 + 59) = 59.5 whole tooth spaces**, measured clockwise from geometry A to geometry B. Since the mean span differs from a whole number of tooth spaces by half a tooth space, the illustrated arrangement of geometries A and B will function correctly, in continuously repeating cycles. Figure 63 is, therefore, a correctly functioning reconfiguration of Harrison's dysfunctional MS3972/3 illustration of two entirely separate twin balance sub-geometries, as explained in detail in '8 - ENTIRELY SEPARATE SUB-GEOMETRIES' (page 51).

Common sense and accepted convention suggest that the mean span of any escapment should be less than half of the escape wheel tooth count. For the 59.5 tooth spaces mean span of Figure 63, therefore, **geometry A** should be referred to as the **'entry'** geometry and **geometry B** should be referred to as the **'exit'** geometry. As promised earlier, in '1 - PALLET ARMS LINES OF ACTION' (pages 48 and 50), this explains the adopted terms '**entry** geometry' and '**entry** angle' for **geometry A** and '**exit** geometry' and '**exit** angle' for **geometry B**.

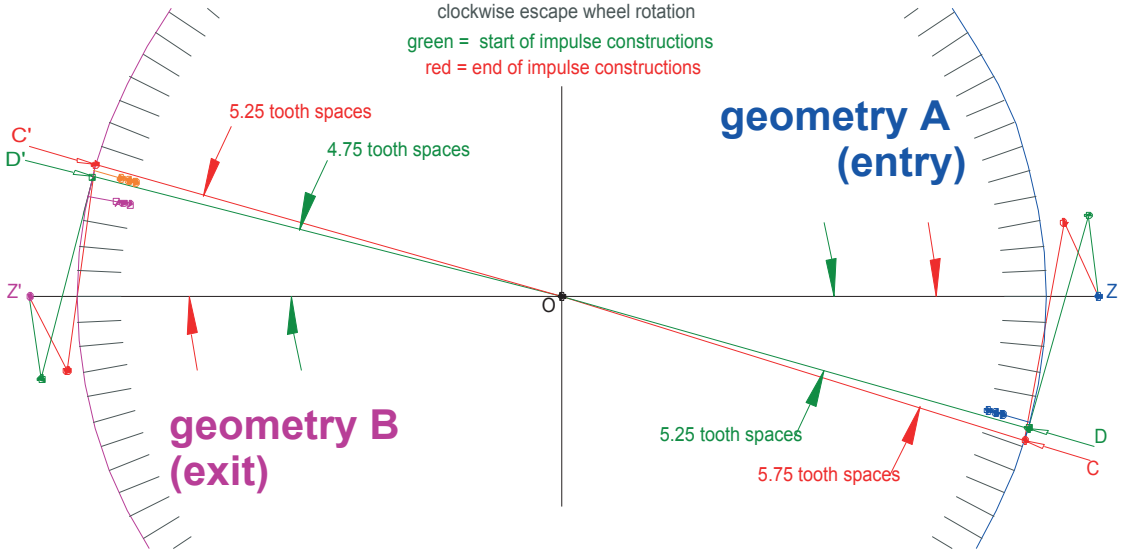

Figure 63 - Correctly functioning arrangement of balance axes and associated sub-geometries.

MS3972/3 AND SEA CLOCK H3

The twin pivot study of PART ONE supported a PART TWO proposal that Harrison originally intended MS3972/3 to be an accompaniment to his manuscript, CSM, published in 1775, the year before his death. On that basis, it is likely that CSM and MS3972/3 were both created towards the end of Harrison's life. It is therefore possible (although by no means certain, without proof of escapement originality) that the twin balance escapement sub-geometries of MS3972/3 illustrate the original escapement of H3 (whether to scale or not), it being unlikely that Harrison would have depicted the twin balance escapement of an earlier, superseded sea clock, or continued the development of large, slow-beating longitude timekeepers beyond H3. Regardless of any of the above, the escapement sub-geometries of H3 are arranged with their balance arbor axes above and below the 120 tooth escape wheel arbor axis, whilst a pair of large, circular balances, arranged as schematically illustrated in **Figure 64**, replace the large twin bar balances of H1 and H2. Figure 63 rotated in its entirety through ninety degrees would represent such a configuration, which may well have been Harrison's undisclosed intention.

Of passing interest, thin metal ribbons and circular arcs, illustrated in green, red and light grey, oblige the balances of H3 to swing in opposition. The upper balance arbor is connected to the movement frame by a short, stiff, spiral spring, the effective rate of which is altered by a temperature-sensitive compensation curb (not illustrated), incorporating what was apparently the first ever 'bimetallic strip', invented by Harrison. Although he was eventually forced to concede that slow balances were fundamentally unsuited to the intended task, Harrison acknowledged the contribution of H3 to the subesequent creation of the much smaller, successful solution, H4. The considerable influence of H3 is also revealed (to this observer, at least) by the incorporation of a circular balance with a high 'velocity' (Harrison's term), a longer, more flexible balance spring, a bimetallic temperature compensation curb acting upon the balance spring and a spring remontoire feeding energy to the escape wheel arbor.

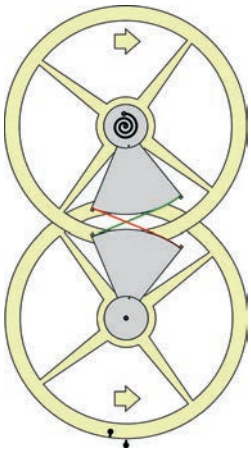

Figure 64 - Linked circular balances and single spiral spring arrangement of H3

CHECKING GEOMETRIES

Upon completion, or at any time beforehand if considered necessary, sub-geometries should be checked. With reference to **Figure 65**, drawn to no particular scale, the following sequence is suggested. Although geometry A labelling is used, the listed checks may be applied, with common sense, to geometry B.

Check (1) COD should be the angle subtended by half a tooth space.
Check (2) DOZ should be the angle subtended by the chosen start of impulse encompassed tooth spaces.
Check (3) The start of impulse encompassed tooth spaces of geometry A should be greater than the start of impulse encompassed tooth spaces of geometry B by an odd integer multiple of half a tooth space.
Check (4) DF should equal CG (equal pallet arm active lengths at the start and end of impulse).
Check (5) FZ should equal GZ (equal pallet arm pivot to balance axis distances at the start and end of impulse).
Check (6) FDO should be the designer-chosen entry angle (geometry A), or should be within (a proposed) two degrees of the initial designer-chosen exit angle (geometry B).
Check (7) FD should be tangential to the smaller torque arm circle at H .
Check (8) CG should be tangential to the larger torque arm circle at E.
Check (9) EZ / HZ should match the designer-chosen end/start ratio, T. For Harrison compliant geometries, the ratio should be 3 / 2.
Check (10) In final sub-geometries, MZ = 0.5 (EZ + HZ) should match the designer-chosen mean torque arm.
Check (11) Angle FZG should match the designer-chosen escaping arc, with at least the chosen degree of precision.

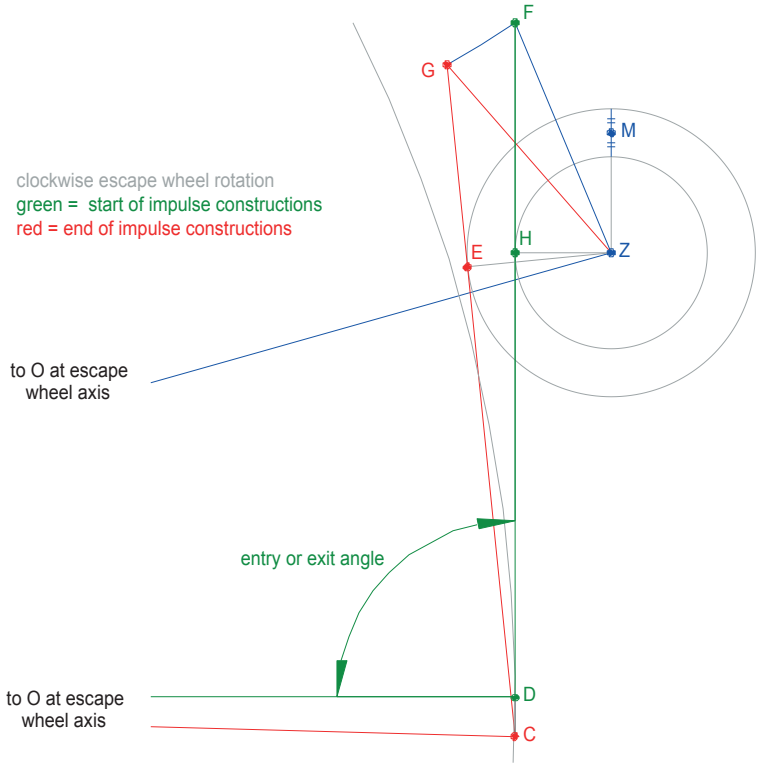

Figure 65 - Checking geometries

BIBLIOGRAPHY

Harrison, John. 1775. *A Description Concerning Such Mechanism as will Afford a Nice, or True Mensuration of Time; Together with Some Account of the Attempts for the Discovery of the Longitude by the Moon; as also an Account of the Discovery of the Scale of Music.* London. CSM is, at the time of writing, freely available on the NAWCC Horological Science Chapter 161 website at http://www.hsn161.com/HSN/CSM.pdf

Heskin, David. June 2011. *Concerning Such Mechanism - An accessible translation of the Horological Content of John Harrison's 1775 manuscript.* First Edition, 2011. ISBN 978-0-9555875-7-3. Soptera Publications, Leicestershire, England. Also freely available on the above website.

Heskin, David. September 2011. *Computer Aided Design of the Harrison Single Pivot Grasshopper Escapement Geometry.* 1st Edition September 2011, ISBN 978-0-9555875-8-0. This publication is, at the time of writing, freely available on the NAWCC Horological Science Chapter 161 website at http://www.hsn161.com/HSN/Heskin.php

MS3972/3 - Catalogued as such in The Worshipful Company of Clockmakers library, London.

APPENDIX

INTRODUCTION

This Appendix describes invaluable properties of the twin pivot exit geometry, the twin pivot entry geometry and either of the twin balance sub-geometries. Thorough familiarity with relevant CAD sequences and mechanical arrangements will be assumed. Supporting calculations will be offered in an economical format. In all illustrations, normal escape wheel advancement is clockwise, green colouring applies to start of impulse constructions and red colouring applies to end of impulse constructions. CAD sequence labelling is preserved. All curves are segments of circular arcs and all lines are straight. Alphabetical labelling of lines and angles is not necessarily observed.

THE TWIN PIVOT EXIT GEOMETRY

UNIVERSAL ESCAPEMENT FRAME ARBOR AXIS AND UNIVERSAL ESCAPING ARC

Figure 67 reproduces, greatly enlarges and applies fresh green and red colouring to the illustrated exit geometries of twin pivot CAD sequence STEP SIX (Figure 40, page 38). The escape wheel arbor axis, O, is beyond the page margin, at the intersection of lines [3], [4] and [10]. The entry geometry is also beyond the page margins.

■ - Three twin pivot grasshopper escapement exit geometries are simultaneously illustrated in Figure 67. **'Geometry QR'** incorporates start and end of impulse pallet arm pivot locations Q and R, respectively. **'Geometry DC'** incorporates theoretically valid start and end of impulse pallet arm pivot locations D and C, respectively. **'Geometry FG'** incorporates start and end of impulse pallet arm pivot locations F and G, respectively.

■ **-** Further additions to the original illustration are small blue label B', at the intersection of line QR with its grey, perpendicular, bisecting line; small orange label M', at the intersection of DC with its grey, perpendicular, bisecting line [30] and small orange label A', at the intersection of line FG with its orange, perpendicular, bisecting line [34].

■ **-** Some features of geometry FG were created in a different order to those of geometries QR and DC, as will be explained shortly. Until then, to avoid any risk of confusion, geometry FG should be completely ignored.

■ **-** Geometry QR start and end of impulse pallet arm active lengths DQ and CR are constructed equal during the CAD sequence, correctly representing the active length of the rigid exit pallet arm in its start and end of impulse positions, when its pivot is at Q and R, respectively. Since the escapement frame arbor axis, labelled W, is located along the grey perpendicular to QR from mid point B', points Q and R are equidistant from W. The rigid connection between W and the pallet arm pivot in its start and end of impulse positions, Q and R respectively, is thereby correctly represented, whence apex angle QWR in isosceles triangle QWR is the escaping arc of geometry QR.

■ **-** Geometry DC incorporates equal start and end of impulse pallet arm active lengths of zero. Active lengths of zero are correctly represented by start and end of impulse pallet arm pivots coincident with the start and end of impulse nib locking corners at D and C, respectively. Such an arrangement is invaluably valid *in theory*, despite being worthless in physical reality. Since the escapement frame arbor axis, labelled W, is located along the grey perpendicular to DC from mid point M', points D and C are equidistant from W. The rigid connection between W and the pallet arm pivot in its start and end of impulse positions, D and C respectively, is thereby correctly represented, whence apex angle DWC in isosceles triangle DWC is the escaping arc of geometry DC.

■ - The illustrated escapement frame arbor axis W, at the point of intersection of the grey perpendiculars from B' and M', is the only sensible location *simultaneously* valid for geometry QR and geometry DC.

■ - It has been demonstrated in the above that DQ = CR, QW = RW and DW = CW. Triangle DWQ therefore matches triangle CWR in every respect. Thus, triangle DWQ is identical to triangle CWR rotated clockwise about W by escaping arc DWC of geometry DC and is also identical to triangle CWR rotated clockwise about W by escaping arc QWR of geometry QR. Escaping arc DWC is therefore equal to escaping arc QWR. The common escaping arc will be referred to as **E**.

■ - DQ in triangle DWQ is identical to CR in triangle CWR rotated clockwise about W by escaping arc E. Therefore, since DQ and CR are aligned with the start and end of impulse lines of action, respectively, the angle between the start and end of impulse lines of action is equal to E.

■ - All of the above could be applied to and incorporated within any one of a potentially infinite number of correctly functioning geometries incorporating W, D, C and the illustrated lines of action. The same location of axis W will be incorporated within any such geometry and may, therefore, be referred to as the **'universal escapement frame arbor axis'**. The escaping arc of any such geometry will be equal to E, which may, therefore, be referred to as the **'universal escaping arc'**.

■ **- SUMMARY - For a given escape wheel tooth count and given start and end of impulse lines of action, all correctly functioning twin pivot grasshopper escapement exit geometries will be compatible with a single, universal escapement frame arbor axis, at which a single, universal escaping arc will match the acute angle between the lines of action.**

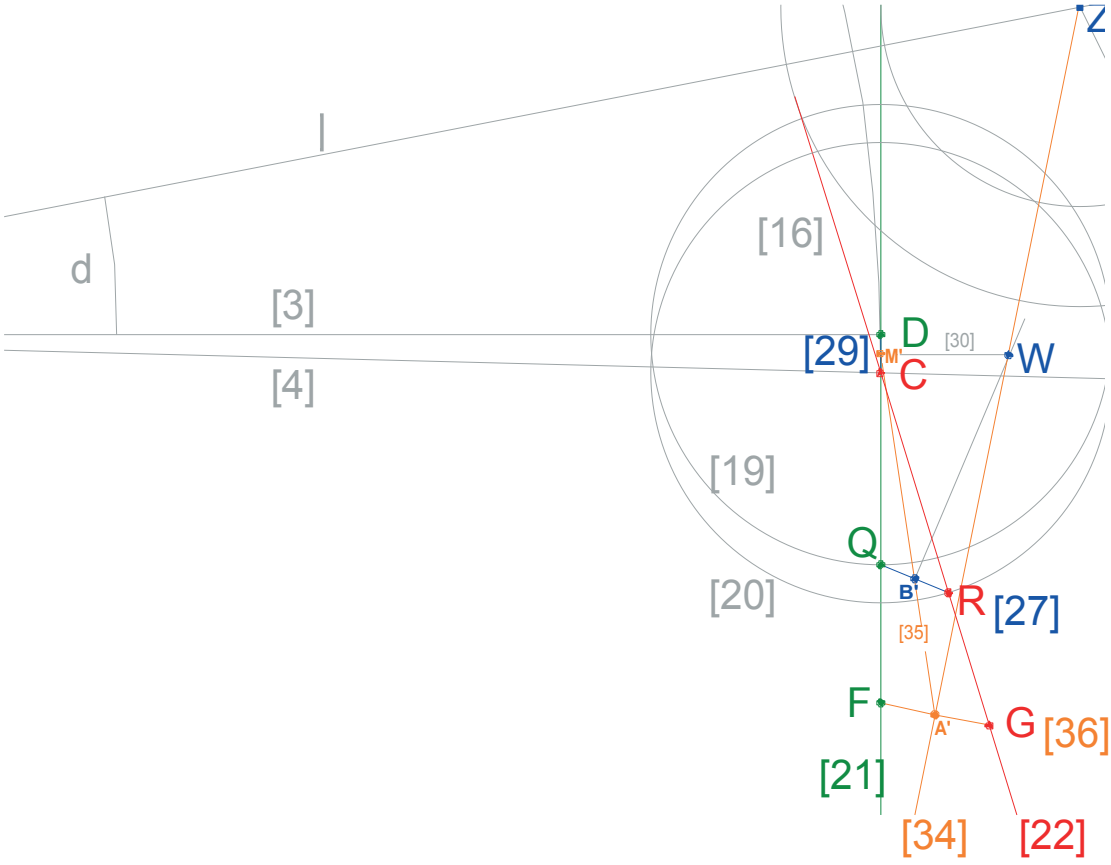

Figure 67 - Three twin pivot CAD sequence STEP SIX exit geometries

THE UNIVERSAL LINE OF INTERSECTIONS

■ - For the purposes of clear description, **Figure 68** (next page) illustrates three greatly magnified twin pivot exit geometries with intentionally exaggerated proportions. '**Geometry DC'** is the equivalent of geometry DC in Figure 67. '**Geometry NA'** is entirely new and incorporates start and end of impulse pallet arm pivot locations N and A, respectively. '**Geometry XY'** is also entirely new and incorporates start and end of impulse pallet arm pivot locations X and Y, respectively. The universal escapement frame arbor axis, beyond the page margin, is labelled W.
■ - As described on page 70, geometry DC start and end of impulse pallet arm active lengths are both zero and the universal escapement frame arbor axis, W, lies along a perpendicular to DC, which bisects DC at M'. DW and CW are therefore equal in length, as is necessary for correct functioning. From the SUMMARY (page 70), DWC is the universal escaping arc, E, matching the acute angle between the green start and red end of impulse lines of action. DWC is an isosceles triangle, whence angles DWM' and CWM' are both equal to E/2, as illustrated.
■ - Geometry NA start of impulse pallet arm pivot location, N, has been deliberately placed at the intersection of the green start of impulse line of action and the red end of impulse line of action. DN is therefore the start of impulse pallet arm active length and line NA lies along the red end of impulse line of action. The end of impulse pallet arm active length, CA, is constructed equal to DN. The universal escapement frame arbor axis, W, lies along a perpendicular to NA, which bisects NA at Y. Thus, NW = AW, as is necessary for correct functioning. From the SUMMARY (page 70), NWA is equal to the universal escaping arc, E. NWA is an isosceles triangle, whence angles NWY and AWY are both equal to E/2, as illustrated. Thus WNY = [90-E/2]. Since acute angle DNC, between the lines of action, is equal to E, the obtuse angle, DNA, between the lines of action is [180-E], half of which is [90-E/2], which matches WNY. NW therefore bisects the obtuse angle between the lines of action.
■ - Geometry XY start and end of impulse pallet arm pivot locations, X and Y, are intentionally defined by perpendiculars to the start and end of impulse lines of action, intersecting at the universal escapement frame arbor axis, W. The universal escapement frame arbor axis, W, lies along a perpendicular to XY, which bisects XY at L. XW and YW are therefore of equal length, as is necessary for correct functioning. From the SUMMARY (page 70), XWY is equal to the universal escaping arc, E. XWY is an isosceles triangle, whence angles XWL and YWL are both equal to E/2, as illustrated. By virtue of symmetry, a short extension of LW would pass through N. LW and NW therefore coincide for most of their lengths, as illustrated.

Continues after Figure 68...

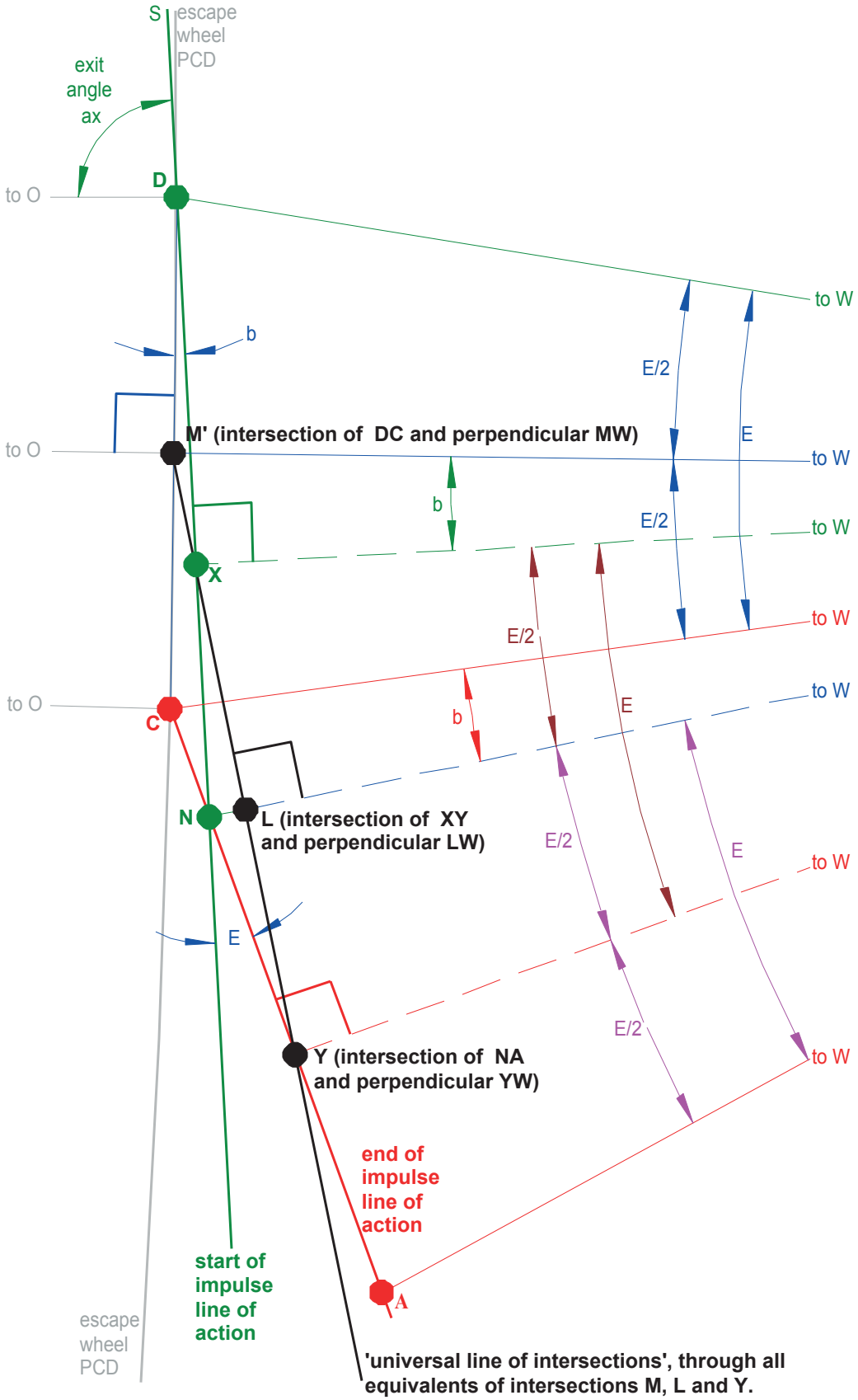

Figure 68 - Universal escapement frame arbor axis (W) and 'universal line of intersections' (in black).

■ - XDO = [180-ax] and M'DO = [90-DOM'], whence **M'DX** = [90+DOM'-ax], hereafter referred to and illustrated as **angle b**. Since M'W is perpendicular to DC and XW is perpendicular to DN, angle **M'WX** is also equal to **angle b**, as illustrated. Angle CWL = [M'WX+XWL-CWM'], angle XWL= E/2 and angle CWM' = E/2, whence angle CWL = [M'WX+E/2-E/2] = M'WX. Angle **CWL** is also, therefore, equal to **angle b**, as illustrated.
■ - The above demonstrates that triangle DWX is identical to triangle CWY, whence geometry XY start and end of impulse pallet arm active lengths DX and CY, respectively, are equal, as is necessary for correct functioning.
■ - With the exception of the black line (to be described shortly) all of the above demonstrates that Figure 68 is correct and that the three Figure 68 geometries would function as twin pivot exit geometries. Observe that the escape wheel tooth count, exit angle and end/start ratio, which define angle E between the lines of action and angle b, are entirely responsible for the forms of all three geometries, as the illustrated angles E, E/2 and b serve to emphasise.
■ - Recall that, in geometry DC, point M' lies at the **perpendicular intersection** of DC and its **bisector**, M'W. In geometry NA, point Y lies at the **perpendicular intersection** of NA and its **bisector**, YW. In geometry XY, point L lies at the **perpendicular intersection** of XY and its **bisector**, LW.
■ - The black line connects point of **perpendicular intersection** Y in geometry NA and point of **perpendicular intersection** L in geometry XY. The line extends to point X, since Y, L and X are aligned in geometry XY.
■ - The black line through Y, L and X extends to point M'. The universal validity of that construction may be demonstrated by incorporating an angle b of zero, achieved by setting ax to [90 + DOM']. Point X in geometry XY thereby coincides with point M' in geometry DC.
■ - **Returning to Figure 67**, the orange line labelled [35] passes through the **perpendicular intersection** of DC and its grey **bisector** [30] in geometry DC and through the **perpendicular intersection** of QR and its grey **bisector** B'W in geometry QR.
■ - From all of the above (and entirely regardless of the deliberately exaggerated proportions of Figure 68), the black line in Figure 68 and orange line [35] in Figure 67 both pass through every point of **perpendicular intersection** of lines between the start and end of impulse pallet arm pivot locations and their corresponding **bisecting** lines. The properties of those two lines (and any extensions) are identical. Either line (and any extensions) may, therefore, be referred to as a **'universal line of intersections'**. The significance of this line is revealed below.

INCORPORATING A SPECIFIC ESCAPEMENT FRAME ARBOR AXIS

In Figure 67, point Z is the CAD sequence STEP TWO location of the escapement frame arbor axis at which the designer-chosen end/start ratio is imposed in STEP THREE. The APPENDIX thus far has, however, only described geometries incorporating the universal escapement frame arbor axis, W, which will always fail to generate the chosen end/start ratio, except by extremely unlikely chance. The devised CAD sequence resolves this difficulty by identifying a single, unique geometry, capable of correct operation at axis W **or** axis Z.

In Figure 67, geometries DC and QR both incorporate the universal escapement frame arbor axis, W. The universal line of intersections, labelled [35], is derived from those two geometries, as described earlier in this Appendix. Geometry FG (which must no longer be ignored) is then created 'in reverse', starting from the universal line of intersections. Thus, a straight orange line, labelled [34], is constructed from the required axis, Z, to the universal axis, W, extending beyond W as far as the universal line of intersections, [35]. The point of intersection of lines [34] and [35] is labelled A'. A perpendicular to [34] is constructed through A' and labelled [36]. The two points of intersection of [36] with the start and end of impulse lines of action define the start and end of impulse pallet arm pivot locations F and G, respectively. Since triangles FWG and FZG are both isosceles, FW = GW and FZ = GZ, thereby representing a valid rigid connection between axis W and pallet arm pivot locations F and G **and** an equally valid, but entirely different rigid connection between axis Z and pallet arm pivot locations F and G. Correct functioning of the W-axis geometry and the target Z-axis geometry is thereby **simultaneously** assured for equal start and end of impulse exit pallet arm active lengths DF and CG, respectively. As required, the designer-chosen end/start ratio has been preserved within the unique Z-axis geometry incorporating D, C, F and G. For the chosen escape wheel and exit angle, no other exit geometry is capable of generating the chosen end start ratio.

THE TWIN PIVOT ENTRY GEOMETRY

Apart from the incorporation of green (start of impulse) and red (end of impulse) colouring, **Figure 69** (overleaf) reproduces the entry geometry from twin pivot CAD sequence STEP SIX. The exit geometry is reproduced in grey, for ease of comparison. The universal escapement frame arbor axis of the entry geometry is labelled 'V', to distinguish it from 'W' of the exit geometry. Although the *mechanical* arrangement of the entry side of the twin pivot grasshopper escapement differs markedly from the exit side, the fundamental principles of the entry and exit *geometries* are identical in every respect. The same approach described earlier for the exit geometry may therefore be applied to the entry geometry. Thus, a universal line of intersections, [32], has been created from universal V-axis **geometry JK** and universal V-axis **geometry ST**. The required Z-axis **geometry PN**, which generates the designer-chosen end/start ratio, is then created 'in reverse', starting from the universal line of intersections.

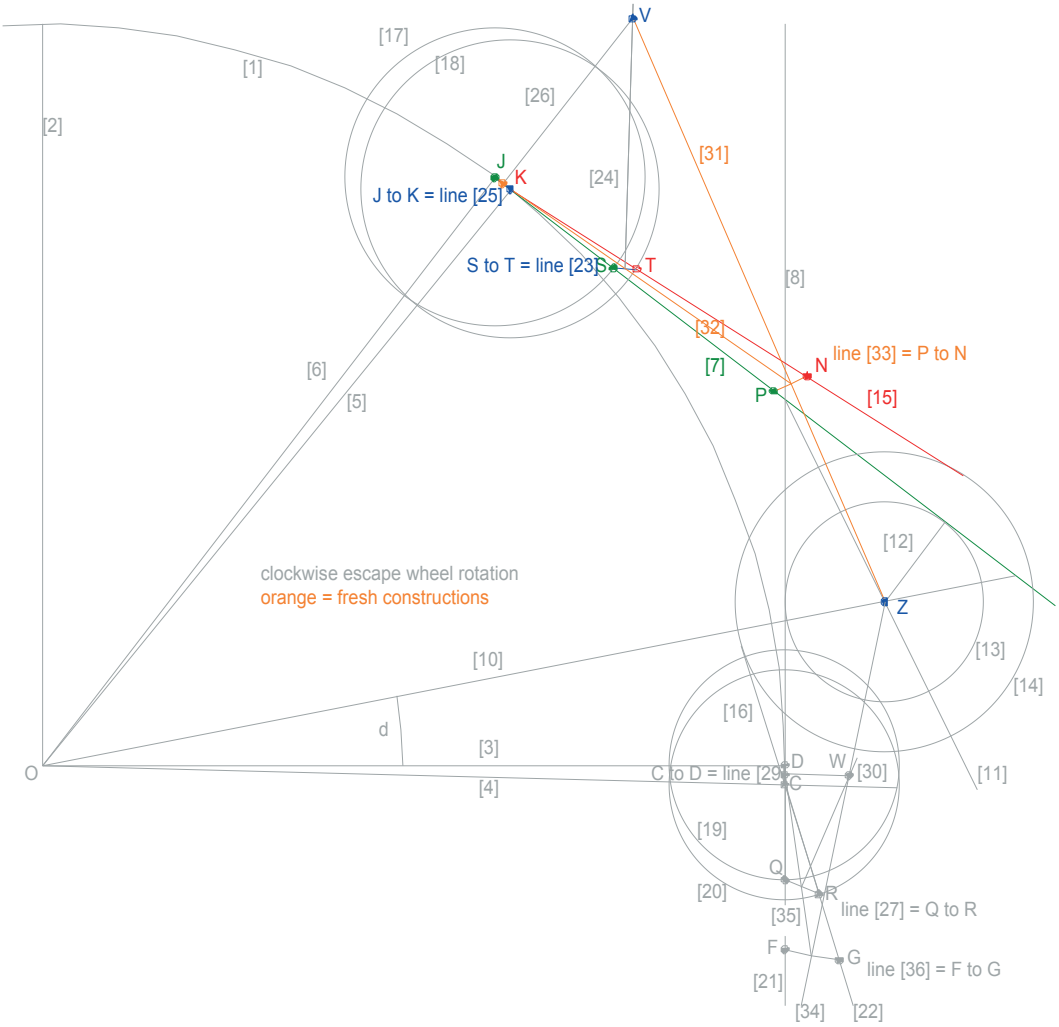

Figure 69 - Two W-axis and one Z-axis twin pivot entry geometries, emphasised in green, red and orange.

EITHER TWIN BALANCE SUB-GEOMETRY

Apart from the incorporation of green (start of impulse) and red (end of impulse) colouring, **Figure 70** (overleaf) reproduces Figure 54 from twin balance CAD sequence STEP FOUR. Although the illustrated proportions and labelling are for twin balance geometry A, the following conclusions are no less valid for twin balance geometry B, or any other twin balance sub-geometry. The universal escapement frame arbor axis is labelled 'W'.

Although the *mechanical* arrangement of the twin balance grasshopper differs from the exit side of the twin pivot exit escapement, the *geometry* of Figure 70 is nothing more than a mirror image of a twin pivot exit geometry, with appropriate exchanges of the start and end of impulse events. The same approach described earlier for the exit geometry may therefore be applied. Thus, a universal line of intersections, [16], has been created from universal W-axis **sub-geometry DC** and universal W-axis **sub-geometry QR**. The required Z-axis **sub-geometry FG**, which generates the designer-chosen end/start ratio, is then created ‘in reverse’, starting from the universal line of intersections.

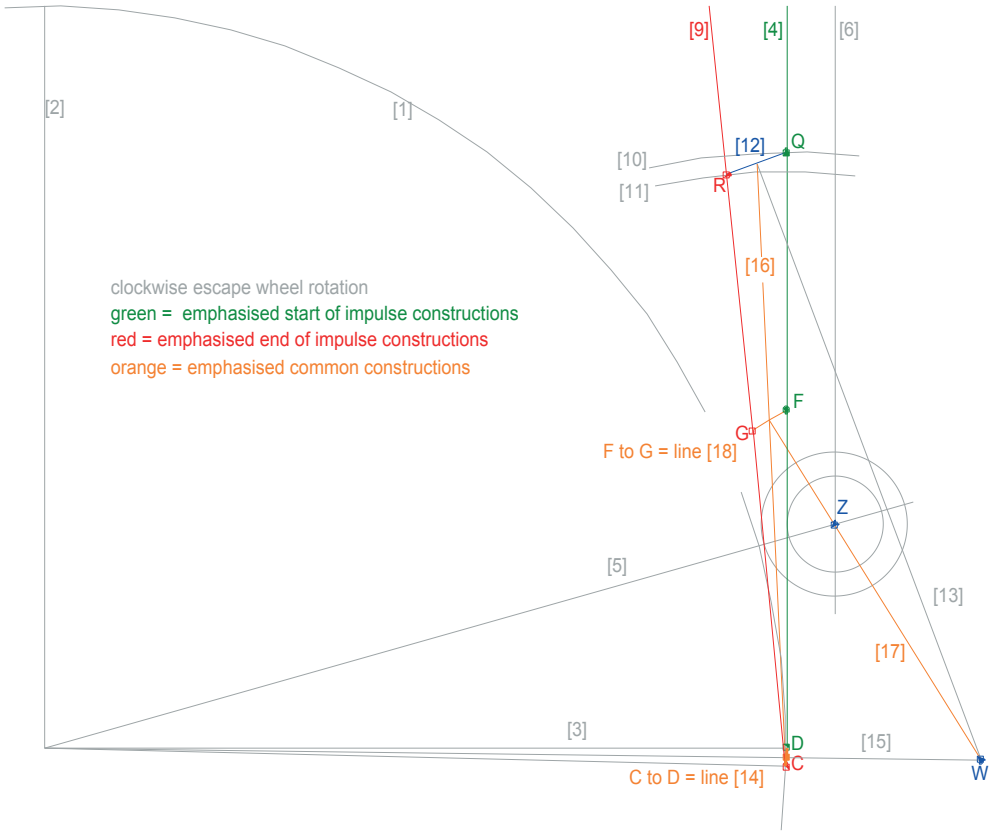

Figure 70 - Two W-axis and one Z-axis twin balance sub-geometries, emphasised in green, red and orange.

OF THE ORDER ORTHOPTERA

As deduced in this APPENDIX, the entry geometry of a twin pivot grasshopper and either sub-geometry of a twin balance configuration incorporate the same fundamental geometrical structure as the exit geometry of a twin pivot escapement. An appraisal of Harrison's single pivot grasshopper escapement geometry also identifies the twin pivot exit geometry as its fundamental geometrical basis, given that a single pivot entry geometry is a twin pivot entry geometry and a single pivot exit geometry is a twin balance sub-geometry. Mechanical arrangements aside, the single pivot configuration is only set apart from the twin pivot and twin balance arrangements by its unavoidably imbalanced entry versus exit impulse characteristics and the unique design process required for their incorporation about a single pallet arm pivot. The latter difference is, to some extent, responsible for the separate publication of '*Computer Aided Design of the Harrison Single Pivot Grasshopper Escapement Geometry* (see BIBLIOGRAPHY).

Darwin might have been pleased.